



# The Paton WELDING JOURNAL

Issue  
**02**  
2019

Published Monthly Since 2000

English translation of the monthly «Avtomaticheskaya Svarka» (Automatic Welding) journal published in Russian since 1948

## EDITORIAL BOARD

### Editor-in-Chief

**B.E. Paton**

*Scientists of PWI, Kyiv*

**S.I. Kuchuk-Yatsenko** (*vice-chief ed.*),

**V.N. Lipodaev** (*vice-chief ed.*),

**Yu.S. Borisov, G.M. Grigorenko,**

**A.T. Zelnichenko, V.V. Knysh,**

**I.V. Krivtsun, Yu.N. Lankin,**

**L.M. Lobanov, V.D. Poznyakov,**

**I.A. Ryabtsev, K.A. Yushchenko**

*Scientists of Ukrainian Universities*

**V.V. Dmitrik**, NTU «KhPI», Kharkov

**V.V. Kvasnitsky**, NTUU «KPI», Kyiv

**E.P. Chvertko**, NTUU «KPI», Kyiv

*Foreign Scientists*

**N.P. Alyoshin**

N.E. Bauman MSTU, Moscow, Russia

**Guan Qiao**

Beijing Aeronautical Institute, China

**M. Zinigrad**

Ariel University, Israel

**V.I. Lysak**

Volgograd STU, Russia

**Ya. Pilarczyk**

Welding Institute, Gliwice, Poland

**U. Reisgen**

Welding and Joining Institute, Aachen, Germany

**G.A. Turichin**

St. Petersburg SPU, Russia

### Founders

E.O. Paton Electric Welding Institute, NASU

International Association «Welding»

### Publisher

International Association «Welding»

### Translators

A.A. Fomin, O.S. Kurochko, I.N. Kutianova

*Editor*

N.G. Khomenko

*Electron galley*

D.I. Sereda, T.Yu. Snegiryova

### Address

E.O. Paton Electric Welding Institute,

International Association «Welding»

11 Kazimir Malevich Str. (former Bozhenko Str.),

03150, Kyiv, Ukraine

Tel.: (38044) 200 60 16, 200 82 77

Fax: (38044) 200 82 77, 200 81 45

E-mail: journal@paton.kiev.ua

www.patonpublishinghouse.com

State Registration Certificate

KV 4790 of 09.01.2001

ISSN 0957-798X

DOI: <http://dx.doi.org/10.15407/tpwj>

### Subscriptions

\$384, 12 issues per year,

air postage and packaging included.

Back issues available.

All rights reserved.

This publication and each of the articles contained

herein are protected by copyright.

Permission to reproduce material contained in this journal must be obtained in writing from the Publisher.

## CONTENTS

PWI Pilot Plant of Welding Equipment is 60 ..... 2

### SCIENTIFIC AND TECHNICAL

*Skulsky V.Yu., Strizhius G.N., Nimko M.A., Gavrik A.R., Kantor A.G. and Konovalenko A.V.* Delayed fracture resistance of welded joints of rotor steel 25Kh2NMFA after welding reheating ..... 7

*Poklyatsky A.G. and Motrunich S.I.* Strength of welded joints of heat-hardenable aluminium alloys in TIG and friction stir welding ..... 13

*Razmyshlyayev A.D., Ageeva M.V. and Lavrova E.V.* Refinement of metal structure in arc surfacing under the effect of longitudinal magnetic field ..... 19

### INDUSTRIAL

*Reisgen U. and Stein L.* Joining of steel and dissimilar material joints with highest strength — there are other ways than conventional welding ..... 22

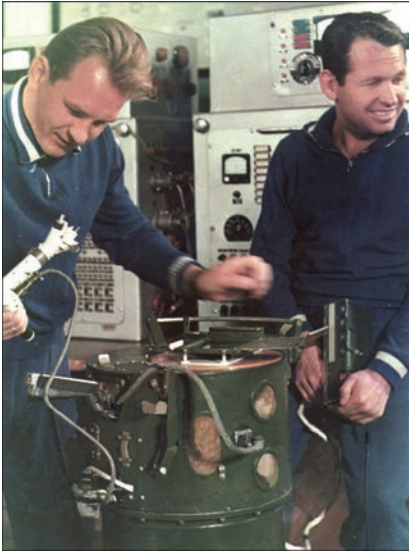
*Ryabtsev I.A., Knysh V.V., Babinets A.A., Solovej S.A. and Senchenkov I.K.* Methods and specimens for comparative investigations of fatigue resistance of parts with multilayer surfacing ..... 29

*Degtyarev V.A.* Methods of evaluation of increase of fatigue resistance in butt welded joints of low-carbon steels after high-frequency mechanical peening ..... 35

*Gubatyuk R.S.* Heat treatment of welded joints of high-strength railway rails (Review) ..... 41

CALENDAR OF FEBRUARY ..... 49

## PWI Pilot Plant of Welding Equipment is 60



Cosmonauts V.N. Kubasov and G.V. Shonin with «Vulkan» unit before Soyuz-6 flight

Welding technologies, similar to many others, do not stay in one place, but have a steady tendency to develop, new materials are created, welding technologies are improved, as well as welding equipment, which becomes more cost-effective, compact and efficient from year to year.

A bright example of successful welding technology development is PWI PPWE, which celebrated its 60th anniversary on January 1, 2019.

From the moment of the start of its operation (1959), the main objective of the Plant was optimizing the technology of manufacturing new welding equipment, developed by PWI scientists. And over the 60 years of its history, the Plant has manufactured hundreds of thousands of equipment units for almost all continents of the world. Welding equipment manufactured by the Pilot Plant, was used for performance of welding operations in a broad range of conditions: from water depths to open space.

Among the known historical events, which were realized with application of PPWE equipment, the following should be noted:

- construction of «Bukhara-Urals» and «Druzhba» gas pipelines (A850 and A943 machines for welding large-diameter pipes);
- first welding operations with the electron beam, plasma and consumable electrode in space, performed by the crew of «Soyuz-6» spaceship (unique «Vulkan» apparatus);
- Soviet-French experiment in near-earth space (special hardware «Araks»);
- world's first cutting, welding, brazing and spraying of metal plates in open space at «Salyut-7» station (portable electron beam unit URI).

In the period from 1992 to 1998, during the unstable economic situation in Ukraine, when many production enterprises were closing, the Pilot Plant of Welding Equipment managed to preserve its production facilities and most valuable personnel resource. During this period the main activity of the Plant was manufacturing transformer equipment.



Laying the main pipeline

In 2004, in parallel with manufacture of classic transformers and rectifiers, a new department is formed, the main purpose of which was development of welding inverters. This department was formed from high class specialists — graduates of NTUU «KPI», who were immediately sent for training to Italy, to one of Europe's leading plants on manufacture of inverter welding machines. This yielded its results — Pilot Plant of welding equipment was the first in Ukraine to master manufacture of inverter-type welding machines, and today the Plant's products take up a considerable share of Ukrainian market of welding equipment. PPWE also is the only plant in Ukraine, capable of manufacturing welding equipment for welding currents from 150 A for household consumers up to 10000 A for Ukrainian industry giants.



PPWE central building

After the Plant has occupied a serious share of Ukrainian market, a decision was taken to actively develop exports. In 2012 the first export delivery of inverter-type welding machines to Equatorial Guinea was carried out. Since 2013 welding machines began to be exported to Georgia, Moldova and Azerbaijan. In 2014 the Pilot Plant received the European Certification CE for inverters, and in 2017 confirmed it for the entire line of inverter-type PATON™ machines. As of 2019 PATON™ products have been supplied to more than 20 countries all over the world — from Latin America to South Korea.

*«During the entire period of its activity the Pilot Plant of Welding Equipment implemented the developments of the Electric Welding Institute. On the one hand, it was a great responsibility, but on the other, it always kept the team's creativity in good shape and allowed working with the newest developments in the field of welding that largely predetermined today's success of the Plant»,* — Victor Koritsky, PWI staff member, shares his impressions.

The Plant carries on close cooperation with PWI and PWI Experimental-Design and Technological Bureau, remaining the production site for manufacturing pilot equipment. Over the last several years, a number of National and International projects have been realized using the Plant production facilities, including:

- development of welding technology and equipment for manufacturing welded combined rotors by automated submerged-arc welding by an order of OJSC «Turboatom» (2013);
- project of State Oil Company of Azerbaijan (SOCAR) on severing two pontoons from a block by directed explosion method at construction of an off-shore stationary platform No.7 in the Caspian Sea (2014);
- project of State Company «Ukrspetsexport» on development and manufacture of a batch of welding equipment for tropical climate, which was supplied to one of shipbuilding plants in South-East Asia (2015);
- development of welding equipment for electroslag welding of metal up to 200–450 mm thick for mechanical engineering plant in Eastern Europe (2016);
- joint development by the Plant and PWI EDTB of multi-operator welding rectifiers VDU-



Anat. V. Stepakhno, Chairman of PPWE Board, is demonstrating new samples of welding power sources to academician B.E. Paton

Acad. I.V. Krivtsun,  
PWI Deputy Director



Pilot Plant of Welding Equipment of the E.O. Paton Electric Welding Institute is one of the main partners of PWI in the field of development and batch production of modern competitive equipment for welding and related technologies. Institute scientists, with the participation of PPWE, perform studies of different welding processes and technologies, determining technical requirements to equipment, which is necessary for their practical realization. The thus obtained results are the base for manufacture of modern power sources and other specialized equipment at PPWE. An example of such fruitful cooperation can be the joint work performed last year on determination of welding-technological properties of inverter power sources for arc welding with expanded functional capabilities, the results of which are already being used by the Plant in manufacture of the line of multifunctional digital inverters. A promising direction of further cooperation of PWI and PPWE can be joint work on organizing mass production of specialized equipment and tools for high-frequency welding and treatment of live biological tissues, developed by the Institute's scientists in cooperation with specialists of different medical institutions of Ukraine.

graded: HAAS turning center, HAAS vertical machining center and specialized rotary table were put into operation. This entire equipment complex is fully automated and allows performing a wide range of operations on manufacture and machining of parts in the shape of bodies of revolution. Conducted refitting and upgrading of production led to improvement of product quality, reduction of labour consumption of complex operations

1202P, which were used to re-equip the carriage works of SCB Foundry in the Czech Republic (2016);

- project for State Company «Ukroboronservis» on development of an automatic mortar coordinating system (2016). The Project was presented with success at XIII International Specialized Exhibition «Arms and Security–2016».

The Plant also continues successfully realizing the Institute's developments in its products, manufacturing classical-type welding equipment. Literally at the end of 2018 the Pilot Plant realized a project on delivery of four multioperator welding rectifiers PATON™ VMG-5000 for welding currents up to 5000 A for top Ukrainian enterprises — leaders of the mining industry and metallurgy. Modern pace of development of science and technology necessitates regular upgrading of production enterprises on the strategic and technological levels. It is impossible to correspond to the status of the national steel manufacturer without continuous investments into development of the industry, which is given special attention by the Plant management.

In order to expand the range of manufactured products and strengthen its market positions, PPWE management took a decision on setting up its own company for production of welding electrodes. As a result, at the beginning of 2016, a new company OJSC «PATON-Elektrod» was established, which began manufacturing welding electrodes of the most popular grades of the classic formulations: ANO-21, ANO-36, ANO-4, UONI 13/45, UONI 13/55, MR-3, special electrodes for surfacing of T-590 grade, for cast iron welding of TsCh-4 grade, for welding high-alloyed steels OZL-8 and TSL-11, as well as electrodes of Elite series by improved PWI formulation. And in 2017 the technology park for electrode manufacture was complemented by a modern line of the capacity of 12 tons per shift, as part of realization of the strategy of development of this sector.

In 2017 the Plant commissioned a section on production of cases for welding machines, which accommodated high-technology equipment of the known TRUMPF brand: coordinate-perforating press for treating large metal sheets, hydraulic bending press to give the required shape to metal parts and line of powder painting of finished products. And in 2018 the section of mechanical production was up-

G.V. Zhuk,  
EDTB Director



Fruitful reliable cooperation of PPWE and EDTB for 60 years is still going on now. A large number of joint projects have been realized over these years. And now, when solving new tasks, EDTB can always rely on the enterprise, which is capable of embodying the most daring ideas. Continuous mutually beneficial cooperation of our organizations allows finding new customers, opening and expanding the markets.

## Export deliveries of PPWE equipment

### Classical equipment



Rectifiers



Transformers



Automatic machines



Multioperator power sources

Kazakhstan

Estonia

Latvia

Lithuania

Belarus

Poland

Uzbekistan

Moldova

Bulgaria

Georgia

Armenia

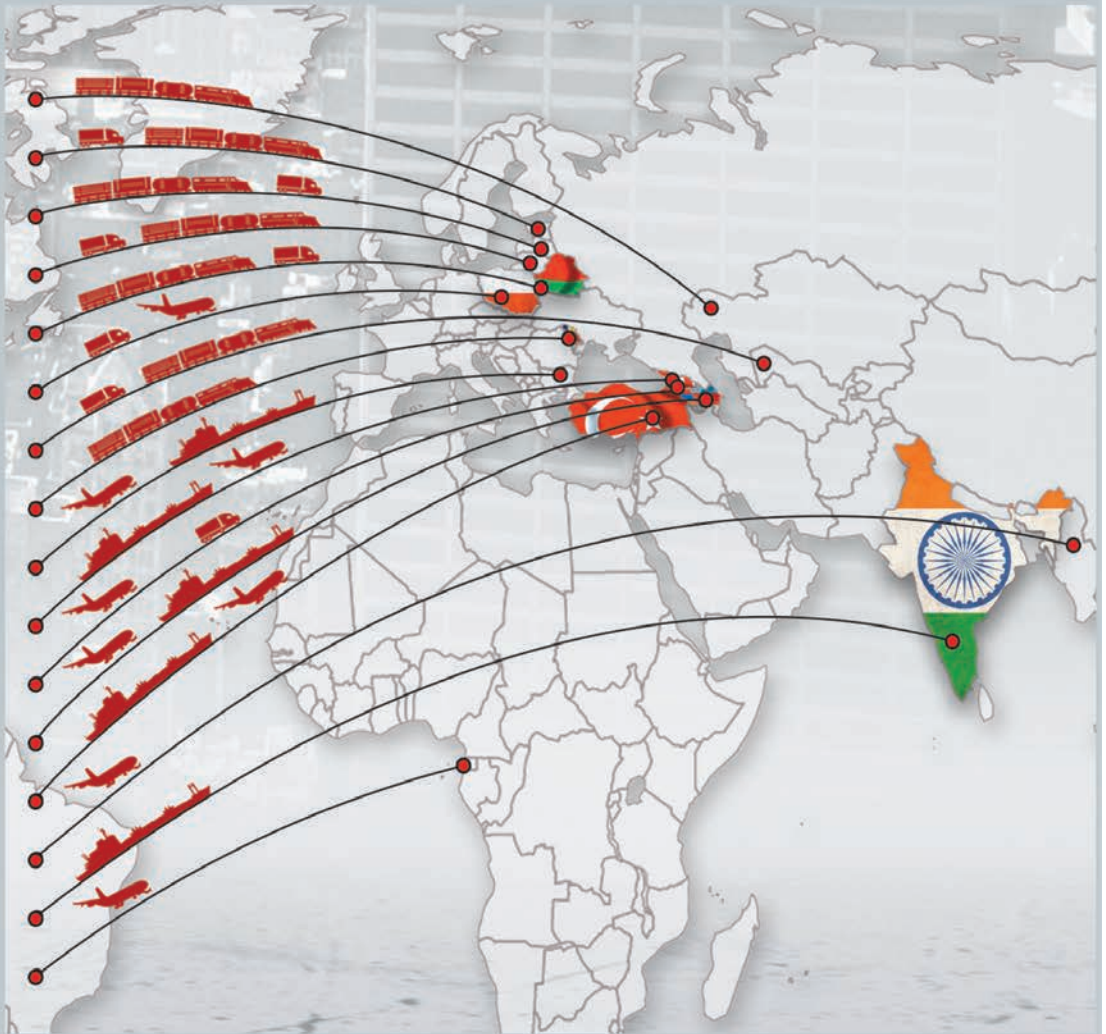
Azerbaijan

Turkey

Myanmar

India

Eq. Guinea



### Inverter equipment



Welding



Semi-automatic



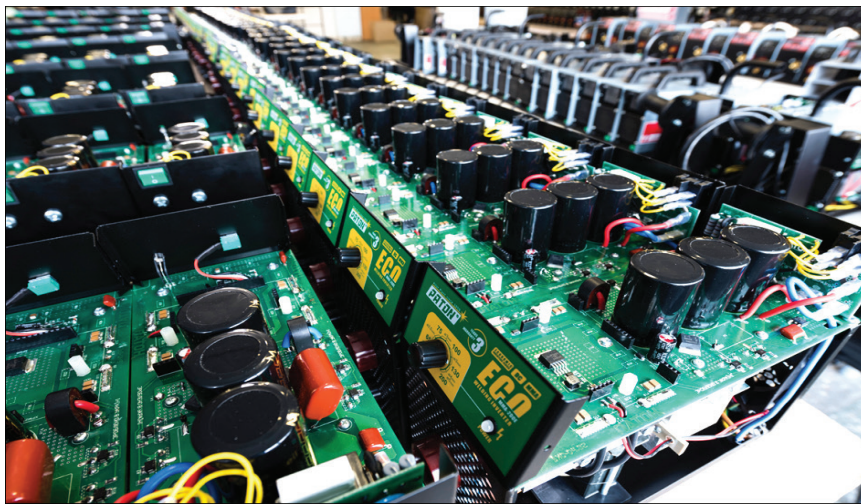
Argon-arc



Apparatuses for air-plasma cutting



Blank production shop



Assembly line of welding power sources

and shortening of certain production cycles, that allowed somewhat slowing down the increase of prices for finished products.

*«The steps taken for upgrading the production facilities of the Pilot Plant and step-by-step realization of development strategy allow us looking to the future with confidence. Today the Plant is focused on development of new samples of welding equipment and extension of the product range. Active development of high-power inverter-type machines with up to 1200 A welding currents is conducted now. We hope that they will complement the line of PATON™ welding inverters in the near future», — Anatolii Stepakhno, Chairman of Plant Board is talking about plans.*

Another important vector of Plant development is active expansion of export of its products. Today, the priority objectives of the enterprise export department include expansion of PATON™ product presence in the markets of the European countries, as well as entering the Central American market. Thus, over the 60 years of its activity the Pilot Plant of Welding Equipment has really gone a long way, with its ups and downs, trying to preserve and multiply its production and personnel potential to a maximum and improve the effectiveness of its operation. In the long run, this allowed it to become a leading Ukrainian manufacturer of welding equipment and materials, and PATON™ products to be in high demand both among Ukrainian welders and welding professionals all over the world.

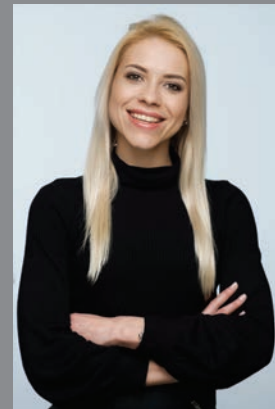
Editorial Board of «The Paton Welding Journal»

Vitalii Sokolyuk,  
Director of  
MasterWeld Sp.z.o.o Company



Our Company has been the official distributor of PATON™ welding equipment and electrodes in the Polish Republic beginning from 2016. During this time, the Plant products have proven their worth. This is high quality equipment and materials for welders of any qualification. This is exactly why PATON™ products are always in high demand, and we increase deliveries every month, accordingly, and see great prospects for PATON™ brand in EC market.

Daria Selina,  
Export Director of the Plant



The Plant has certain achievements — in January 2019 we shipped a trial batch of PATON™ products to Costa-Rica, which, as we think, will be the start of subsequent effective operation in this region.

# DELAYED FRACTURE RESISTANCE OF WELDED JOINTS OF ROTOR STEEL 25Kh2NMFA AFTER WELDING REHEATING

V.Yu. SKULSKY<sup>1</sup>, G.N. STRIZHIUS<sup>1</sup>, M.A. NIMKO<sup>1</sup>,  
A.R. GAVRIK<sup>1</sup>, A.G. KANTOR<sup>2</sup> and A.V. KONOVALENKO<sup>2</sup>

<sup>1</sup>E.O. Paton Electric Welding Institute of the NAS of Ukraine  
11 Kazimir Malevich Str., 03150, Kyiv, Ukraine. E-mail: [office@paton.kiev.ua](mailto:office@paton.kiev.ua)

<sup>2</sup>JSC «Turboatom»  
199 Moskovsky Ave., 61037, Kharkov, Ukraine. E-mail: [office@turboatom.com.ua](mailto:office@turboatom.com.ua)

The work is dedicated to experimental investigation of influence of repeated thermal effects under conditions of manual arc welding of hardening heat-resistant steel on delayed fracture resistance of metal in HAZ region of earlier performed passes. Applicable to different schemes of temper bead deposition using Implant method there were determined quantitative characteristics of change of delayed fracture resistance. It is shown that obtained crack resistance in welding without preheating can be compared with resistance in welding with heating. Effect of reheating on change of structural and hydrogen factor, influencing crack formation was evaluated. 22 Ref., 7 Figures.

**Keywords:** *hardening heat-resistant steel, welding reheating, delayed fracture, structural and hydrogen factors, Implant method, quantitative change of cracking resistance*

A classical problem of production of welded joints from hardening steels is high level of risk of cold cracks appearance in metal of heat-affected zone (HAZ) or weld. Multiple investigations showed that the main conditions of cold crack formation are generation of hardening structures in a joint zone, saturation of this zone with hydrogen (diffusion-mobile) and effect of tensile (welding) stresses due to shrinkage of metal being heated in welding and crystallized weld [1, 2]. For such types of defects following from their physical and chemical nature the next synonymous terms are also used, i.e. crack formation, related with effect of hydrogen or hydrogen-assisted cracking, hydrogen-induced cracking, delayed cracking [3, 4] or delayed fracture [5].

Cracking resistance is regulated by technological conditions of welding. For example, there is favorable fact in increase of metal cooling duration after completion of austenite transformation with formation of martensite that is related with effect of «self-tempering of martensite». Partial tempering of hardening structure will rise with increase of transformation temperature interval [3, 6, 7]. Temperatures below the transformation completion ones, including intervals of low-temperature martensite decay (around 160–70 °C [8–10]), provide tempering effect. In addition to redistribution of carbon in the process of such low-temperature tempering there also will be thermally activated diffusion scattering of hydrogen and decrease of its concentration of a dangerous zone. In this connection, the main technological methods in welding of hardening steels are preliminary (concurrent) heating and post weld heating-through of the welded joint (cooling down) at

temperature close to heating temperature [11]. However, such operation can be difficult for performance and rise energy expenses of welding works.

Welding heating results in accumulation of heat and creation of effect similar to concurrent heating [12]. Continuous deposition of beads allows reaching significant decrease of metal cooling rate in the zone of welding. Work [13] shows that deposition on steel surface of an area in several passes being performed without breaks was accompanied by two times decrease of HAZ metal cooling rate in comparison with performance of single bead using the same mode (manual arc welding by 3 mm diameter electrodes,  $I_w = 120\text{--}130$  A,  $U_a = 24$  V, preheating 250 °C:  $w_{6/5}$  in deposition of area of 20×60 mm — 3.3 °C/s, in performance of single bead — 6.7 °C/s). The positive moment in such an approach is possibility of performance of welding operations in repair of products of hardening steels without heating, as, for example, in process of «transverse hill» welding [14]. However, in separate cases uncontrolled increase of temperature of metal of welded joint due to heat accumulation can result in undesirable structural changes and deterioration of mechanical properties. In such cases it is necessary to limit the temperature in the joint zone and provide cooling rates eliminating formation of the structures having negative effect on properties of separate areas of the welded joints (for example, residual austenite in bainite-martensite structure, upper bainite) [12, 15, 16].

In welding of modern power machine building steels of bainite and martensite classes the temperature between the passes is limited at approximately 250–300 °C level [17–20]. At that a procedure of multipass welding with small-section beads is recom-

mended. Function of such a method, first of all, lies in achievement of fine-grain structure in overheating area of HAZ metal resulted from initially performed passes due to next application of temperatures of normalizing interval as well as partial tempering of quenched areas in performance of next passes. The joints with such structure are less susceptible to cracks in high tempering after welding. Applicable to the joints of martensite chromium steels, which are characterized with reduced weld metal impact toughness, a multi-pass welding with thin beads allows rising impact energy. Improvement of toughness is related with obtaining finer and disoriented crystallization structure and partial metal tempering in earlier performed layers; finer the beads the higher the result is. As a variant of welding with deposition of temper beads it was recommended a method using grinding of initially performed beads to the middle of their thickness for better heating of metal in this zone; however, the method is difficult and requires special training of welders, rises cost and time of work performance that limits its application [22].

Welding reheating of metal in the area of earlier performed layers, in addition to structure refinement and partial tempering also promotes increase of cold crack resistance [22]. However, how big, in quantitative concept, is the growth of technological strength under conditions of multipass welding shall be specified.

The aim of work is the quantitative evaluation of change of resistance of HAZ metal of hardening steels to delayed fracture under effect of welding reheating.

Rotor steel of the next alloying system, wt.% 0.23–0.27 C; 1.8–2.2 Cr; 1.3–1.6 Ni; 0.4–0.6 Mo; 0.05 V was used in the investigations as a test material. The values of carbon equivalent  $P_{cm}$  0.4–0.51 wt.% (calculated on Ito and Bessyo equation) [4] corresponds to change of alloying elements within the limits of steel content. The tests were carried out on known method Implant [3]: samples of investigated steel of 8 mm diameter with spiral stress concentrator in a working part in form of 0.5 mm depth V-groove with expansion angle  $40^\circ$  and rounding radius in the tip 1 mm were used. Implant samples were welded to base plate (of steel 20 of 16 mm thickness) by manual arc welding by coated electrodes of 3.2 mm diameter using

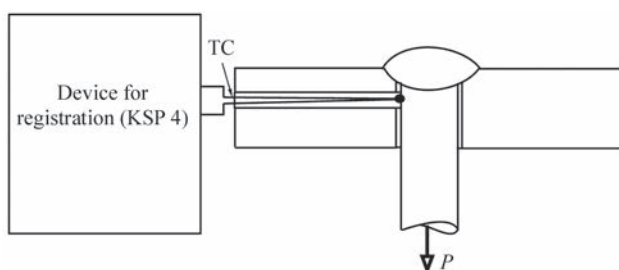


**Figure 1.** Scheme of measurement of temperature in Implant sample

alloying system of deposited metal 0.07C2CrMoV. After electrodes baking at 400–450 °C, 2 h, content of diffusion hydrogen in the deposited metal  $[H]_{diff}$  (alcoholic analysis [11]) made approximately 0.96 cm<sup>3</sup>/100 g of Me. Control of temperature in HAZ of the samples (in welding with heating and at measurement of thermal cycles) was carried out using chromel-alumel thermocouple (TC) in a ceramic insulating shell, passed through a hole drilled from the edge of the base plate at around 4 mm depth in parallel with its surface (Figure 1). TC were welded to the samples with the help of capacitor-discharge machine, another end was connected to recording potentiometer. Application of load to tested joints was performed after cooling of metal in HAZ of the samples to room temperature, i.e. the joints were cooled under natural conditions to 100 °C, below, for making it faster, with blowing by air. A criterion of cracking resistance was a critical stress  $\sigma_{cr}$  promoting delayed fracture. Test joints, which withstood the load without failure for not less than 24 h are considered to be not susceptible to delayed fracture. Measurements of hardness were carried out by Vickers method at 5 kg loading.

In welding of the samples with the plate and in deposition of new beads the next mode of welding (if not indicated additionally) was used:  $I_w = 95\text{--}100$  A,  $U_a = 22$  V,  $v \approx 0.194$  cm/s (7 m/h), heat input  $q/v \approx 8.5\text{--}9.0$  kJ/cm (at calculated efficiency of arc  $\eta = 0.8$ ). The following schemes of welding of test joints with simple (without grinding) bead and with grinding of the first bead to the middle of thickness (half bead) (Figure 2) were used:

- welding with one bead («1 bead» – basic variant of comparison);
- welding in two layers with deposition of one bead on the first (1 + 1);
- welding in two layers with deposition of two beads in the second layer on one bead in the first layer (1 + 2);
- welding in three layers with deposition on the first single bead of two beads in the second and third layers (1 + 2 + 2) as well as in three layers using 1 + 2 + 5 scheme;
- welding with half bead (1/2) in the first layer with deposition in the second layer of one bead (1/2 + 1) and two beads (1/2 + 2), grinding of the first bead was carried out on joint cooling stage using manual grinding machine.

Deposition of new beads on initial weld was carried out after decrease of metal temperature of the first bead to 100 °C, except for 1 + 2 + 5 variant (Figure 3, where at measurement of thermal cycles on scheme from Figure 1 the maximum temperature of heating does not exceed approximately 600 °C due to removal of place of TC welding to the plate surface for a value of around 4 mm that exceeded real width of harden-

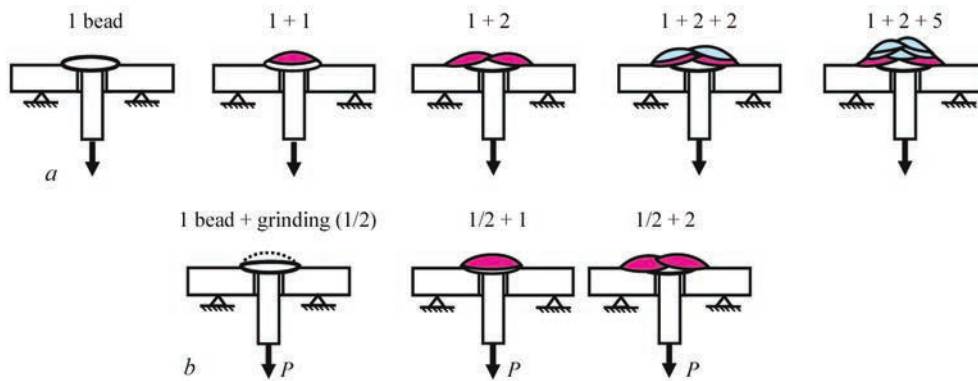


**Figure 2.** Technological schemes of welding of test joints: *a* — welding with simple beads; *b* — welding with first bead grinding

ing area). It should be noted that such position of TC was acceptable for control of approximate temperature in the sample before deposition of the next beads. In the latter variant, deposition of the new beads was accompanied with gradual increase of temperature in the joint that to some extent reconstruct the conditions similar to «transverse hill» welding.

The results of tests of the welded joints produced with preheating as well as without heating (Figure 4) show that reheating of HAZ metal in the area of the first bead results in increase of cold cracking resistance. Effect of deposition of two or more beads on the first weld (schemes 1 + 2, 1 + 2 + 2, etc.) is highly obvious. Deposition of only one bead (for example, schemes 1 + 1 and 1/2 + 1 (Figure 4, *a, b*) in welding without heating, and 1 + 1 in welding with heating (Figure 4, *c*) is less effective.

Efficiency of reheating, influencing the technological strength, can be judged based on the results of measurements of hardness in hardening area in the first bead by the example of 1 + 2 scheme, i.e. in the initial state the maximum value of hardness made *HV* 460, after deposition of one bead — *HV* 430, after deposition of the second bead — *HV* 360.

Increase of welding current in performance of temper beads also had positive effect on rise of cracking resistance due to larger heat input into the welded joint (see test results in welding on 1/2 + 2 scheme with  $I_w = 130$  A in comparison with the same variant performed on 100 A current, which was used in all experiments (Figure 4, *b*). However, as it was mentioned above, it is reasonable to limit growth of current.

Quantitative rise of cracking resistance can be evaluated by relationship of  $\sigma_{cr}$  values for one of the technological variants to  $\sigma_{cr}$  of initial variant – welding with single bead. Thus, for example, (see Figure 4, *a*) in welding on 1 + 2, 1 + 2 + 2 and 1 + 2 + 5 schemes the delayed fracture resistance increased approximately 2.3 and 4.7 times, respectively.

As can be seen from Figure 5, reheating in welding without preheating on schemes 1 + 2 + 2 and 1 + 2 + 5 allows reaching cracking resistance, close to welding with heating to 220 and 250 °C order. Reheating on

scheme 1 + 2 creates an effect close to welding with heating around 150 °C. The effect becomes more significant when using preheating.

It was experimentally determined that efficiency of tempering influence depends on welding modes and level of overlapping of the first and deposited beads. As an example, Figure 6 shows the schemes illustrating distribution of the maximum temperatures in the near-weld zone in deposition of a new bead on the earlier performed. The test material was martensite steel 0.1C9CrMoVNb of 14 mm thickness, depo-

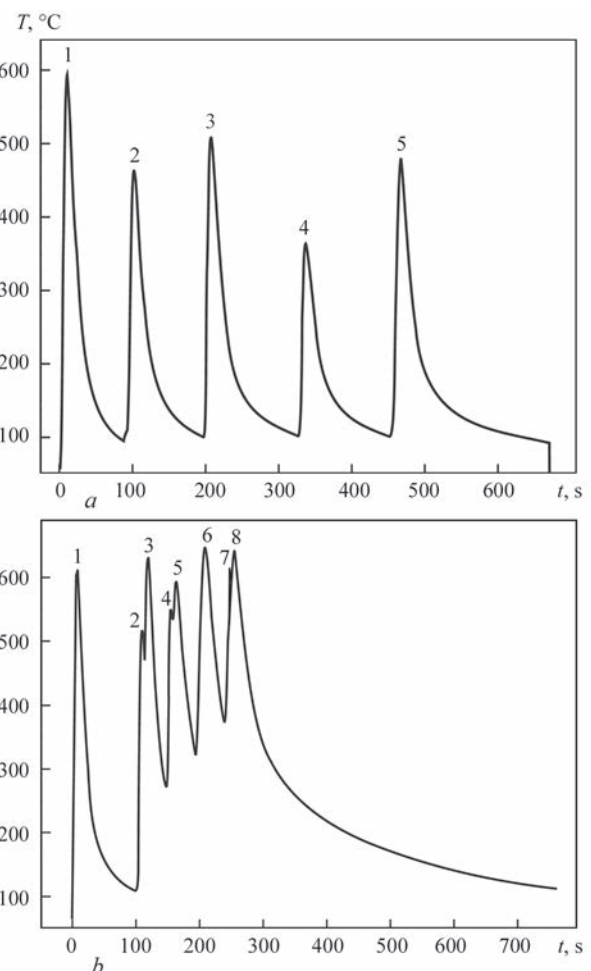


**Figure 3.** Thermal cycles in place of TC welding to sample in performance of test joints on 1 + 2 + 2 beads scheme (*a*) and on 1 + 2 + 5 beads scheme using principle of «transverse hill» welding (*b*)

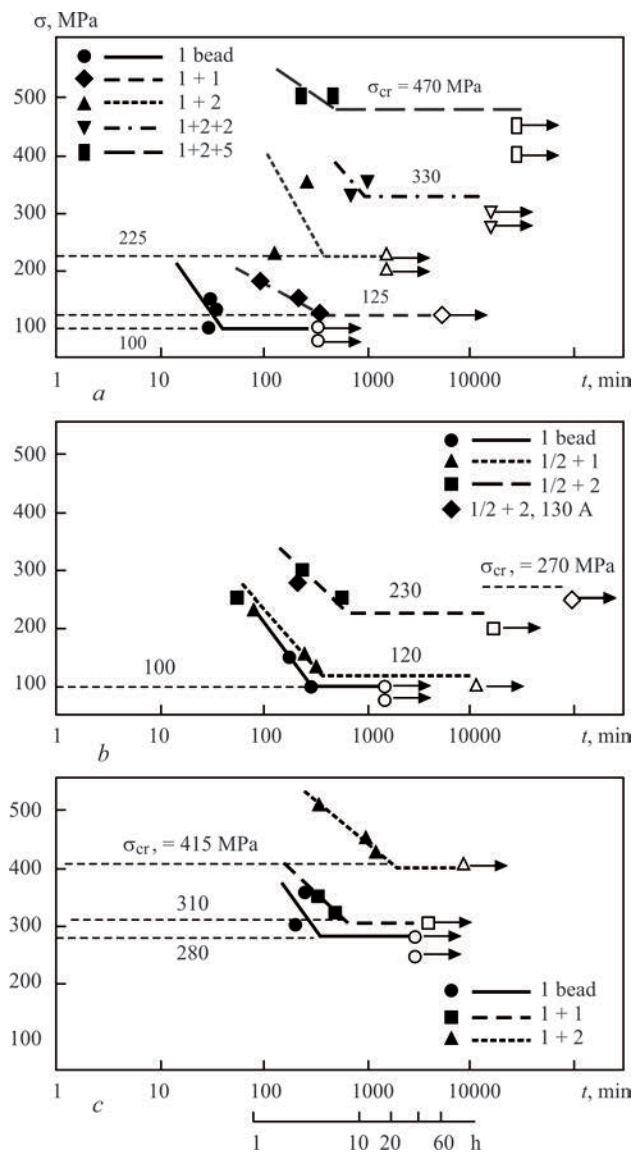


**Figure 4.** Results of tests: *a* — welding without heating with simple bead; *b* — welding without heating with grinding of the first bead for 1/2 of its thickness; *c* — welding with 200 °C preheating (dark and light marks — joints with and without fractures)

sition of beads was carried out using MAW with electrodes of similar alloying system of 3.2 mm diameter at two modes with 200 °C heating. There were used the results of determination of maximum heating temperatures at different depth from steel surface in deposition of the single bead as well as real dimensions of bead and hardening area, measured in cross-sections. In this case, record of thermal cycles was carried out simultaneous with two TC, passed through from below into the holes, drilled across the plate thickness to different distance from assumed fusion line and located with displacement one from another. Bead-on-plate deposition was carried out along the line of TC location. As it is shown on Figure 6, *a, b*, deposition of the second bead on the first creates a new hardening area of metal (in HAZ 2) being heated over  $A_{c1}-A_{c3}$  interval temperature. Temperatures below  $A_{c1}$  promote partial tempering of metal, hardened in per-

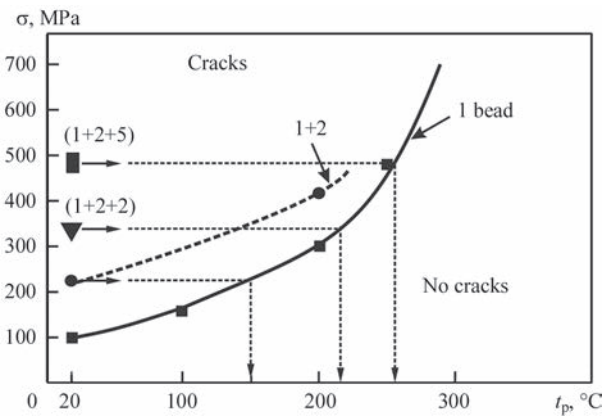


**Figure 5.** Comparison of the test results in welding with reheating without preheating ( $t_p = 20$  °C) and welding with preheating ( $t_p$  — temperature of preheating)

formance of the first bead. Such a situation will take place in deposition of the second bead in the zenith of the first (on scheme 1 + 1). In this case tempering will affect the biggest part of hardened metal in HAZ 1 in the first bead. When grinding the first bead to half thickness (scheme 1/2 + 1, Figure 6, *c*) area of hardening of the second bead will «make layers» on the bigger part of hardened metal from the first bead (HAZ 1). Lower part of hardened metal in HAZ 1 will be subjected to tempering. Probably, this is the reason why insufficient tempering effect had small influence on  $\sigma_{cr}$  increase on Figure 4, *b*. Similar situation with overlaying of the second and first hardening areas can take place in welding with simple bead, but at deposition of the second bead at higher current (Figure 6, *d*). In this case, a favorable factor, from point of view of heat effect on hardened metal, is input of larger amount of heat into the welding zone.

Also it was interesting to evaluate the effect of reheating on amount of diffusion hydrogen remaining in the metal. The pencil probes [11], deposited with TML-5 electrodes (alloying of 06Kh1M type) in a condition after long-term storage without baking, were used in the experiments carried for this purpose. The probes after deposition were cooled in water for registration of initial concentration of diffusion hydrogen, then their reheating using gas flame and alcohol analysis were carried out. Temperature was controlled by pyrometer. In high-temperature heating (500 °C and more) immediately after reaching the necessary temperature the metal was cooled in water, in heating to 300 °C it was cooled in air to 100 °C and then in water. At combined cycles the initial probe was heated to higher temperature, firstly cooled in air to approximately 100 °C, then in water, after that the probe was heated to the next temperature with the same gradual cooling (air/water). At 200 °C longer furnace heating was also carried out for simulation of the conditions of postweld cooling down. Using TC, fastened in the middle of thickness of the pencil probe, there was car-

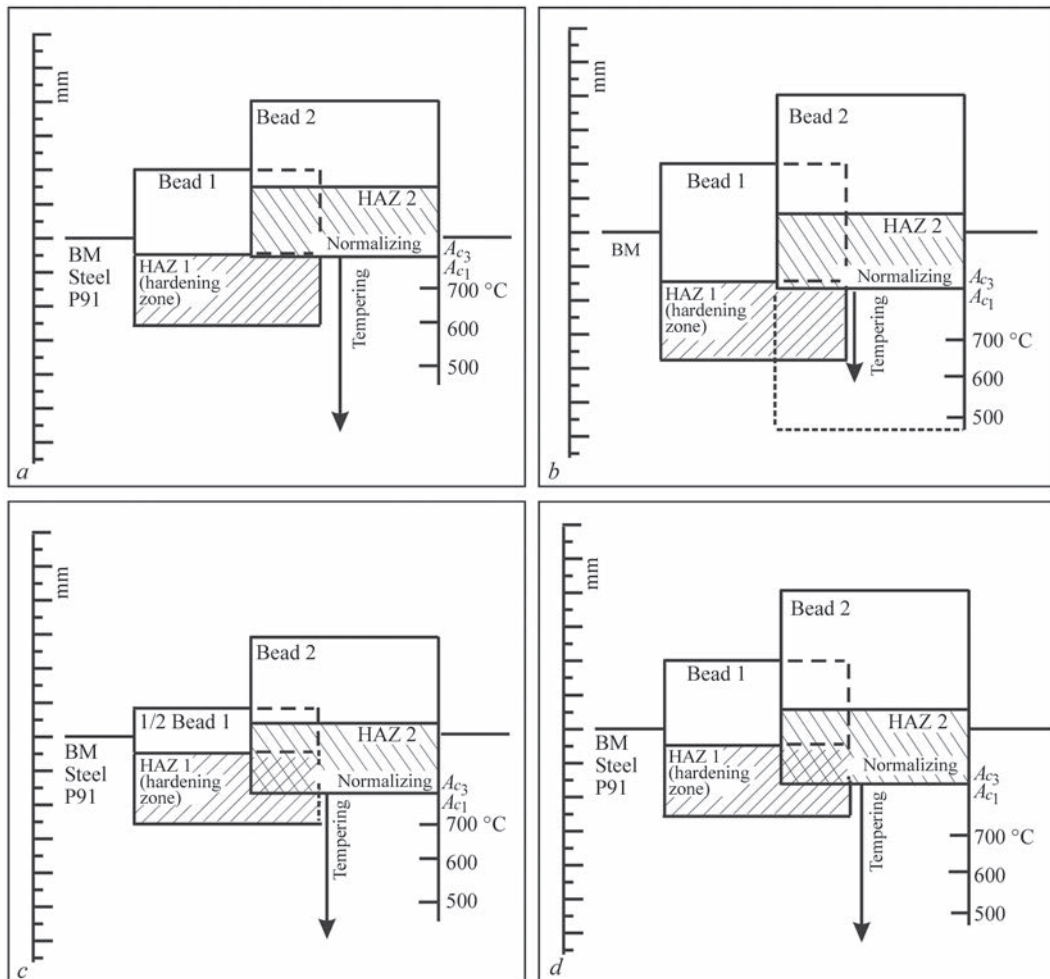


**Figure 6.** Distribution of temperatures in near-weld zone in performance of two beads (*a, b* — conventional welding: *a* —  $I_w = 100$  A,  $q/v = 8.3$  kJ/cm; *b* —  $I_w = 160$  A,  $q/v = 11.38$  kJ/cm; *c* — welding with first bead grinding,  $I_w = 100$  A; *d* — welding with simple bead, first bead is made on current  $I_w = 100$  A; second — 160 A)

ried out an evaluation of time of gas heating to 1000, 500, 300, 200 and 100 °C temperatures, which made, respectively, 15; 5.5; 2.9; 2 and 1.3 s. Duration of probe cooling in smooth air in 300–100, 200–100 °C intervals made 300 and 200 s. At the same time HAZ of Implant samples demonstrates quicker drop of the temperature in the indicated intervals, on average 2.3 and 3 times more, nevertheless the durations of heating to 500 °C were close. Considering the available differences in the thermal cycles with real welded samples, it can be assumed that the experimental approach allows only tracing the tendency of change of diffusion hydrogen content in the reheatings.

**Effect of reheating on emission of diffusion hydrogen  $[H]_{diff}$ , cm<sup>3</sup>/100 g Me) from deposited metal (pencil probes)**

initial state (after deposition) . . . . .	7.55–5.37
1000 °C . . . . .	~0.2
700 °C . . . . .	~0.2
500 °C . . . . .	~0.7
300 °C . . . . .	0.96
200 °C . . . . .	2.26
500 °C + 300 °C. . . . .	~0.2
300 °C + 200 °C. . . . .	0.26
200 °C, 20 min . . . . .	0

The results showed that at short-term high-temperature effect the concentration of diffusion hydrogen reduces by order and more. Heating to 200–300 °C results in 2–3 times decrease of  $[H]_{diff}$ . At combined cycles the concentration  $[H]_{diff}$  also reduces for more than order. Cooling down is the most efficient; similar effect will, probably, take place in welding with preheating.

Summing up the set forth material, it is noted that cold cracks are the consequence of critical combination of three factors in their specific quantitative expression (Figure 7, *a*): welding stresses, in MPa, created by shrinkage, are determined with the help of special procedures, under Implant test conditions they are set by tension force of the sample in the joint; condition of hardening structure can be evaluated by hardness value, hydrogen factor is usually evaluated on amount of diffusion hydrogen in the probes of the deposited metal or in the samples of the welded joint. Weakening of effect of one or several of them results in appearance of «reserve» in cracking resistance (that, as an example, on scheme of Figure 7, *b* is symbolized by white sector as a result of weakening of a negative role of the structural factor). High tem-

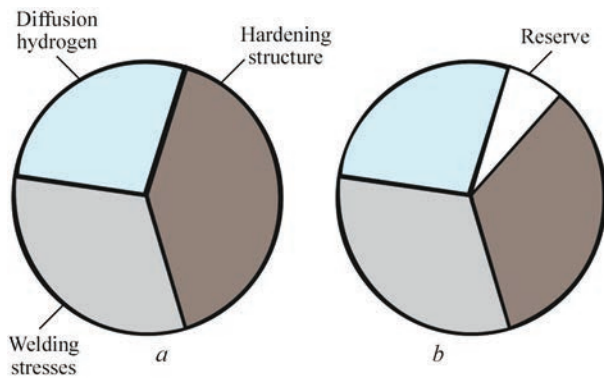


**Figure 7.** Factors, promoting delayed fracture of welded joints (*a* — critical state; *b* — state with reserve of cracking resistance)

pering of welded joints can be assumed an extreme measure for reaching high crack resistance that leads to relaxation of the residual stresses, maximum decrease of hydrogen content and transfer of hardened metal in a state close to equilibrium one, being characterized with improved ductility. As it is shown in present work, reheating of metal in the area of earlier performed passes develops a positive effect under conditions of multipass welding. The consequence is improvement of structural state of metal and, probably, reduction to some level of diffusion hydrogen concentration in the hardening zone in the area of earlier performed passes as a result of its diffusion redistribution and scattering.

## Conclusions

1. By the example of tests on Implant method using the samples of hardening heat-resistant 25Kh2NMFA steel it is shown that under conditions of manual arc welding with coated electrodes welding reheating allows significantly increasing the delayed fracture resistance of the hardened metal in the area of earlier made passes. Effect is revealed in welding without preheating as well as with heating.

It was experimentally demonstrated that the critical stresses promoting crack formation depending on number of cycles of repeated thermal effect at deposition of new layers of tempering beads can be increased approximately 2–4 times. At that welding without preheating can provide cracking resistance equivalent to resistance in welding with heating to 150–250 °C.

2. The results of carried experiments allow assuming that welding reheating in multipass welding simultaneously effects two factors influencing delayed fracture, namely structural, creating partial tempering of hardened layers in the area of earlier performed passes, and hydrogen, promoting reduction of diffusion hydrogen concentration in them.

1. Tsaryuk, A.K., Brednev, V.I. (1996) Problem of prevention of cold cracks. *Avtomatich. Svarka*, **1**, 36–40 [in Russian].
2. Kasatkin, O.G. (1994) Peculiarities of hydrogen embrittlement of high-strength steels in welding. *Ibid.*, **1**, 3–7 [in Russian].
3. Sawhill, J.M., Dix, A.W., Savage, W.F. (1974) Modified Implant test for studying delayed cracking. *Welding J.*, **12**, 554-s–560-s.
4. Lippold, J.C. (2015) *Welding metallurgy and weldability*. USA, John Wiley & Sons, Inc.
5. Brednev, V.I., Kasatkin, B.S. (1988) Specific work of formation of cold crack centers in welding of low-alloy high-strength steels. *Avtomatich. Svarka*, **11**, 6–11 [in Russian].
6. Makara, A.M., Mosendz, N.A. (1971) Welding of high-strength steels. Kiev, Tekhnika [in Russian].
7. Snisar, V.V., Demchenko, E.L. (1990) Prevention of cold cracks in welded joints of high-strength steel 15Kh2N4MDA with austenite-martensite weld. *Avtomatich. Svarka*, **2**, 24–27 [in Russian].
8. Kurdyumov, G.V., Utevsky, L.M., Entin, R.I. (1977) *Transformations in iron and steel*. Moscow, Nauka [in Russian].
9. Gulyaev, A.P. (1978) *Metals science*. Moscow, Metallurgiya [in Russian].
10. Skulsky, V.Yu. (2009) Peculiarities of kinetics of delayed fracture of welded joints of hardening steels. *The Paton Welding J.*, **7**, 12–17.
11. Kozlov, R.A. (1986) *Welding of heat-resistant steels*. Leningrad, Mashinostroenie [in Russian].
12. Burashenko, I.A., Zvezdin, Yu.I., Tsukanov, V.V. (1981) Substantiation of preheating temperature in welding of chromium-nickel-molybdenum steels of martensite class. *Avtomatich. Svarka*, **11**, 16–20 [in Russian].
13. Skulsky, V.Yu., Tsaryuk, A.K., Vasiliev, V.G., Strizhius, G.N. (2003) Structural transformations and weldability of hardening high-strength steel 20KhN4FA. *The Paton Welding J.*, **2**, 27–21.
14. Sinadsky, S.E. (1967) *Method of multipass welding*. Author's cert. 202383. *Byulleten Izobretenij*, **19**, 4.09.1967 [in Russian].
15. Novikov, I.I. (1971) *Theory of heat treatment*. Moscow, Metallurgiya [in Russian].
16. Novikova, D.P., Bogachek, Yu.L., Semenov, S.E. et al. (1976) Influence of cooling and deformation on impact toughness of weld metal in welding of high-strength steel joints. *Avtomatich. Svarka*, **10**, 21–23 [in Russian].
17. Metting, G.F., Hausen, T. (2014) Welche stähle wie Schweissen? *Der Praktiker*, **4**, 142–147 [in German].
18. Irvin, A.B. (1991) Promising chrome-moly steel returns to American shores. *Welding J.*, **12**, 35–40.
19. Zeman, M., Blacha, S. (2014) Spawalne martenzytyczne stale zarowitrymale nowej generacji. *Przegląd Spawalnictwa*, **4**, 51–61 [in Polish].
20. Hoizer, G. (1977) Filler materials for welding power machine building. *Avtomatich. Svarka*, **9**, 40–44, 47 [in Russian].
21. Herold, H., Krebs, S., Arjakin, N. (2002) New methods of orbital welding — a contribution towards joinability of new materials. In: *Proc. of Int. Conf. on Welding — Quality — Competitiveness* (October 23–24, 2002, Moscow).
22. Wang, Y., Lundin, C.D., Qiao, C.Y.P. et al. (2005) Halfbead temper-bead controlled deposition techniques for improvement of fabrication and service performance of Cr–Mo steels. *WRC, Bulletin*, **506**.

Received 14.01.2019

# STRENGTH OF WELDED JOINTS OF HEAT-HARDENABLE ALUMINIUM ALLOYS IN TIG AND FRICTION STIR WELDING

A.G. POKLYATSKY and S.I. MOTRUNICH

E.O. Paton Electric Welding Institute of the NAS of Ukraine  
11 Kazimir Malevich Str., 03150, Kyiv, Ukraine. E-mail: [office@paton.kiev.ua](mailto:office@paton.kiev.ua)

Influence of zirconium and scandium modifiers in the filler wire and of arc oscillations due to electric current flowing through the filler section in nonconsumable electrode argon-arc welding, as well as of friction stir welding process on formation of weld structure in sheet aluminium alloys 1460 and 1201, was studied. Curves of metal hardness distribution in the zone of permanent joint formation were plotted, and ultimate strength of samples was determined directly after welding and after their artificial ageing. It is shown that application of friction stir welding yields higher values of ultimate strength of the metal of welds and welded joints on aluminium alloys 1460 and 1201, than in automatic non-consumable electrode argon-arc welding with weld pool oscillations, even at application of welding wire with zirconium and scandium. Here, the maximum strength level (75 % for alloy 1201 and 86 % for alloy 1460), compared to base material, is achieved after artificial ageing of samples, at which phase transformations and processes of stabilization of the structure of metal after thermal impact, take place. 16 Ref., 1 Table, 4 Figures.

**Keywords:** heat-hardenable aluminium alloy, argon-arc welding with arc oscillations, friction stir welding, micro-structure, hardness, strength

In fabrication of structures from aluminium alloys, permanent joints are produced by fusion welding in most of the cases, where weld formation occurs as a result of melting of the edges being welded and welding wire with their subsequent crystallization [1–3]. Metal of such a weld has a cast, usually coarse-crystalline structure. Moreover, high-temperature heating of the blanks being welded leads to surface melting of grain boundaries and partial precipitation of secondary phases and eutectics along them in the zone of weld fusion with the base material. As a result the ultimate strength of welded joints is equal to 60–70 % for most of the heat-hardenable alloys, whereas the weld metal ultimate strength is equal to just 50–60 % of this value for base material [4].

Therefore, measures which are aimed at creating conditions for formation of a disoriented fine-crystalline structure of the welds and lowering of metal heating temperature in the zone of permanent joint formation, can be effective for increasing the strength of welds and welded joints as a whole. Among the known widely applied methods of influencing the crystallization processes in the weld pool, an important place is taken by application of zirconium as modifier of the 1st kind in the welding wire. It has a structure isomorphous to the crystallizing alloy, and acts as forced crystallization centers. Over the recent years, scandium, a modifier of the 2<sup>nd</sup> kind, has been used additionally. It creates favourable conditions for initiation and growth of new crystallization centers due

to formation of Al<sub>3</sub>Sc phase, having dimensional and structural similarity with aluminium crystalline lattice [5–7]. Moreover, microadditives of this element to aluminium alloys promote their hardening after artificial ageing, stabilizing the structural components of base material and weld metal exposed to thermal impact [8–10].

The nature of metal crystallization during welding can be changed also due to abrupt oscillations of weld pool melt, which are due to periodical change of the force impact of the arc as a result of welding current pulsations or arc deviation from its vertical position [11–13]. Such oscillations of molten metal lead to disturbance of the continuity of formation of extended oriented crystals as a result of melting of second-order axes and increase of activity of crystallization centers due to periodical change of crystallizing metal temperature.

An essential lowering of metal heating temperature in the zone of permanent joint formation can be achieved at application of one of the new methods of solid-phase welding — friction stir welding (FSW) [14]. Weld formation here occurs due to heating through friction by a special tool of a certain volume of the materials being joined in their contact zone to a plastic state and its stirring in a closed space that allows avoiding the problems of high-temperature heating, melting and crystallization of metal. Intensive plastic deformation of metal at FSW promotes formation of an ultradispersed structure in the weld nugget, and of long, extended along the metal movement path

and fine recrystallized grains in the adjacent thermo-mechanical impact zone (TMIZ) [15].

The research objective was to study the influence of zirconium and scandium modifiers in the filler wire and arc oscillations, due to passage of electric current through the filler section in nonconsumable electrode argon-arc welding, as well as FSW process on formation of the structure of welds, metal softening and ultimate strength of butt joints of sheet aluminium alloys 1201 and 1460 directly after welding and after artificial ageing of the samples.

**Experimental procedure.** Automatic nonconsumable electrode argon-arc welding (automatic TIG) of aluminium alloys 1201 (wt.%: 6.3 Cu; 0.3 Mn; 0.06 Ti; 0.17 Zr; 0.1 V; bal. being Al) and 1460 (wt.%: 3.0 Cu; 2.0 Li; 0.1 Mg; 0.12 Ti; 0.008 Sc; bal. being Al) 2 mm thick was performed at square wave alternating current of 200 Hz frequency with welding head ASTV-2m. MW-450 (Fronius, Austria) was used as the power source of the welding arc. Welding speed was 20 m/h; welding current was 170 A, and feed rate of 1.6 mm welding wire was 82 m/h. Batch-produced welding wire Sv1201(Al-6 % Cu-0.1 % Ti-0.3 % Mn-0.2 % Zr) and experimental welding wire Sv1201Sc of the same composition, but additionally containing 0.5 % Sc were used in welding. In order to induce arc oscillations, arising as a result of interaction of electromagnetic fields, generated at current flowing through the arc gap and filler wire [13], direct current (200 A) from power source TR-200 (Fronius, Austria) was passed through filler wire section 25 mm long directly before it entered the head part of the weld pool. Continuous variation of the arc force impact due to its deviation from the vertical position results in oscillations of weld pool molten metal, which disturb the continuity of its crystallization, and formation of a fine-crystalline structure of the welds. It should be noted that standard automatic TIG welding was not used for alloy 1460 in order to assess the ultimate strength of the welded joints, as extended oxide film inclusions form in the welds, while current passage through the filler wire section allows avoiding these defects.

FSW process was conducted in a laboratory unit developed at PWI. Speed of rotation of a special welding tool with a conical tip and 12 mm dia shoulder was 1420 rpm, and the speed of its linear displacement (welding speed) was 14 m/h. Before welding the sheet blanks were treated by chemical etching by the conventional technology. Mechanical scraping of just the end faces of the edges to be welded was performed for FSW, and for automatic TIG welding also the surface layers 0.10–0.15 mm thick were removed to avoid porosity in the welded joints.

Metal hardness was measured on the face surfaces of the produced welded joints. Degree of metal softening in the welding zone was assessed in Rockwell instrument at  $P = 600$  N load. Evaluation of structural features of welded joints was performed using optical electron microscope MIM-8. Ultimate strength of welded joints produced by automatic TIG welding was determined at static tension in a universal servo-hydraulic system MTS 318.25, of standard flat samples with 15 mm width of the test portion and with reinforcement and removed weld back bead, while weld metal ultimate strength was measured on samples with removed weld reinforcement and back bead. Samples produced by FSW, were tested without reinforcement and back bead, as such a shape of the weld is due to the features of the process of producing permanent joints. To assess the effect of heat treatment on strength properties of welded joints, standard artificial ageing of samples of alloy 1201 was performed at the temperature of 170 °C for 17 h, and those of alloy 1460 were aged at the temperature of 130 °C for 20 h, and then at the temperature of 160 °C for 16 h.

**Research results and discussion.** As a result of the performed research it was found that in conventional automatic TIG welding of the studied aluminium alloys 1201 and 1460 the weld metal develops a fine dendritic structure with individual elements of the central crystallite, which form large crystals in some sections of the weld central part (Figure 1, *a*). Application of filler wire, containing zirconium and scandium, leads to refinement of weld metal crystalline structure due to partial formation of a subdendritic shape of the crystallites (Figure 1, *b*). Here, it is not possible to form a subdendritic structure of the crystallites over the entire volume of the weld. This is, apparently, attributable to the fact that in welding of sheet joints, when the share of filler wire in the weld is small, a sufficient (0.3–0.4 % [16]) concentration of scandium in the weld metal cannot be achieved. However, owing to weld pool molten metal oscillations, arising as a result of the arc deviation from its vertical position due to electric current passing through a section of filler wire Sv1201Sc, periodical melting of the crystallizing dendrites occurs during crystallization, that ensures formation of fine equiaxed crystals over the entire weld section (Figure 1, *c*).

However, the finest structure of weld metal forms at FSW as a result of intensive plastic deformation of metal in the zone of permanent joint formation. Figure 2 shows very well how grain refinement occurs on the surface of the metal being welded at the edge of the tool shoulder on the boundary of HAZ (left) and TMIZ (right). An abrupt grain refinement occurs in the sections of the weld and TMIZ directly subjected

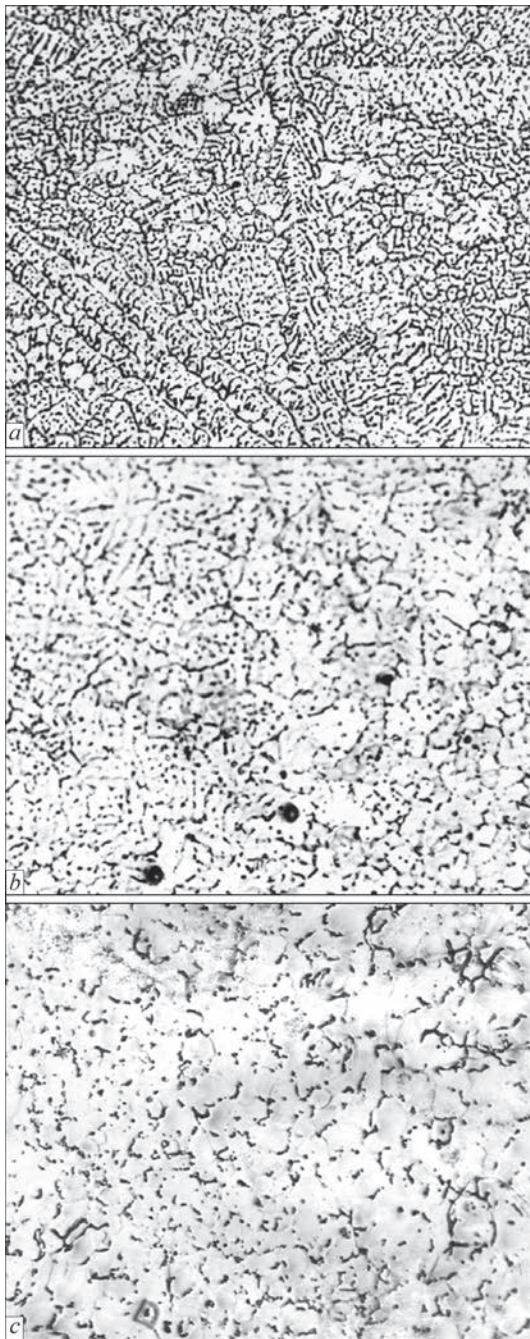


**Figure 1.** Microstructure ( $\times 200$ ) of welds, made by nonconsumable electrode argon-arc welding of 2 mm sheets of alloy 1460 with application of filler wires Sv1201 (*a*) and Sv1201Sc (*b*), as well as arc oscillations, arising at current passing through the section of filler wire Sv1201Sc (*c*)

to the impact of the tool working surfaces (side surfaces of the tip and shoulder end face). Analysis of the transverse microstructure of joints produced by FSW showed that a nugget with finely-dispersed ( $3\text{--}5\ \mu\text{m}$ ) structure forms in the weld central part developing as a result of displacement of plasticized metal by the tool working surfaces. As the grain size is 5–7 times smaller than that in the base material, the volume fraction of their boundaries increases significantly (Figure 3). Here, deformed extended grains oriented in the direction of displacement of plasticized metal by the

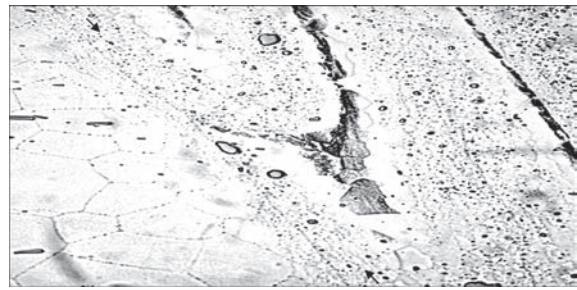


**Figure 2.** Microstructure ( $\times 500$ ) of the surface of FSW joint of 2 mm alloy 1201

tool working surfaces, and fine-equiaxed grains, the size of which varies within  $5\text{ to }10\ \mu\text{m}$  are observed in TMIZ. On the other hand, at conventional automatic TIG welding of these alloys using filler wire Sv1201 the weld forms a characteristic cast structure with dendrite dimensions of  $0.15\text{--}0.20\ \text{mm}$ . Moreover, high-temperature heating of the edges being welded near the weld causes melting of structural components of the grain boundaries. This results in formation of a coarse continuous network of fine-grained interlayers in the section adjacent to the weld metal. Such structural transformations in the metal in the zone of permanent joint formation lead to a change of metal hardness and its strength.

Measurements of metal hardness on samples of FSW joints showed that it is much higher than in samples produced by automatic TIG welding. Such welded joints of alloy 1460 have metal hardness in the weld and zone of its transition to base material (at about 1.5 mm distance from weld axis) on the level of *HRB* 90, and minimum hardness *HRB* 88–89 at about 5.8 mm distance from weld axis on TMIZ and HAZ boundary (Figure 4, *a*). On the other hand, in automatic TIG welding of this alloy even with application of filler wire Sv1201Sc and arc oscillations, metal hardness in the weld central part is equal to just *HRB* 69, and in the zone of weld fusion with base material (at about 3.3 mm distance) it is *HRB* 76–77.

In FSW of alloy 1201 metal hardness in the weld central part is on the level of *HRB* 82, in the zone of weld transition to base material it is *HRB* 81, and on the boundary of TMIZ and HAZ it is *HRB* 95–96 (Figure 4, *b*). Joints produced by automatic TIG welding with application of scandium-containing filler wire and arc oscillations, have weld metal hardness on the level of *HRB* 71, and in the zone of its fusion with base material it is *HRB* 73–74.

Metal softening in zone of permanent joint formation in welding of these heat-hardenable alloys occurs not only due to structural transformations, but also as a result of partial decomposition of the solid solution and coagulation of particles of the main alloying elements in zones, subjected to heating even

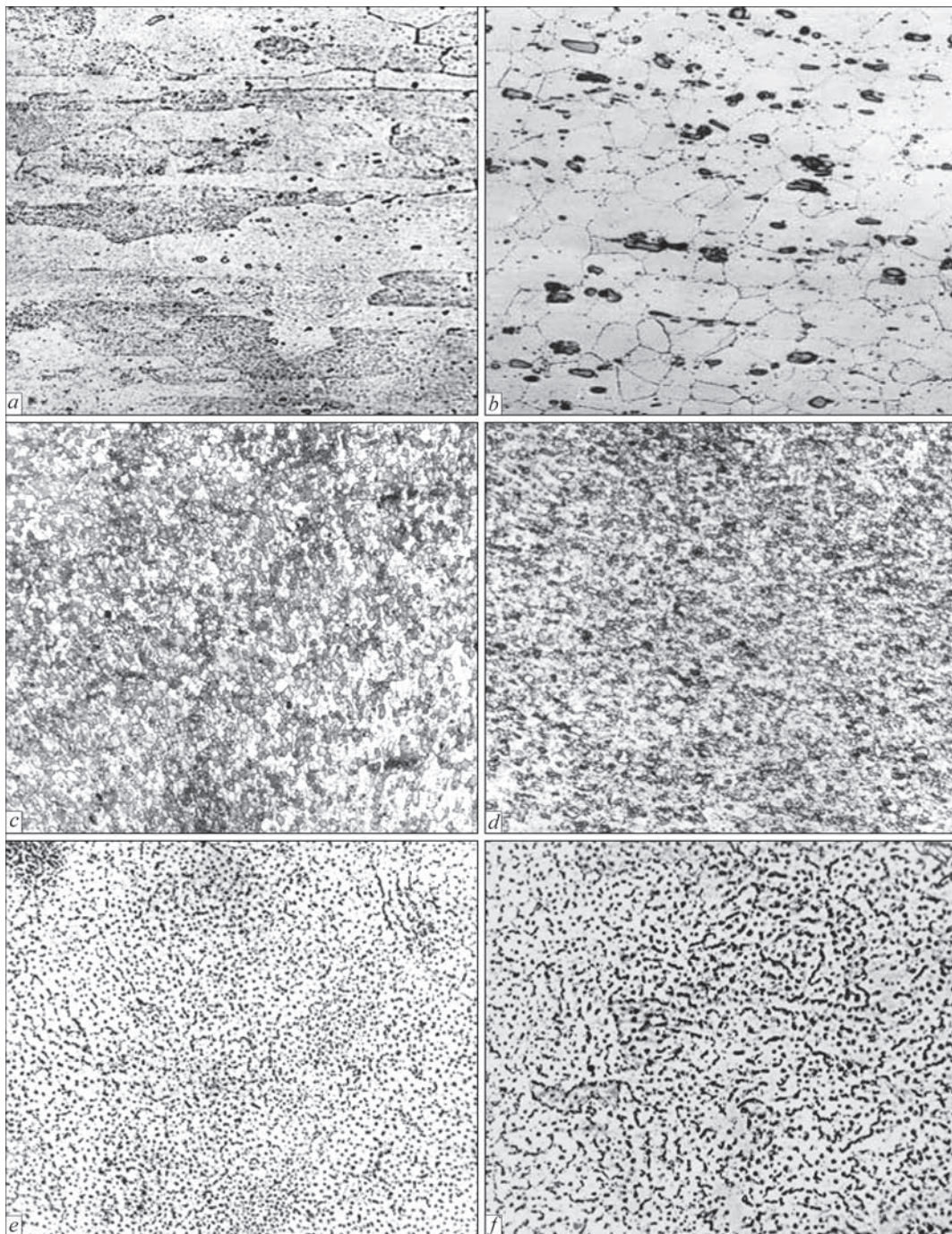


**Figure 3.** Microstructure ( $\times 400$ ) of base metal (*a, b*) and welds (*c–f*) produced at FSW (*c, d*) and automatic TIG welding (*e, f*) of 2 mm alloys 1460 (*a, c, d*) and 1201 (*b, d, f*)

in FSW process. Therefore, heat treatment (HT) is used for their welded joints, if required. It involves artificial ageing, resulting in metal hardening due to phase transformations and metal structure stabilization. Analysis of metal hardness distribution in FSW joints of alloy 1460 after artificial ageing of the samples (see Figure 4, *a*), showed that metal hardness in the weld and in the zone of its transition to base material increased up to *HRB* 104. Here, the same hardness level is observed right up to the boundary of TMIZ and HAZ, where it decreases to *HRB* 100, and then smoothly increases up to base material hardness level

(*HRB* 108–109). In welded joints produced by automatic TIG welding with filler wire Sv1201Sc, through a section of which electric current was passed to induce arc oscillations, increase of metal hardness also occurred after heat treatment. However, it increased just to *HRB* 80 in the weld central part, and up to *HRB* 90–91 in the zone of fusion of the weld with base material.

Such changes of metal hardness after artificial ageing of the samples are observed also in welded joints of 1201 alloy (see Figure 4, *b*). In FSW weld, metal hardness increases up to *HRB* 86, and in the

zone of its transition to base material it increases up to *HRB* 85. On the other hand, at automatic TIG welding weld metal hardness increases just to *HRB* 77, and in the zone of its fusion with base material — up to *HRB* 81–82.

Nature of metal hardness distribution in the zone of permanent joint formation allows finding the weakest regions, in which fractures are the most probable at mechanical testing of the samples. So, at static tension of samples without weld back bead and reinforcement, produced at automatic TIG welding of alloy 1460 with filler wire Sv1201Sc and arc oscillations, their fracture occurs across the weld metal, where metal hardness is minimal. Their ultimate strength is on the level of 265 MPa (Table). Similar samples with weld reinforcement fail in the zone of weld fusion with the base material and their ultimate strength is about 285 MPa. Here, FSW joints have the highest ultimate strength (345 MPa). Samples of such joints without either weld back bead or reinforcement (owing to the features of this welding process), fail on the boundary of TMIZ and HAZ from the tool retreating side.

Postweld heat treatment allowed increasing the weld metal ultimate strength up to 275 MPa, and welded joint ultimate strength — up to 300 MPa. However, artificial ageing has the maximum effect on FSW joints. Their ultimate strength rises up to

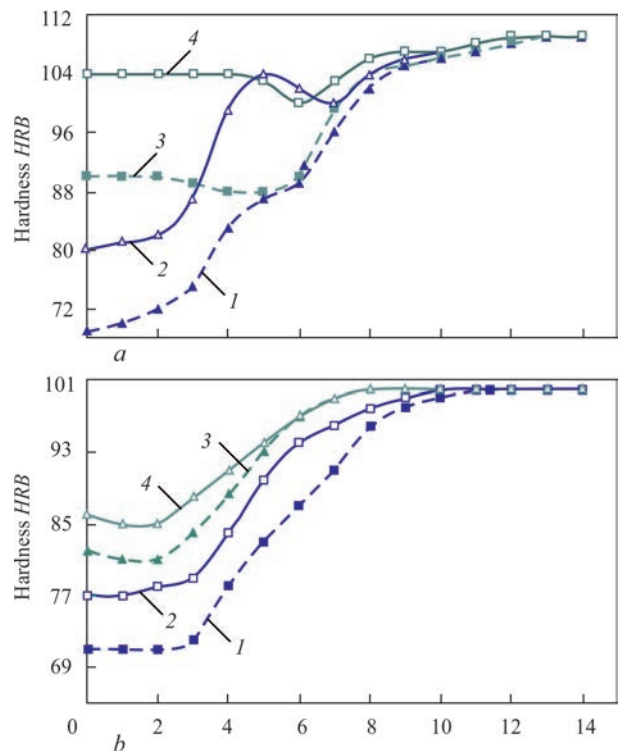


**Figure 4.** Hardness distribution in welded joints of 2 mm alloys 1460 (a) and 1201 (b) produced by automatic TIG welding with arc oscillations with application of filler wire Sv1201Sc and by FSW, directly after welding and after heat treatment of the samples: 1 — Sv1201Sc; 2 — Sv1201Sc (HT); 3 — FSW; 4 — FSW (HT)

Ultimate strength of butt joints of 2 mm aluminium alloys 1460 and 1201 produced by FSW and automatic TIG welding

Alloy	Welding process	Condition	Filler wire	Ultimate strength $\sigma$ , MPa	
				Samples without back bead with weld reinforcement	Samples without back and without weld reinforcement
1460	FSW	After welding	—	—	339–348 345
		After HT	—	—	416–424 420
	Automatic TIG welding with arc oscillations	After welding	Sv1201Sc	283–289 285	262–270 265
		After HT		295–309 300	269–279 275
1201	FSW	After welding	—	305–315 310	
		After HT	—	318–323 320	
	Automatic TIG welding	After welding	Sv1201	274–277 275	232–237 235
		After HT		303–315 307	259–264 261
	Automatic TIG welding with arc oscillations	After welding	Sv1201Sc	287–296 290	240–252 245
		After HT		310–317 315	265–277 270

*Note.* The numerator gives the maximum values of the parameter; and the denominator — its average values by the results of testing three — five samples.

420 MPa, that is equal to 86 % of ultimate strength for base material. Here the sample fracture location remains unchanged, as metal hardness in the zone of welded joint formation, increases, but the nature of its distribution practically does not change — regions of minimum metal hardness remain after artificial ageing in the same locations as immediately after welding.

Samples of welded joints of alloy 1201 produced by FSW, fail under static tension in TMZ in the region of weld transition to base material. Here, their ultimate strength is on the level of 310 MPa, directly after welding and on the level of 320 MPa after artificial ageing. Fracture of samples with weld reinforcement produced by automatic TIG welding with filler wire Sv1201Sc and arc oscillations, runs in the zone of weld fusion with base material. Their ultimate strength directly after welding is equal to 290 MPa, and after heat treatment it is 315 MPa. After removal of weld reinforcement the site of sample fracture at their tension becomes the weld metal, the ultimate strength of which is on the level of 245 MPa after welding and 270 MPa after artificial ageing.

### Conclusions

1. Application of welding wire Sv1201Sc, containing 0.2 % Zr and 0.5 % Sc, in nonconsumable electrode argon-arc welding of aluminium alloys 1460 and 1201 with arc oscillations, due to its deviations from the vertical position as a result of electric current passage through the filler section, ensures formation of fine equiaxed crystals over the entire section of the weld. However, at FSW, intensive plastic deformation of metal in the zone of permanent joint formation results in development of the finest (3–5  $\mu\text{m}$ ) structure in the weld.

2. Formation of a permanent joint in the solid phase without melting of the edges being welded and of fine structure of welds at FSW allows achieving higher values of ultimate strength of the metal of welds and welded joints of aluminium alloys 1460 and 1201, than at automatic TIG welding with welding pool oscillations, even with application of welding wire containing zirconium and scandium.

3. Artificial ageing of welded joints, when phase transformations and processes of stabilization of the structure of metal subjected to thermal impact take place, promotes their strengthening. Here, the maximum level of strength (75 % for alloy 1201 and

86 % for 1460 alloy), compared to base material, is achieved after such heat treatment of FSW samples.

1. Ishchenko, A.Ya., Labur, T.M. (2013) *Welding of modern structures of aluminium alloys*. Kiev, SPE NASU [in Russian].
2. Beletsky, V.M., Krivov, G.A. (2005) *Aluminium alloys (composition, properties, technology, application): Refer. Book*. Ed. by I.N. Fridlyander. Kiev, COMINTEX [in Russian].
3. Ishchenko, A.Ya., Labur, T.M., Bernadsky, V.N., Makovetskaia, O.K. (2006) *Aluminium and its alloys in modern welded structures*. Kiev, Ekotekhnologiya [in Russian].
4. Mashin, V.S., Poklyatsky, A.G., Fedorchuk, V.E. (2005) Mechanical properties of aluminium alloys in consumable and nonconsumable electrode arc welding. *The Paton Welding J.*, **9**, 39–45.
5. Lukin, V.I. (1996) Sc is the promising alloying element for filler materials. *Svarochn. Proizvodstvo*, **6**, 13–14 [in Russian].
6. Ishchenko, A.Ya. (2003) Aluminium high-strength alloys for welded structures. Vol. 1: *Advanced materials and technologies*. Kyiv, Akadempriodyka, 50–82 [in Russian].
7. Davydov, V.G., Elagin, V.I., Zakharov, V.V., Rostova, T.D. (1996) On alloying of aluminium alloys with additions of scandium and zirconium. *Metallovedenie i Termich. Obrab. Metallov*, **8**, 25–30 [in Russian].
8. Bondarev, B.I., Elagin, V.I. (1992) New aluminium alloys, doped with scandium. *Tekhnologiya Lyogkikh Splavov*, **5**, 22–28 [in Russian].
9. Ishchenko, A.Ya., Labur, T.M. (1997) Weldable scandium-containing aluminium alloys. *Welding and Surfacing Review, Harwood Academic Publisher*, **9**.
10. Zakharov, V.V. (1997) Stability of scandium solid solution in aluminium. *Metallovedenie i Termich. Obrab. Metallov*, **2**, 15–20 [in Russian].
11. Ishchenko, A.Ya., Poklyatsky, A.G., LOzovskaya, A.V. et al. (1990) Influence of parameters of low-frequency modulation of rectangular bipolar current on weld structure in welding of aluminium alloys. *Avtomatich. Svarka*, **9**, 23–27 [in Russian].
12. Brodyagina, I.V. (1998) Arc welding of aluminium alloys using magnetic fields. *Svarochn. Proizvodstvo*, **9**, 48–51 [in Russian].
13. Poklyatsky, A.G., Ishchenko, A.Ya., Grinyuk, A.A. et al. (2002) Non-consumable electrode argon-arc welding of aluminium alloys with arc oscillations. *The Paton Welding J.*, **18**–22.
14. Thomas, W.M., Nicholas, E.D., Needham, J.C., Church, M.G., Templesmith, P., Dawes, C.J. (1991) *Friction stir butt welding*. Int. Pat. Appl. PCT/GB 92/02203; GB Pat. Appl. 9125978.8.
15. Markashova, L.I., Poklyatsky, A.G., Kushnaryova, O.S. (2013) Influence of welding processes on the structure and mechanical properties of welded joints of aluminium alloy 1460. *The Paton Welding J.*, **3**, 18–23.
16. Fedorchuk, V.E., Kushnaryova, O.S., Alekseenko, T.A., Falchenko, Yu.V. (2014) Peculiarities of alloying of weld metal of high-strength aluminium alloy welded joints with scandium. *Ibid.*, **5**, 28–32.

Received 23.10.2018

# REFINEMENT OF METAL STRUCTURE IN ARC SURFACING UNDER THE EFFECT OF LONGITUDINAL MAGNETIC FIELD

A.D. RAZMYSHLYAEV<sup>1</sup>, M.V. AGEEVA<sup>2</sup> and E.V. LAVROVA<sup>1</sup>

<sup>1</sup>State Higher Education Institute Pryazov State Technical University  
7 Universitetskaya Str., 87500, Mariupol, Ukraine. E-mail: razmyshljaev@gmail.com

<sup>2</sup>Donbass State Machine Building Academy  
72 Akademicheskaya Str., 84313, Kramatorsk, Ukraine. E-mail: maryna\_ah@ukr.net

It is shown that if the deposited iron-based metal contains less than 0.15 % carbon, and more than 16 % chromium, then during its crystallization austenitic dendrites will form at the stage of primary crystallization, and during further cooling austenite will be transformed into ferrite. In this case, ferrite is formed within the boundaries of austenitic dendrites, and further on it does not undergo polymorphic transformations. Taking this statement into account, the deposits were produced using flux-cored wire, which provided carbon content of 0.08 % and that of chromium of 17–19.5 % in the deposits. The deposits were made without the effect of a longitudinal magnetic field and under the effect of this alternating field of 6, 12, 24 and 33 Hz frequency. Studies of macro- and microstructure of the deposited metal showed that under the effect of the magnetic field in the frequency range of 6–24 Hz, a significant decrease in the width and length of dendrites was observed in the deposited metal structure. The conclusion was made that refinement of the structure (of dendrites) during submerged-arc surfacing with wire is caused by movement of liquid metal in the pool under the effect of the magnetic field, and the influence on primary crystallization, and not on the stage of polymorphous transformations of metal in the solid state. 4 Ref., 1 Table, 3 Figures.

**Keywords:** *arc surfacing, magnetic field, crystallization, dendrite, austenite, ferrite*

Known is a considerable number of works, devoted to study of the features of the process of electric arc welding and surfacing under the effect of a controlling longitudinal magnetic field (LMF). In particular, in [1] it is shown that in welding under the effect of LMF, the melting rate of electrode wire becomes higher, the depth and area of base metal penetration zone is reduced, structure of weld or deposit metal is refined. However, the mechanism of refinement of structural components of welds (deposited metal) under LMF effect has not been unambiguously established. Brief overview of the currently available opinions of researchers on this subject is given in work [2].

In work [2] it is shown that the question about the stage of crystallization of weld metal in welding under LMF effect, at which weld structure refinement occurs, is still not solved. A number of researchers believe that this occurs at primary crystallization of welds, other authors think that this is due to phase transformations in the solid state (polymorphous transformations).

In works [3, 4] it is shown that in low-carbon high-chromium iron-based alloys (less than 0.15 % carbon and more than 16 % chromium) ferrite forms at austenite decomposition at temperature below  $A_{r3}$  point (of the order of 700 °C). This ferrite forms at decomposition of austenitic dendrites so that the available boundaries of dendrites (austenite) are pre-

served. Moreover, the alloy produced after crystallization, does not change its structure at heat treatment (quenching, or heating). Thus, if an alloy of such a composition is deposited under LMF effect and refinement of dendrites (grains) takes place, it will mean that refinement of the deposited metal structure occurred at primary crystallization of molten metal in the weld pool.

The objective of this work is obtaining the following information: at what stage — primary crystallization or that of phase transformations in the solid state does refinement of the structure of welds (deposits) take place in submerged-arc welding (surfacing) with wire under the effect of LMF.

In order to achieve this objective, the following experiment was performed. Reverse polarity submerged-arc surfacing with wires was conducted by automatic machine of ADS-1002 type using a rectifier of VDU-1202 type.

Surfacing was performed on a plate from low-carbon steel VMSt3sp(killed) 20 mm thick (250 mm wide, 400 mm long). First a sublayer was deposited in two passes (see Figure 1 — layer I, II) with 3.6 mm flux-cored wire PP12Kh13 using AN-26P flux.

Surfacing mode was as follows:  $I_s = 400\text{--}420$  A;  $U_a = 32\text{--}33$  W;  $v_s = 27$  m/h. Bead overlapping — deposition step  $L$  was equal to 12–13 mm. Total thickness of the two layers of the sublayer was  $\delta = 6\text{--}7$  mm

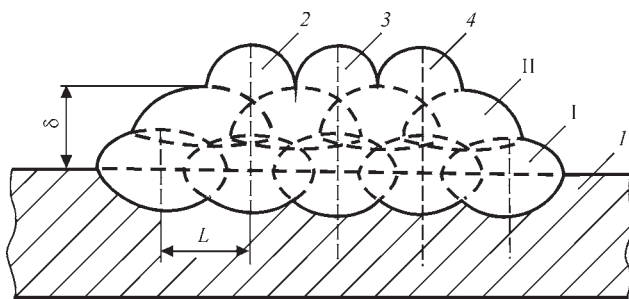


**Figure 1.** Deposition scheme: I, II — first and second passes of the sublayer, respectively; I — base metal; 2–4 — deposited beads

(Figure 1). A bead was deposited on the sublayer with specially made 4 mm flux-cored wire of 10Kh20 type using AN-26P flux under the effect of alternating LMF of 6, 12, 24, 33 Hz frequency. One bead was deposited without the LMF impact. Value of longitudinal component of LMF induction was 25–30 MT (measured before deposition under the electrode end face, which was located at 5 mm distance from the sublayer). LMF input device (ID) consisted of a solenoid with a ferromagnetic core, mounted coaxially with the electrode. The number of turns in the solenoid winding was  $W = 150$ . Power to LMF ID winding was supplied from a special power source, which generated rectangular current pulses in the winding with pause  $t_p = 0.01$  s. LMF ID design is described in detail in work [1].

Transverse templates 25–30 mm thick were cut out of the deposits. The template surfaces were ground, polished and etched with aqua-regia to study the macro- and microstructure. By the data of chemical analysis in all the deposit samples element content was equal to, wt.%: 0.08 C; 17–19.5 Cr; 0.34–0.36 Si; 0.29–0.30 Mn.

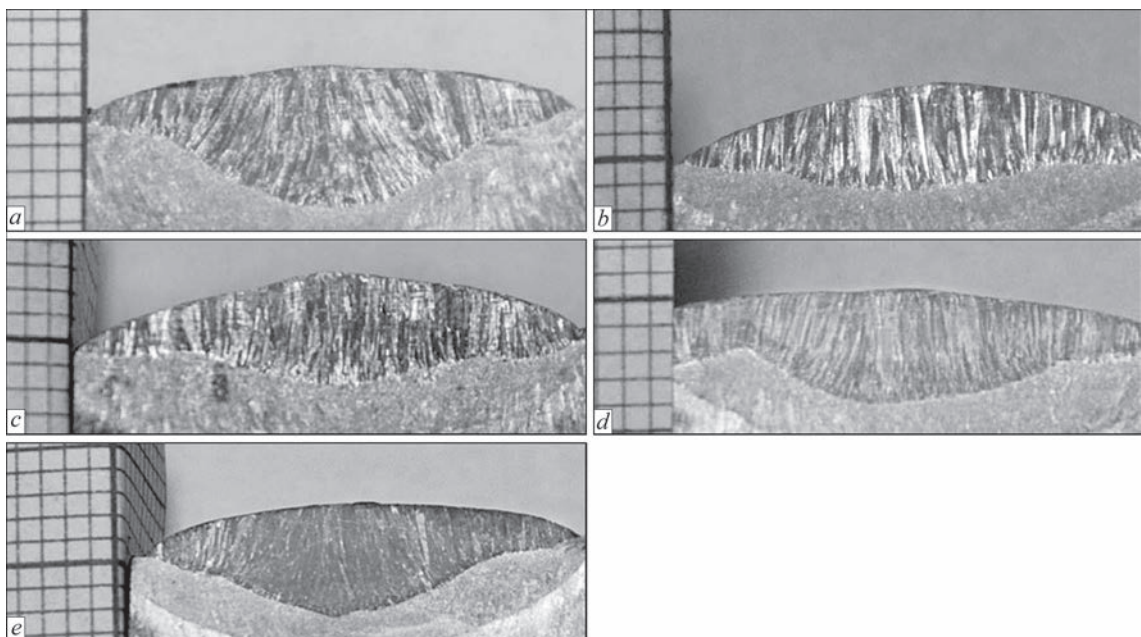
Dendrite dimensions in the deposited metal

Surfacing method	Dendrite dimensions	
	Width, $\mu\text{m}$	Length, mm
Without LMF	$\frac{130}{100-50}$	$\frac{0.130}{0.100-0.140}$
LMF, $f = 6$ Hz	$\frac{110}{100-150}$	$\frac{0.098}{0.080-0.120}$
LMF, $f = 12$ Hz	$\frac{83}{80-140}$	$\frac{0.100}{0.085-0.115}$
LMF, $f = 24$ Hz	$\frac{90}{80-20}$	$\frac{0.100}{0.080-0.120}$
ИПМПД, $f = 33$ Гц	$\frac{140}{100-200}$	$\frac{0.130}{0.100-0.150}$

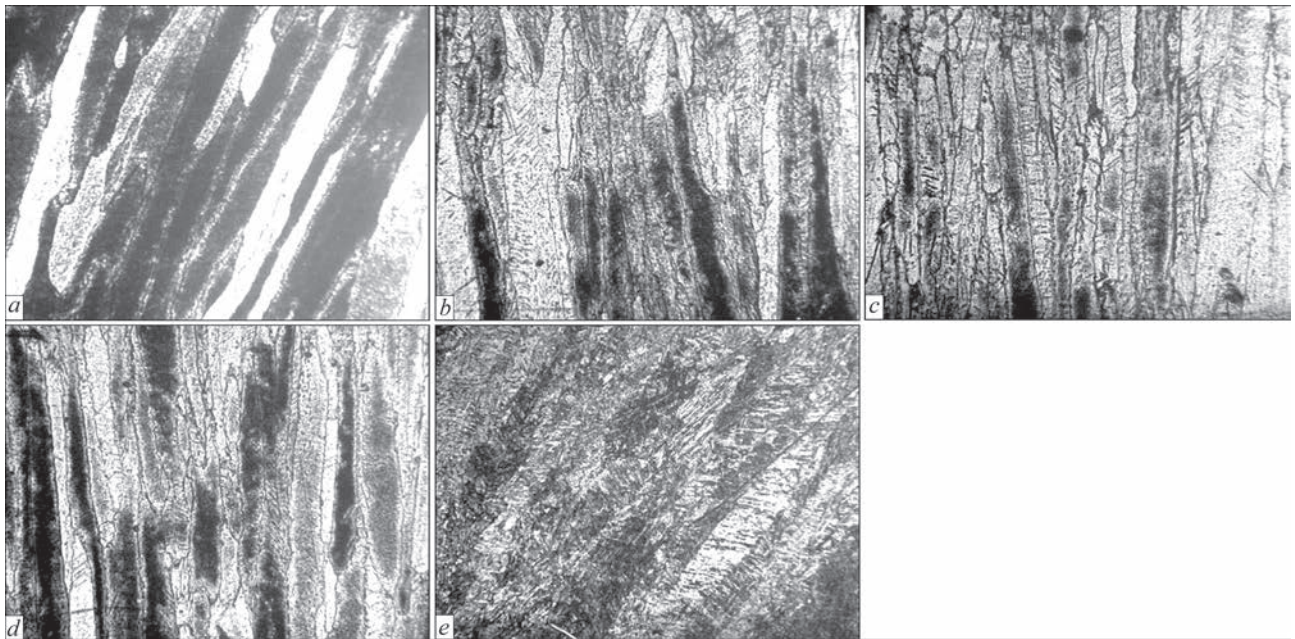
*Note.* The numerator gives average values, the denominator — minimum and maximum values.

Figure 2 shows the appearance of deposit macrostructures in their central part. It is characteristic that a dendritic structure is found at surfacing without LMF impact (Figure 2, a). In deposits, produced under the effect of LMF (Figure 2, b–e), a columnar dendritic structure is observed, oriented normal to the heat removal surface (towards the fusion line). Transverse dimensions of columnar dendrites decreased noticeably in deposits produced under LMF effect.

The microstructure of deposits, the appearance of which is given in Figure 3, was studied for a more detailed investigation of dendrite dimensions. The secant method was used to determine the width of dendrites, the data on which are given in the Table. It is characteristic that the scatter of this value is con-



**Figure 2.** Deposited metal macrostructures: a — without LFM; b, c, d, e — under the effect of LMF of the following frequency: 6, 12, 24, 33 Hz



**Figure 3.** Microstructures of deposited metal ( $\times 60$ ): *a* — without LMF; *b, c, d, e* — under the effect of LMF of 6, 12, 24, 33 Hz frequency, respectively

siderable for deposits made without LMF impact and under the effect of LMF. Average values of dendrite width are as follows: without LMF impact — 130  $\mu\text{m}$ , under LMF effect:  $f = 6$  Hz — 110  $\mu\text{m}$ ; 12 Hz — 83  $\mu\text{m}$ ; 24 Hz — 90  $\mu\text{m}$ ; 33 Hz — 140  $\mu\text{m}$ . Thus, in the frequency range of 12–24 Hz, the dendrite width decreased considerably (from 130 to 83–90  $\mu\text{m}$ ). At 33 Hz frequency this size is not smaller than in deposits made without LMF impact. This is associated with the fact that at 33 Hz frequency of LMF the metal molten in the pool did not move under the impact of alternating LMF, because of its inertia; the melt moved at lower LMF frequencies (right down to 24 Hz inclusive). The length of dendrites in the photo of deposit microstructures was also measured. The table data showed that the average length of dendrites in the deposits made without LMF impact, is equal to 0.13 mm, and decreases to values of the order of 0.10 mm in deposits, made under the effect of LMF of 6–24 Hz frequency. In deposits made under the effect of LMF of 33 Hz frequency, the length of dendrites is the same as in the deposits, made without LMF impact. As all the deposits contained:  $< 0.1\%$  C;  $> 16\%$  Cr, then, as was noted above, the effect of structure refinement in the deposits, made under the impact of LMF, was obtained at the stage of primary crystallization of liquid pool metal in arc surfacing. Thus, refinement of the structure (of dendrites) in

submerged-arc surfacing with wire is associated with LMF impact (movement of liquid pool metal) at the stage of primary crystallization, and not at the stage of phase transformations of metal in the solid state (polymorphous transformations).

### Conclusions

1. A significant reduction of the width and length of dendrites in the deposits is observed in submerged-arc surfacing with wire of iron-based alloy with 0.08 % C and 17–19.5 % Cr, under the effect of an alternating magnetic field of 6–24 Hz frequency.
2. Refinement of structural components in the metal of deposits in submerged-arc surfacing with wire under the effect of controlling longitudinal magnetic field is due to the process of this field impact on the stage of primary crystallization of liquid pool metal, and not on the stage of polymorphous transformations of metal in the solid state.

1. Razmyshlyayev, A.D., Mironova, M.V. (2009) *Magnetic control of formation of beads and welds in arc surfacing and welding*. Mariupol, PGU [in Russian].
2. Razmyshlyayev, A.D., Ageeva, M.V. (2018) On mechanism of weld metal structure refinement in arc welding under action of magnetic fields (Review). *The Paton Welding J.*, **3**, 25–18.
3. Lakhtin, Yu.M. (1977) *Metals science and heat treatment of metals*. Moscow, Metallurgiya [in Russian].
4. Bagryansky, K.V., Dobrotina, Z.A., Khrenov, K.K. (1976) *Theory of welding processes*. Kiev, Vyscha Shkola [in Russian].

Received 12.11.2018

# JOINING OF STEEL AND DISSIMILAR MATERIAL JOINTS WITH HIGHEST STRENGTH — THERE ARE OTHER WAYS THAN CONVENTIONAL WELDING

U. REISGEN and L. STEIN  
RWTH Aachen University (ISF)

Pontstrasse 49, 52062, Aachen, Germany. E-mail: [reisgen@isf.rwth-aachen.de](mailto:reisgen@isf.rwth-aachen.de)

Technological products are undergoing a continuous evolution, which, in many cases, require new materials and material combinations. In turn, these novel material concepts require their own special joining technology. Although classical joining methods can frequently be adapted, there are often drawbacks connected with these adaptations. Novel joining processes, such as Laser Beam Welding in Vacuum, MIG-Brazing of aluminium to steel or novel technologies for bonding steel to fiber-reinforced plastics aim at overcoming existing price or design limits and also at providing engineers with new possibilities for challenging future products. 7 Ref., 16 Figures.

Technological products are undergoing a continuous evolution driven by market demands for products that have less weight, are more energy-efficient, provide more and better functions, are smarter and cheaper or boast with new and spectacular designs. Meeting these demands is in many cases a challenge requiring new materials and material combinations, which in turn require their own special joining technology.

Even though classical joining methods can often be adapted to meet these new challenges, there are often drawbacks connected with these adaptations, such as price and design limits. Novel joining processes, as they are discussed in this article, aim at overcoming existing price or design limits and providing engineers with new possibilities for challenging future products.

## Laser beam welding in vacuum (LaVa) [1, 2].

Laser beam welding is a well-known and well-established process in industry. Therefore, laser beam welding can meanwhile be called a conventional welding process. It provides high-speed welding and low distortion for a great variety of materials. Nevertheless, the development of a large plasma plume leads to a shielding of the workpiece, thus limiting energy transfer into the workpiece and in consequence also limiting possible penetration depth.

The reduction of the ambient pressure (as far as to a vacuum) leads to an enormous change in the metal vapor plume above the keyhole and in the inner weld seam geometry. The plasma plume can be completely suppressed by the vacuum. Especially with a low welding speed, the weld seam becomes much more narrow and the penetration depth is increased by a factor of two, Figure 1. The process efficiency relating to the amount of molten material remains unaffected.

In the course of the research work of the past years, it was possible to demonstrate that the effect of increased penetration depth and narrow weld seam at low welding speeds can be transferred to deep penetration welding for industrial applications. Single-pass joint welds on a plate thickness of 50 mm for unalloyed steels and of 30 mm for high alloyed steels are achieved, Figure 2. With the double-sided single-pass welding technique, joint welds for a plate thickness of up to 110 mm have become possible. Spatter for-

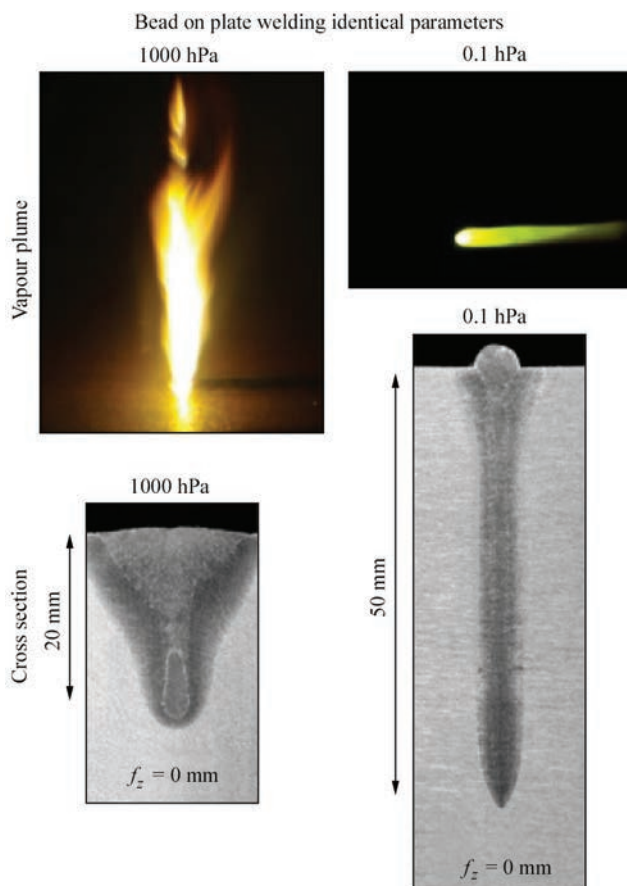


Figure 1. Vapor plume and bead-on-plate welding

mation on the weld top side is strongly reduced, very finely rippled top weld beads can be produced and the tendency to pore formation is reduced by facilitated degassing in the reduced pressure.

Comparative studies of LaVa-welding of copper (copper with high residual phosphorus Cu-DHP) at atmospheric pressure of 1000 hPa and vacuum pressure of 0.2 hPa with basic welding parameters (focus position on the surface, without beam oscillation) prove that a significant stabilization of the welding process by the reduction of the ambient pressure is the result, Figure 3.

At a working pressure of 0.2 hPa and a welding speed of 1.5 m/min weld metal ejections can be completely avoided up to the maximum power of 16 kW. Comparative welding trials with identical welding parameters and identical equipment at a pressure of 1000 hPa show the typical welding defects. This process stabilization can also be observed at even lower speeds around 1 m/min but the welds start to develop weld metal ejections at high power levels above 12 kW, Figure 6. The latest research results prove that these process limits can be further reduced by an optimization of the welding parameters.

At a laser power level of 8 kW (multimode disc laser, spot diameter 0.3 mm) and pressure level of 0.1 hPa, welding at low welding speeds (range of 1.5 m/min down to 0.5 m/min) is possible without weld metal ejections. In comparison to welding at atmospheric pressure, high penetration depth values (5 mm at 1.5 m/min up to 8.5 mm at 0.5 m/min) are

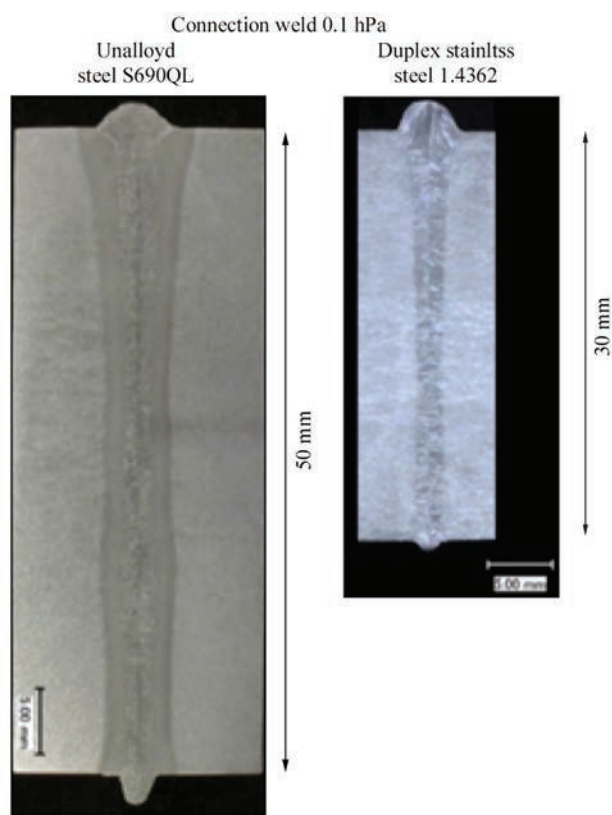


**Figure 2.** Connection weld unalloyed steel (50 mm) and duplex stainless steel (30 mm)

achieved with high process reliability. It can also be observed that the stabilization at the start of the welding process and achievement of the nominal penetration depth needs a distance of 5 to 10 mm, which is independent from the welding speed, Figure 4.

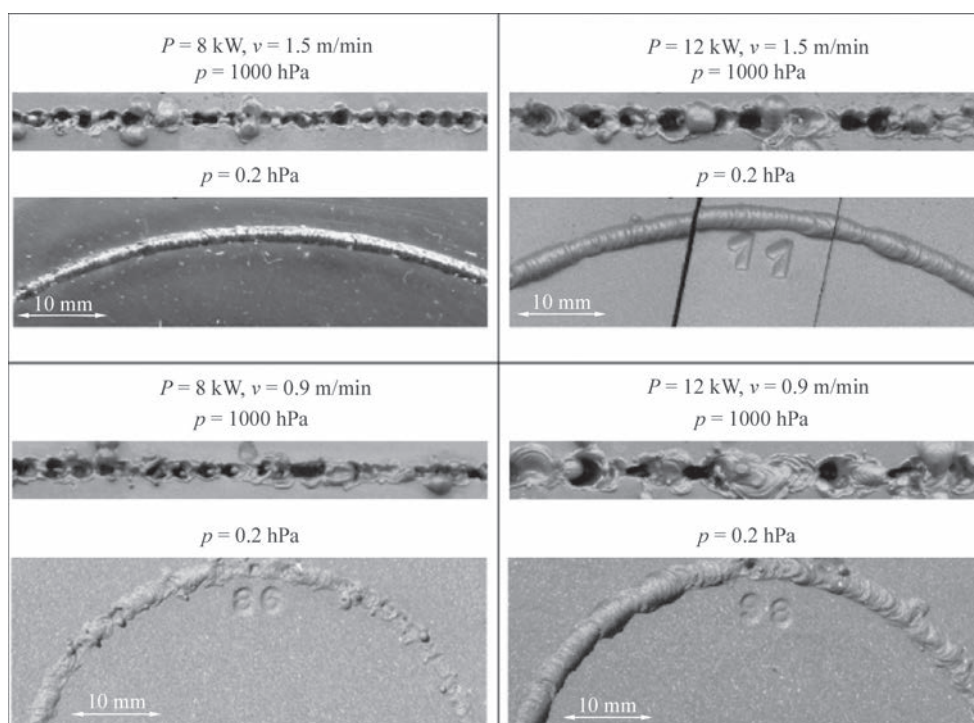


**Figure 3.** LaVa-welding of copper — weld metal ejections at ambient pressure and at 0.2 hPa

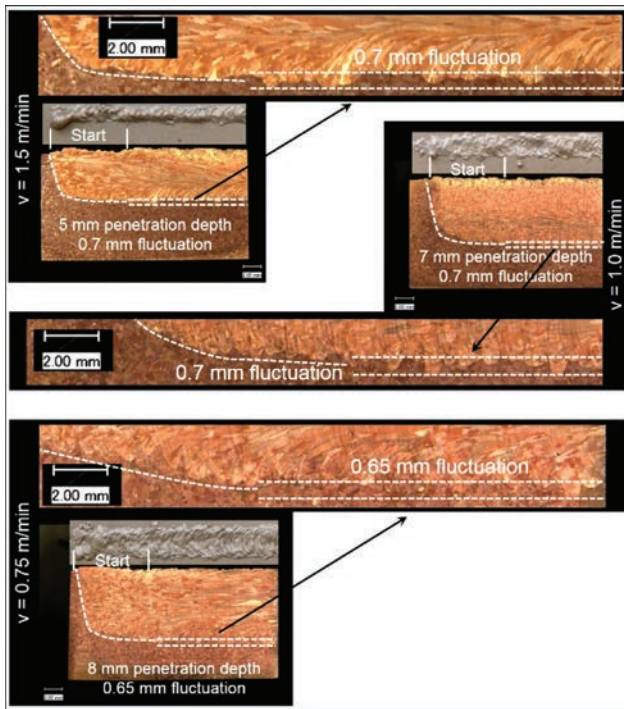


**Figure 4.** LaVa-welding of copper — penetration depth and fluctuation of penetration at different welding velocities

Reducing the work pressure had a great influence on the process stability when welding copper or aluminum. For this reason and to minimize oxidation during welding the laser beam under vacuum (LaVa) process was used to weld copper to aluminum, a joint of special interest for electrical engineering. In order to change the dilution of the mixed material joint by melting less copper, the focal position of the laser beam was changed parallel to the welding direction as

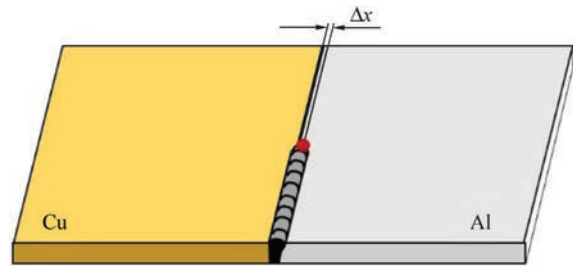


**Figure 5.** Schematic representation of the LBW process and focal off-set

shown in Figure 5. Additionally, circular beam oscillation was used to influence the dilution of the joint.

Sound welds of the material combination aluminum-copper were produced using laser beam welding under reduced ambient pressure. The trials done in this work all show very small narrow weld seams with a very low content of copper. The reason for that is most probably the fact, that aluminum and copper show different absorption rates for infrared laser energy. The laser intensity and energy per unit length used in this work was high enough to melt the aluminum base material but was almost totally reflected by the copper. This presumption is supported by the fact that the fusion line on the copper side is a straight line (joint preparation) and the weld seam area increases when using a beam off-set towards the aluminum side (Figure 6). Thus, an uncontrolled formation of brittle intermetallic is avoided. The joint can therefore be described as a weld on the aluminum side and as a braze weld towards the copper joining member.

To evaluate the quality of a Cu–Al material joint, the electrical resistance  $R_v$  was measured. All connections showed an electrical resistance between that

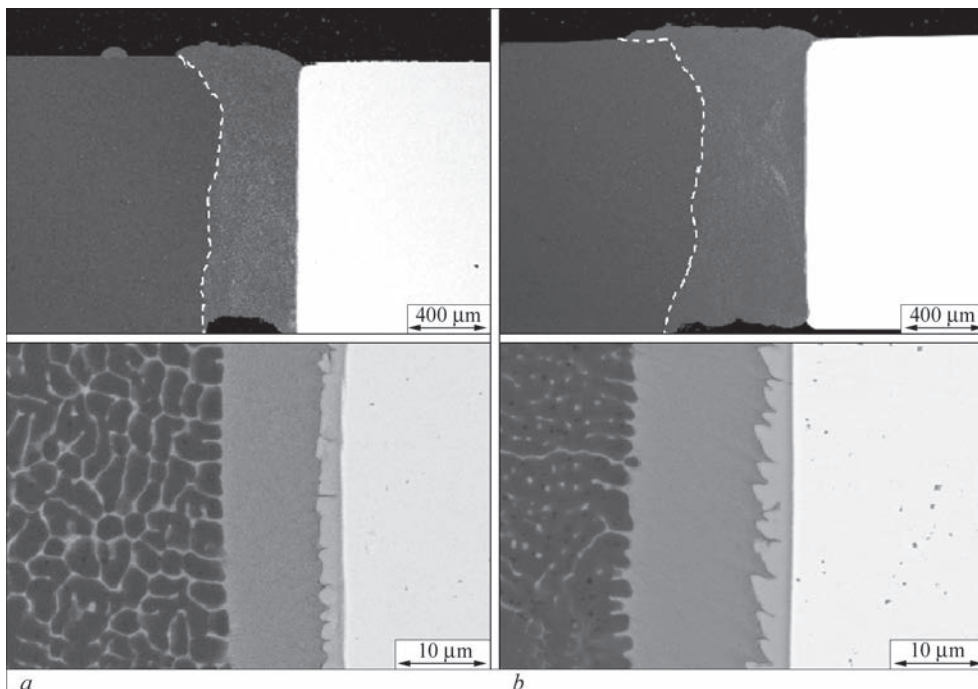


**Figure 6.** BSE analysis of a laser beam under vacuum Al-Cu joint: *a* — off-set = 0,1 mm; *b* — off-set = 0.3 mm

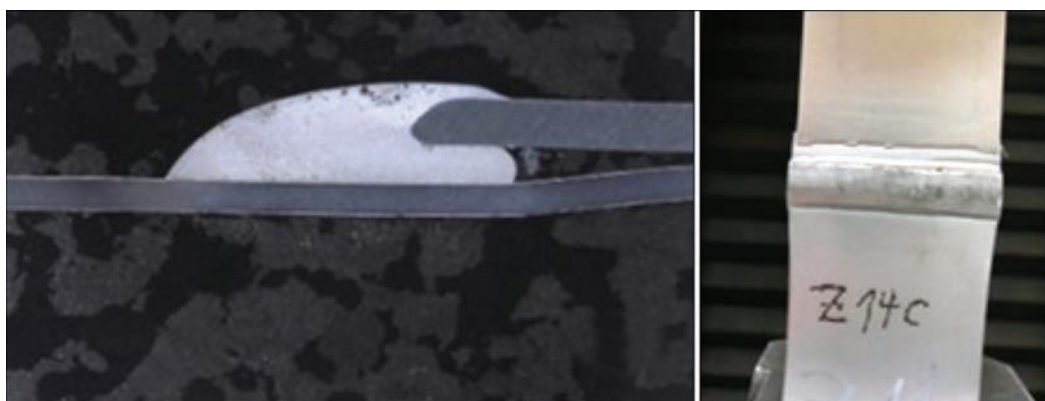


**Figure 7.** Steel-aluminum mixed joint with the brazing wire ZnAl4

of the base materials. A current flow of 200 A resulted in a decrease, followed by an increase of the connection resistance  $R_v$  over time. A growth of the intermetallic phase could not be observed after applying a current for two weeks.

**MIG-brazing of aluminium to steel [3].** Optimised lightweight car body building often involves multi-material designs. One of the desired combinations that excludes conventional welding because of the formation of brittle intermetallic phases is the joining of aluminium to steel. For this reason joining is done, despite of the costs, mainly by punch riveting, self-tapping fasteners, adhesive bonding or other non thermal joining technologies.

Thermal joining is mostly rejected by the industry due to the challenges it presents. In addition to the different physical properties of the two materials, such as heat conductivity and thermal expansion, the metallurgical incompatibility of steel and aluminum results in the formation of intermetallic phases during and after the joining process. Arc brazing processes using a zinc based wire have the potential for use in thermal joining of steel and aluminum, pursuing a lightweight strategy through multi-material design. Different from the use of aluminum-based wires where the brittle intermetallic phase layer emerges in form of a continuous seam along the steel-aluminum interface thus making this area susceptible to crack development and propagation, the use of a zinc-based wire allows to avoid the continuous formation of the intermetallic phases. This way, the negative impact of intermetallic phase formation on the mechanical properties of the joint is limited.

Compared with steel and aluminium, zinc-based brazing materials have a lower melting point which allows to reduce the heat required for the joining process and thus also the accompanying distortion of the component. Moreover, less heat influence on the base materials and the surface coatings is also possible. As in joining of steel-aluminium dissimilar material joints with aluminium-based brazing wires, the joining point is brazed

on the side of the steel and welded on the aluminium side. So far, a great challenge when applying different arc processes has been the low melting temperature of zinc which has a negative influence on the arc stability. Due to the controlled arc processes, the heat input and the droplet detachment is modified in such way that the arc is used as local heat source and, at the same time, it is possible to achieve a defined and sufficient deposition of molten filler material into the joining zone.

Among other things, overlap joints on hot-dip galvanised steel sheets DX 56 with a thickness of 1.0 mm and on aluminium sheets EN AW 6016 T4 with a thickness of 1.15 mm were carried out. With sufficient wetting of the steel sheet, the specimen fails in the heat-affected zone of the aluminium sheet. On the side of the steel, this material combination exceeds 90 % of the tensile strength with respective constriction of the specimens, Figure 7. The zinc layer of the steel sheet is not affected alongside the seam and also not on the sheet bottom side which allows for corrosion resistance without needing finishing work. It can be shown that constant strength can be obtained for overlap joints with a gap bridging ability of more than 1 mm. This should be sufficient to tackle production

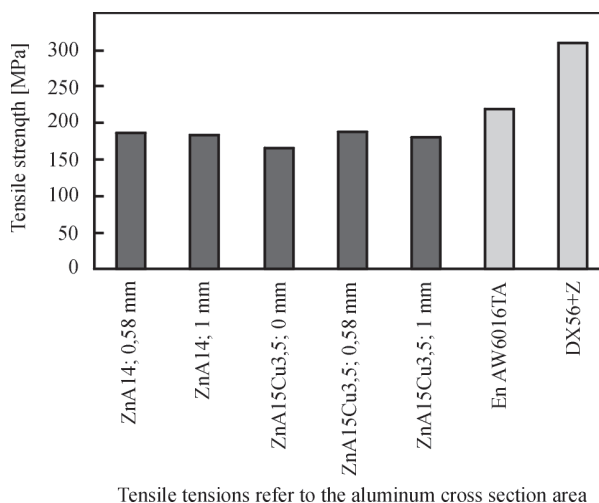


**Figure 8.** Tensile strength of steel-aluminum joints using different wires and defined gaps

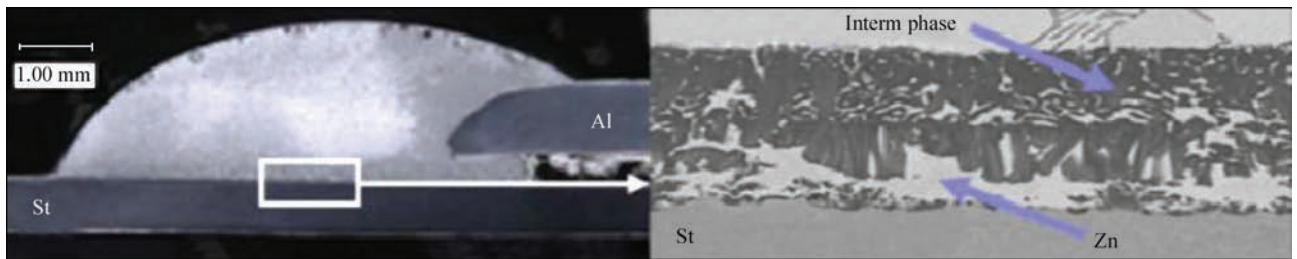


**Figure 9.** Intermetallic phase formation when using a zinc-based wire

tolerances that are common in practical applications, (Figure 8).

It was possible to produce steel-aluminium dissimilar joints with mechanically favourable seam geometries without the application of flux (Figure 9, left).

Metallographical examinations established that the brittle intermetallic phases are embedded in a ductile zinc matrix. Due to this structure, the negative influence which the brittle phases exert on the mechanical properties of the steel-aluminium dissimilar joints is reduced [4]. In a cooperation with the automotive industry, a demonstrator has finally been designed and constructed which shows the possibilities of the application of zinc-based brazing materials. In doing so, the same wire was used for joining steel with aluminium and also steel with steel. In both joining tasks, the strength of the base material was successfully achieved.

#### Joining of steel to fiber-reinforced plastics [5].

Lightweight design is constantly gaining importance in a variety of industries (aero-space, automotive, sports equipment, etc.). Materials with high specific densities, such as steel, are replaced by materials with a more favourable ratio of strength (or rigidity)

to their weight like fiber-reinforced plastics (FRP). However, the favourable properties of FRP can only be fully exploited in fiber direction. Moreover, metallic materials are more suitable for the induction of complex forces and are characterized by a higher abrasive wear resistance. In order to take advantage of both materials, FRP composites need to be integrated within metallic structures. Joining metallic structures to FRP composites therefore is one of the challenge in the area of lightweight design.

Existing joining technologies for solving this task are adhesive bonding and formfitting connections, in most cases rivets or bolts. In case of failure, form-fitting elements show a ductile behavior in most cases. This leads to a high process reliability and a high user acceptance. However, this kind of formfitting connections involve recesses in the components, which require an additional process step and lead to an interruption of the fiber formation of the composite materials. This, in turn, leads to the weakening of the supporting cross-section and, due to the notch effect, to high stress concentrations close to the recess, which are almost always the source of fatigue cracks.

Adhesive bonding is a well suited connection technique which transfers the forces homogeneously into the composite and is commonly used in this field. The supporting cross-sections are not reduced and the notch effect is avoided. Particularly for hybrid connections between FRP and metals, adhesive bonding is often regarded as the most convenient procedure. One disadvantage is the sensitivity of adhesives against high temperatures and humidity as well as the restricted ductility of adhesive bonds. In most cases

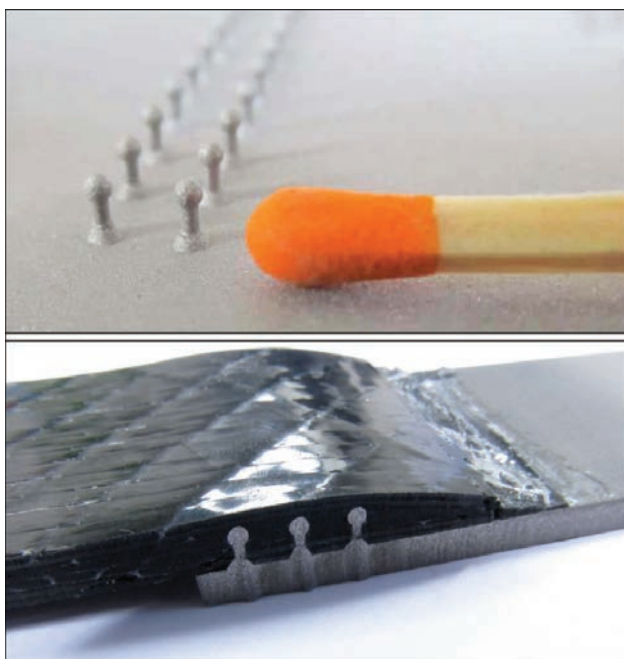


**Figure 10.** CMT pin structures as shear connectors

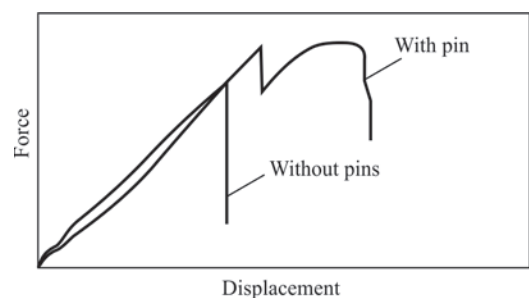


**Figure 11.** Multi-stage failure behavior by pin structures (schematic)

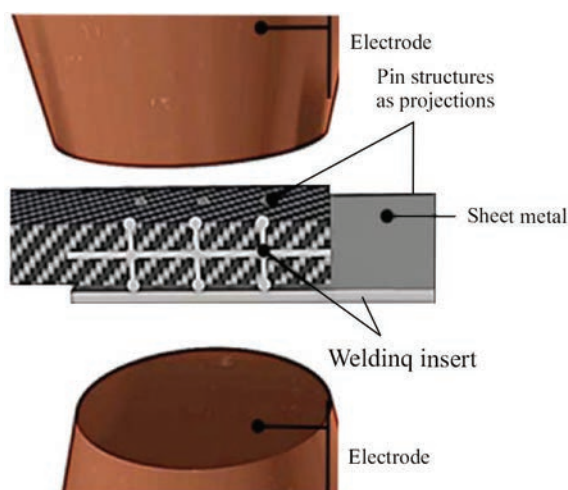


**Figure 12.** Welding insert for metal — FRP joints

the connections suffer brittle failure with absolutely no warning signs beforehand.

A new approach is based on an innovative, modified arc welding process where metallic pin structures are formed directly from the welding wire in one step with no additional prefabricated components needed (see Figure 10).

The pins are freely modifiable with regard to their geometry and arrangement. Therefore, they can be adjusted to the respective FRP structure.

The pin structures can be used as form-fitting elements within adhesive bonds, as has been demonstrated in the research work of the Austrian Institute of Technology in Austria. They are, moreover, suitable for moment transmission in drive shafts. Here, the drive shafts are fitted with pin structures and finally braided or wrapped with technical textiles. However, they have not yet been used to create a multistep failure behavior as it is presented in the following.

For this, the fibres are arranged around the CMT pins. The matrix resin is applied in a wet lamination process and can be directly used as an adhesive. The CMT pins transfer forces into underlying laminate layer, but also create a two-step failure behaviour:

When overloading the joint, first the adhesive bond (whose strength can be set to defined values via surface pre-treatment) fails. The forces are transported



**Figure 13.** Shear studs in civil engineering (source: Schöler + Bolte)

via the pin structures until they also fail. This failure event can be influenced via the pins' geometry and their arrangement and/or their number (see Figure 11).

The primary failure event can be detected by an integrated monitoring system. The force level of the secondary failure event needs to be above the force level of the primary failure event for a sufficient fail-safe backup which ensures a residual load capacity for countermeasures.

A modification of the described joining process [6, 7] enables direct welding of (fibre-reinforced) plastics to metals by resistance projection welding. In this way, continuous fiber-reinforced plastics can be processed without damaging the fibers. In particular, the fabricators can continue to use existing resistance welding systems in the usual way, with minor modifications if necessary. For this, an insert is integrated locally into the (fibre-reinforced) plastic prior to lamination as part of the FRP manufacturing process. This insert consists of a carrier plate with small metallic pin structures that penetrate the fibres and the surrounding plastic, Figure 12. The insert allows current to flow through the electrically non-conductive resin and enables indirect resistance welding to metallic structures.

Steel-concrete-combinations are already known in constructions like bridges in the use of a form-fit connection by shear studs, Figure 13. However, these shear studs build an oversized connector element

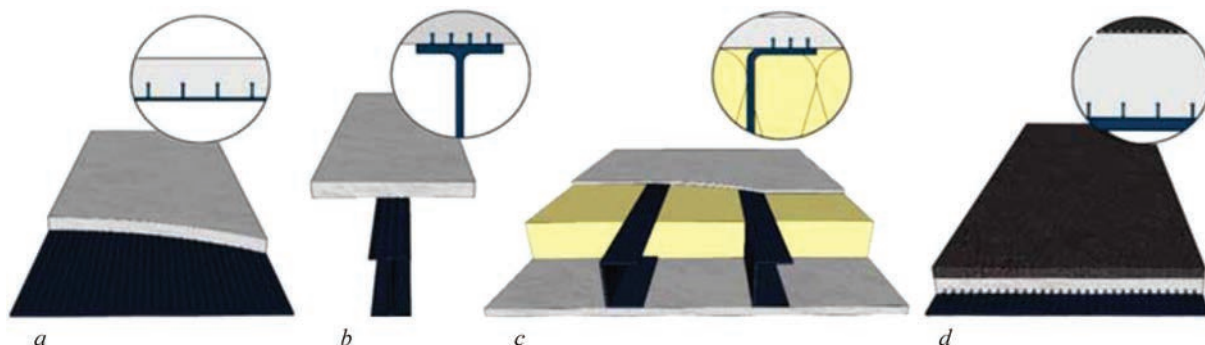


**Figure 14.** Applications for small-scale shear connectors

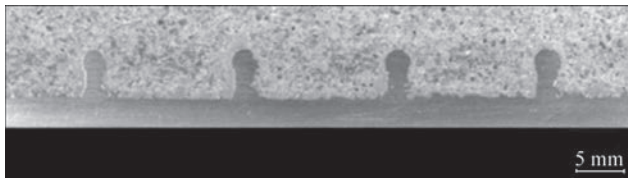


**Figure 15.** CMT pins embedded in concrete

for filigree designs, such as floor panels, roof girders, facade elements or bridge decks, Figure 14. The availability of small-scale connection elements such as CMT pins offers new possibilities for resource savings in lightweight constructions in civil engineering.

Strength and failure mode of the steel concrete combination vary with load and concrete type. Component tests with I-beams with concrete components on the top were performed under bending load in four point-bending tests (Figure 15).

Completely dowelled panels fail in the pressure zone of the concrete slab in the area of the load application. In contrast to this, partly dowelled panels collapse in the composite joint. The occurring failure of those panels was caused by die cutting of the concrete without a pin break (Figure 16).

### Summary

Innovative new joining methods enable innovation in product design. In competition with established joining processes, they improve effectiveness or costs and open new product or production possibilities.

1. Reisgen, U., Olschok, S., Turner, C. (2017) Welding of thick plate copper with laser beam welding under vacuum. *J. of Laser Applications*, **29**, 022402; doi: 10.2351/1.4983165.
2. Reisgen, U., Olschok, S., Holtum, N. (2018) Influencing the electrical properties of laser beam vacuum-welded Cu–Al



**Figure 16.** Die cutting failure of concrete-pin connection

mixed joints. In: *Proc. of 37th Int. Congress on Applications of Lasers & Electro-Optic, ICALEO* (October 14–18, 2018, Orlando, FL, USA); paper 202. Laser Institute of America (LIA), Orlando, FL, USA.

3. Angerhausen, M., Reisgen, U., Geffers, C., Pipinikas, A., Barthelmie, J., Wesling, V. (2016) New opportunities of thermal joining by using zinc- and copper-based brazing materials for modern car manufacturing. In: *Proc. of 36th FISITA World Automotive Congress* (September 26–30, 2016, Busan, South Korea), F2016-MFMG-002.
4. Angerhausen, M., Reisgen, U. (2015) *Method for producing a bonded joint, and structural element*. Rheinisch-Westfälische Technische Hochschule Aachen, RWTH Inventor: 26.11.2015DE, WO002015149756A3.
5. Lotte, J., Reisgen, U., Schiebahn, A. (2015) Smart multi material joint — hybrid joint of steel and FRP. *Mat. Sci. Forum*, 825–826, 314–318; *Transact. Tech. Publications*, Switzerland, doi:10.4028/www.scientific.net/MSF.825-826.314.
6. Reisgen, U., Lotte, J. *Hybrid components can be welded*, Produktion NRW, Cluster Maschinenbau/Produktionstechnik, 28–29, VDMA Publishing, D-Redaktion, Oberndorf.
7. Reisgen, U., Willms, K., Schäfer, J. et al. (2015) Small-scale pin structures: Requirement for a multi material joint CWA. *J. de l'ACS*, **11(5)**, 52–61. Canadian Welding Ass., Milton, Ontario, Canada.

Received 26.11.2018

**SAVE THE DATE**



**THE 72<sup>ND</sup> IIW ANNUAL ASSEMBLY AND INTERNATIONAL CONFERENCE**

**Bratislava, Slovakia**

**7<sup>th</sup> – 12<sup>th</sup> July 2019**

The annual event of the International Institute of Welding IIW 2019

[www.iiw2019.com](http://www.iiw2019.com)



The main topic of the International Conference:

**New Progressive Materials and Welding Methods in the Automotive Industry**

Hosted by



Conference Secretariat



## METHODS AND SPECIMENS FOR COMPARATIVE INVESTIGATIONS OF FATIGUE RESISTANCE OF PARTS WITH MULTILAYER SURFACING

I.A. RYABTSEV<sup>1</sup>, V.V. KNYSH<sup>1</sup>, A.A. BABINETS<sup>1</sup>, S.A. SOLOVEJ<sup>1</sup> and I.K. SENCHENKOV<sup>2</sup>

<sup>1</sup>E.O. Paton Electric Welding Institute of the NAS of Ukraine  
11 Kazimir Malevich Str., 03150, Kyiv, Ukraine. E-mail: [office@paton.kiev.ua](mailto:office@paton.kiev.ua)

<sup>2</sup>S.P. Timoshenko Institute of Mechanics of the NAS of Ukraine,  
3 Nesterova Str., 03057, Kyiv, Ukraine

The design of specimens and methods for experimental evaluation of fatigue life of multilayer deposited specimens at the cyclic mechanical loading were developed. The design of specimens simulates the design of real deposited parts, which allows performing a comparative evaluation of influence of chemical composition of the base metal and deposited layers, as well as technique and technology of surfacing separate beads or layers on their fatigue life. For investigations of fatigue life of specimens, the appropriate loading schemes were chosen, which with certain assumptions reproduce cyclic power loads characteristic for real parts: large-modulus gears, pressing screws of rolling mills, mill rolls, MCCB rollers, etc. The results of experimental investigations of the cyclic fatigue life of specimens according to the proposed methods are given. It was established that the developed investigation methods should be used for evaluation of the fatigue life of different parts when selecting materials, equipment and technology of restoration or manufacturing multilayer surfacing. 11 Ref., 1 Table, 8 Figures.

**Keywords:** *arc surfacing, multilayer surfacing, fatigue testing methods, fatigue, cyclic fatigue life, design of multilayer specimen*

Indices of fatigue life are one of the most important characteristics of deposited parts, operating under cyclic load conditions. This problem is particularly acute when restoring worn parts by surfacing methods. These parts have already passed a certain period of operation and exhausted a part of the life margin preset during their designing and manufacturing. When selecting surfacing materials and developing the technology of restoration surfacing of such parts, it is necessary to evaluate the effect of preliminary operating time on the residual service life of a restored part.

At present, there are no generally accepted methods for testing fatigue life of deposited specimens under cyclic mechanical loads. Standardized methods of testing fatigue life [1–3] are difficult for adaptation to the operating conditions which are typical for many of the deposited parts, since the specimens used in these methods have either a cylindrical solid (thickness of up to 25 mm) or hollow (wall thickness of 2 mm) section, or they represent flat specimens of up to 10 mm thickness. The specimens of such a shape and small dimensions do not allow investigating the influence of chemical composition of surfacing materials and structures of deposited layers in multilayer deposited specimens on their cyclic fatigue life. Using the standard specimens it is also impossible to evaluate

the influence of specifics of the performance of repair-restoration and manufacturing surfacing on the characteristics of fatigue life resistance of parts. As a result, the tests are usually carried out in specialized experimental installations, on specimens of different design which rarely simulate the operation of full-scale parts during their service, which leads to the results, which differ significantly for the same material and surfacing technology [4–8].

It should be noted that during surfacing of some parts, for example, mill rolls, dies, BCCM (billet continuous casting machine) rollers, etc., surfacing materials are used, which provide producing the deposited metal of the type of tool steels of a sufficiently high hardness ( $HRC > 45$ ) and wear resistance. A high hardness of the deposited metal greatly complicates the technology of manufacturing the appropriate specimens for fatigue tests, requiring a complete heat treatment cycle. At the same time, under the production conditions, the parts after surfacing, as a rule, do not pass a complete heat treatment and, therefore, it is only indirectly possible to judge about a cyclic fatigue life of deposited parts.

The aim of this work is to develop the design of specimens and methods of comparative investigations of the fatigue resistance of parts with multilayer sur-

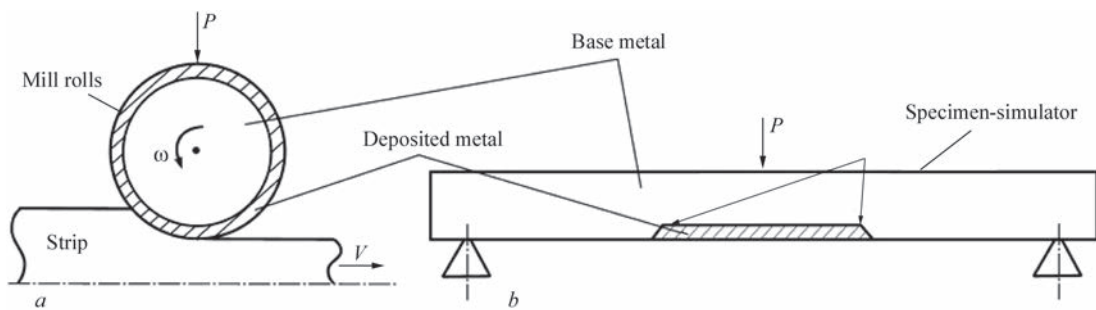


**Figure 1.** Scheme of strip rolling (a) and specimen-simulator loading according to the three-point bending scheme (b). Arrows indicate the transition from base metal to deposited one

facing, which will take into account the influence of chemical composition of the deposited layers, their geometric dimensions and the technology of surfacing and cyclic fatigue life.

For fatigue tests of welded or deposited specimens, tension, pure or circular bending is used [4, 6–9]. Based on the conditions of operation of parts of metallurgical equipment and some other parts requiring repair using surfacing, it is advisable to carry out tests at cantilever or three-point bending of specimens [4]. All the parts of the machines mentioned in this article can be divided into two groups: simple (mill rolls, BCCM rollers, etc.) and complex (gears, buttress thread, etc.) shapes.

**Group 1.** For the specimens, simulating deposited parts such as mill rolls, BCCM rollers, etc., it was proposed to use loading of specimens according to the scheme of three-point bending with application of from zero cyclic load on the specimen centre (Figure 1). Tests according to this scheme reproduce the power loads characteristic of these parts with a certain assumption and, in addition, in the process of testing, it is possible to conduct a visual evaluation of the rate of a fatigue crack propagation. When selecting the dimensions of the specimen, it is necessary to take into account the influence of the scale factor on the characteristics of fatigue resistance, i.e., the width of the specimen should be selected based on the condition of preserving uniaxial stressed state at all points of the specimen [1].

The shape and dimensions of the specimens for fatigue tests should be preset not only on the basis of the abovementioned requirements, but also on the assumption that the specimen should sufficiently simulate a deposited multilayer structure of a real part. Since surfacing on the specimen is performed only on one side, then its dimensions should be such that the deformation of the specimen after surfacing was minimal. Based on the available experience [10, 11] and the results of preliminary experiments, a design of prismatic specimens (in the shape of a rectangular parallelepiped) was developed, having dimensions of 20×40×300 mm with a groove for surfacing of 150 mm width and 10 mm depth (Figure 2).

When it is necessary to manufacture specimens that differ in geometrical parameters from the specimens shown in Figure 2, to calculate the dimensions of the groove for surfacing, it is recommended to use the results of the work [10]. The main requirement is the places of transition from deposited to the base metal (indicated by arrows in Figure 1, b) which should not be a potential place for initiation of fatigue cracks due to being too close to the place of application of the outer load.

To evaluate the cyclic fatigue life of the parts, the deposited metal of which has high hardness (*HRC* 46–50), the following technology was developed for the manufacture of specimens. Semi-products with a small tolerance for subsequent machining are assembled in a pack using technological inserts

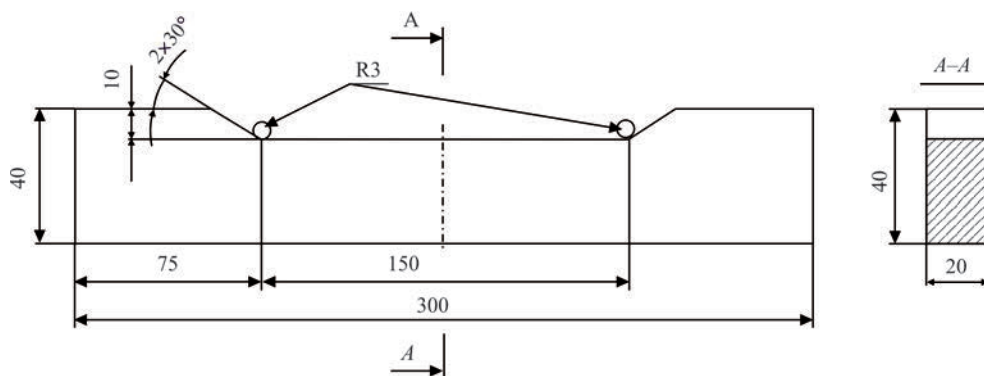


**Figure 2.** Specimen semi-product for investigation of fatigue life with a groove for surfacing with dimensions of 10×20×150 mm

of 5 mm thickness. On the sides of such a pack, run-out tabs are welded-on and automatic arc multilayer surfacing of the packages is performed (Figure 3). After that, the deposited pack of semi-products is cut by abrasive discs through technological inserts into separate semi-products and the metal layer, overheated during the cutting process, is removed in the grinding machine (during the machining of specimens, their heating above 50 °C is not allowed). After finishing grinding of all four sides, the specimens are ready for fatigue tests. This specimen manufacturing technology provides preserving of their transverse dimensions and does not allow any curvature along any axis, providing surface roughness by the class 9–10 according to GOST 2789–73.

**Group 2.** For the specimens, simulating deposited parts of a complex shape (teeth of large-modulus gears, large threading of pressing roll mill screws, buttress threading of suspended cones of conic crushers, crankpins, etc.), the design of specimens was developed, taking into account the features of wear and application of power loads in the parts of this group. In such parts, the wear zone and the application of cyclic load do not coincide with the zone of the most probable occurrence of fatigue damages (Figure 4, *a, b*). For example, the friction forces, occurring in the process of gears operation, lead to their wear and formation of cavities along their polar line (Figure 4, *b*). Moreover, during operation, cyclic stresses reach maximum values at the root of the tooth, and the zone of maximum wear is located higher. In addition, the transition from the tooth root to the cavity is a stress concentrator [10].

In practice, two schemes for surfacing a tooth are possible: the first one is restorative (Figure 5, *b*), the aim of which is the surfacing of only a worn area; the second is restorative-hardening (Figure 5, *c*), the aim of which is not only to restore the shape of the tooth, but also to apply a deposited metal to replace a damaged part of the material in the stress concentration zone at the base of the tooth.

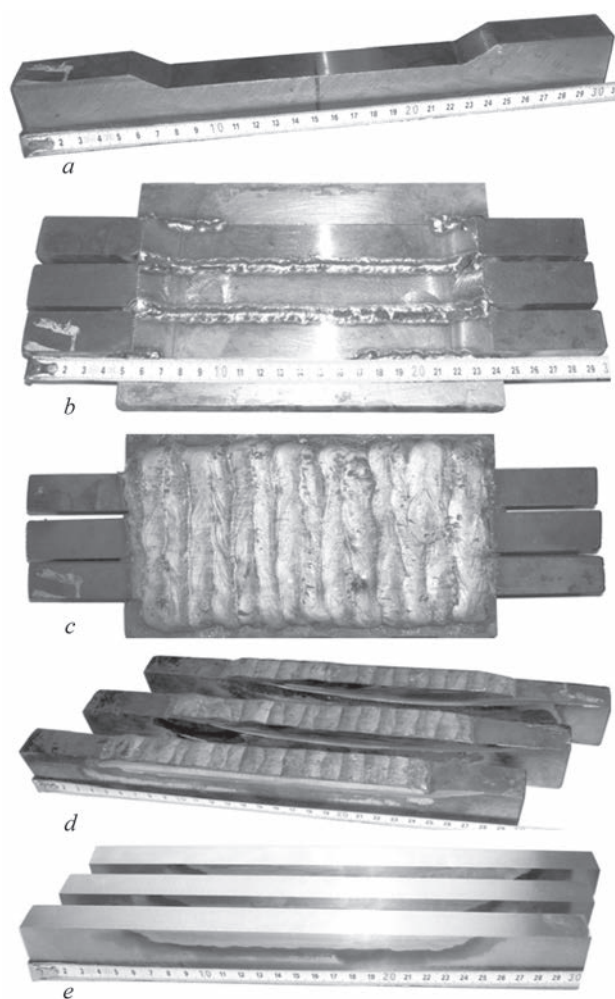


**Figure 3.** Stages of manufacturing deposited specimens: semi-product with a groove for surfacing (*a*); semi-products, assembled into a pack (*b*), after surfacing (*c*), cutting (*d*) and finishing grinding (*e*)

A characteristic feature of these schemes is a significant difference in the distribution of residual stresses after surfacing, which can have an impact on the life of a deposited part. Thus, if only a worn area is deposited and only a shape of the tooth is restored, then tensile welding stresses can significantly reduce the fatigue life of a restored part. Restoration of geometrical dimensions of worn parts without eliminat-

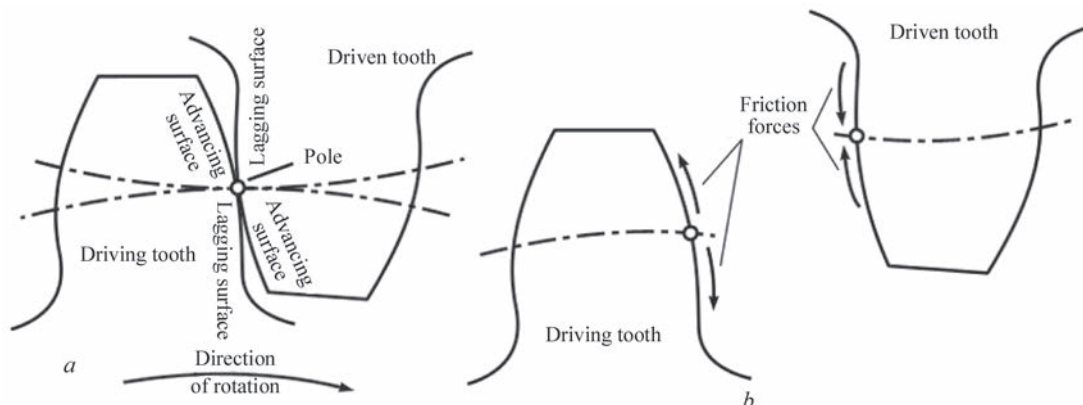


**Figure 4.** Location of lagging and advancing surfaces (*a*) and direction of friction forces (*b*) on driving and driven profiles of the teeth [10]

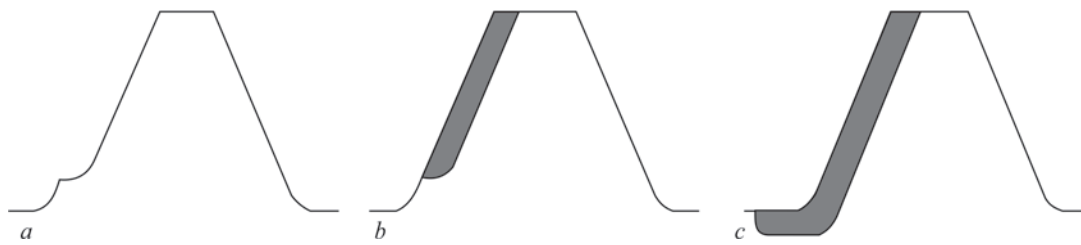


**Figure 5.** Shape of worn tooth (*a*) and possible schemes of its surfacing: *b* — restoration of initial dimensions of a tooth (scheme 1); *c* — restoration-strengthening surfacing with a replacement of damaged material in the stress concentration zone near the tooth root (scheme 2)

ing fatigue damages outside the wear zone does not give the positive results [10].

Based on the fact that a fracture of the gear tooth occurs due to the formation of a fatigue crack near its base, for experimental evaluation of fatigue life, a design of specimens was developed having a similar stress concentrator (Figure 6). The size of the transition radius in the specimens is selected based on the determining dimensions of teeth of real large-modulus gears. Fatigue tests, taking into account the application of real loads on the part, should be carried out at from zero cantilever bending.

Depending on the used scheme of surfacing (see Figure 5) for fatigue tests, the following specimens were manufactured: with a stress concentrator (Figure 7, *a*), with a groove for surfacing according to the scheme 1 (Figure 7, *b*) or with a groove for surfacing according to the scheme 2 (Figure 7, *c*).

The developed designs of specimens and testing methods were tested during investigation of fatigue life of materials used for surfacing the parts of metallurgical equipment, which are made of medium and high-carbon unalloyed or low-alloyed structural steels of type 35KhM, 40Kh, 50 Kh, 50KhN, etc. Two

batches of specimens were manufactured, respectively, for the study of cyclic fatigue life of parts of simple (mill rolls, etc.) and complex (teeth, etc.) shapes.

The first batch of specimens (see Figure 2) consisted of three series (three specimens in each series) for tests according to three-point bending scheme (see Figure 1, *b*). The first series of specimens of steel 40Kh was tested in the initial state (without surfacing); the specimens of the second series — after surfacing using flux-cored wire PP-Np-25Kh5FMS with a diameter of 2.0 mm under the flux AN-26P (surfacing mode: voltage is 24–26 V; current is 230–250 A; rate of surfacing is 20 m/h); the specimens of the third series — after surfacing and at the same modes of the intermediate layer using the solid wire Sv-08 of 2.0 mm diameter under the flux AN-348A and after the subsequent surfacing using the flux-cored wire PP-Np-25Kh5FMS under the flux AN-26P.

The second batch of specimens (see Figure 7) consisted of four series (three specimens in each series) for testing according to the scheme of cantilever bending (see Figure 6). The first series of specimens of steel 35KhM was tested in the initial state (without surfacing); the specimens of the second series — after

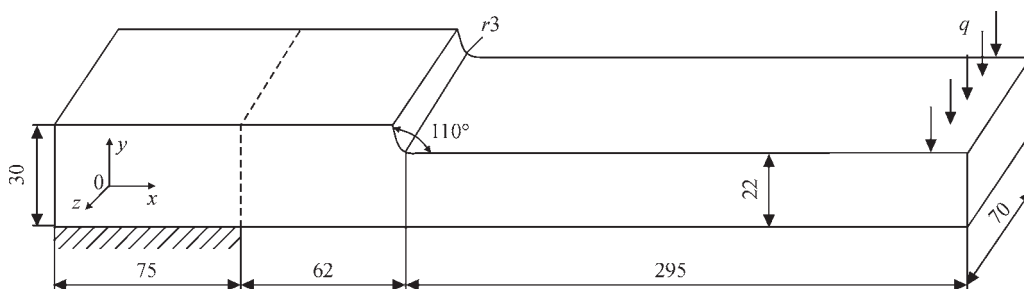


**Figure 6.** Scheme of loading the model specimen for investigation of cyclic fatigue life of a gear tooth (*q* — applied from zero cyclic outer loading)

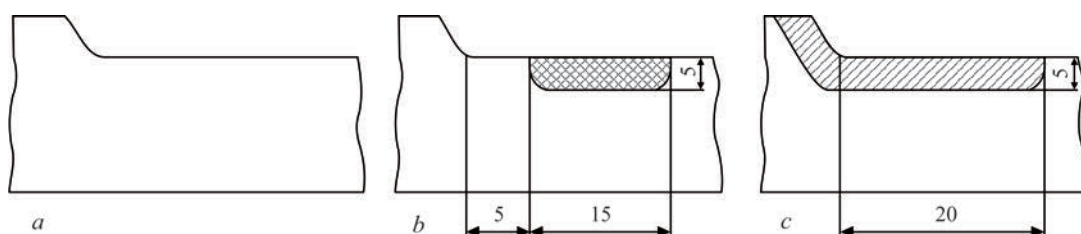


**Figure 7.** Schemes for performing restorative surfacing of specimens for fatigue tests: initial (*a*); with preparation for surfacing according to the scheme 1 (*b*) and with a groove for surfacing according to the scheme 2 (*c*)

## Results of tests of fatigue life of specimens under cyclic mechanical loading

Specimen type and dimensions	Specimen material	Number of cycles before appearance of cracks in specimens			Average number of cycles before crack appearance
		1	2	3	
Specimens with dimensions of 20×40×300 mm for testing under the three-point bending (Figure 2)					
Solid specimen without preparation and surfacing	Steel 40Kh	190500	199750	215300	201850
With surfacing without sublayer	Steel 40Kh + 25Kh5FMS	120100	134300	124800	126400
With surfacing with sublayer	Steel 40Kh + 08kp + 25Kh5FMS	179300	165100	180600	175000
Specimens with dimensions of 30×70×432 mm for testing according to the scheme of cantilever bending (Figure 7, a–c)					
Solid specimen without preparation and surfacing	Steel 35KhM	185700	176900	178900	180500
With preparation and surfacing according to the scheme 1	Steel 35KhM + Np-30KhGSA	111350	126800	134450	124200
With preparation and surfacing according to the scheme 1*	Same	17200	20100	18800	18700
With preparation and surfacing according to the scheme 2*	»	214800	220100	234700	223200

\*Specimens before preparation and surfacing were loaded for 10<sup>5</sup> cycles.

surfacing using the solid wire Np-30KhGSA with a diameter of 2.2 mm under the flux AN-26P according to the scheme 1 (surfacing mode: voltage is 32 V; current is 300 A; deposition rate is 18 m/h); the specimens of the third series — after preliminary operating time of 10<sup>5</sup> cycles and the subsequent preparation and surfacing using the solid wire Np-30KhGSA with a diameter of 2.2 mm under the flux AN-26P according to the scheme 1 (surfacing mode: voltage is 32 V; current is 300 A; deposition rate is 18 m/h); the specimens of the fourth series — after a preliminary operating time of 10<sup>5</sup> cycles and the subsequent preparation and surfacing using the solid wire Np-30KhGSA with a diameter of 2.2 mm under the flux AN-26P according to the scheme 1 (surfacing mode: voltage is 32 V; current is 300 A; deposition rate is 18 m/h).

The calculation of ultimate loads and a number of cycles before fracture was selected from the following prerequisites. As far as the tests had a comparative nature, then to shorten a period of tests, a relatively small number of cycles was selected: 2·10<sup>5</sup> [11]. A calculation of loads was carried out which could provide such a number of cycles until a fatigue crack appeared in the specimen. For specimens of steels 40Kh and 35KhM, to this number of cycles the maximum number of applied stresses equal to 500 MPa is corresponded. The test results of two batches of specimens are given in the Table.

In the process of tests, each specimen is under the constant visual control (inspection is every 15–30 min), during which the side polished etched surfaces of the specimen are lubricated with kerosene to reveal the location of crack initiation. The test report records the number of specimen loading cycles until

one or several cracks with a length of 1.0–1.5 mm appear, after which the tests are stopped. For example, Figure 8 shows the outer appearance of the specimen with fatigue cracks.

Tests of specimens (Table), made of base metal without and with surfacing, confirmed the reasonable accepted design loads and showed that the developed methods and specimens can be successfully used for comparative evaluation of fatigue life of deposited parts. The obtained experimental results clearly illustrate the influence of the chemical composition of surfacing materials, the structure of deposited layers and the surfacing scheme on the cyclic fatigue life of the specimens.

The cyclic fatigue life of specimens of the first type of steel 40Kh with a deposited wear-resistant layer such as steel 25Kh5FMS decreased by about 38 % as compared to the cyclic fatigue life of specimens of the base metal without surfacing. Deposition of the underlayer of plastic material (of type of low-carbon steel 08(semi-killed)), provided a significant (approximately by 38 %) increase in the cyclic fatigue life as compared to the specimens, deposited without an un-

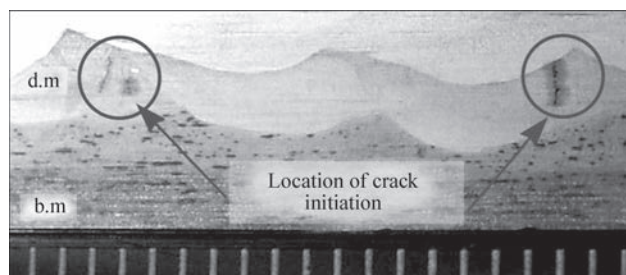


Figure 8. Outer appearance of the side surface of the specimen with the areas where fatigue cracks initiated: b.m. — base metal; d.m — deposited metal

derlayer. The decrease in life as compared to non-deposited specimens in this case does not exceed 14 %.

As follows from the data of the Table, fatigue tests of specimens of steel 35KhM simulating the teeth of large-modulus gears showed that preliminary cyclic fatigue life for  $10^5$  cycles has a significant effect on the life of deposited specimens, since it leads to accumulation of fatigue damages in the area of stress concentrator at the tooth root. The performance of restoration surfacing according to the scheme 1 without removing the base metal, that has fatigue damages, is impractical because it actually leads to a significant reduction in the residual cyclic fatigue life. The performance of restorative-hardening surfacing according to the scheme 2, with the removal of a damaged metal layer near the stress concentrator, allows even 1.2 times increasing the residual fatigue life of the teeth restored by surfacing as compared to the initial state.

### Conclusions

1. The designs of multilayer deposited specimens and corresponding methods for evaluation of their fatigue life under cyclic mechanical loading were developed. These methods and specimens allow carrying out a comparative evaluation of the effect of multilayer surfacing, chemical composition of deposited layers, their thickness, technology and technique of surfacing on the fatigue life of deposited parts.

2. During approbation of the methods, it was found that the use of a low-carbon steel of type 08(ps-killed) as an underlayer in wear-resistant surfacing of specimens of steel 40Kh, simulating operating conditions of mill rolls allowed increasing their cyclic fatigue life by 38 % as compared to specimens produced without underlayer. The similar results were obtained

when testing specimens, simulating operating conditions of the teeth of large-modulus gears. Performing surfacing and removing the damaged layer of the base metal allows 1.2 times increasing the life of the teeth restored by surfacing as compared to the initial state.

1. Shkolnik, L.M. (1978) *Procedure of fatigue tests*. Moscow, Metallurgiya [in Russian].
2. Troshchenko, V.T. (1978) *Strength of metals under alternating loads*. Kiev, Naukova Dumka [in Russian].
3. *GOST 25.502-79 (1979): Methods of mechanical testing of metals. Methods of fatigue tests* [in Russian].
4. Troshchenko, V.T., Sosnovsky, L.A. (1987) *Fatigue resistance of metals and alloys*. Pt 1. Kiev, Naukova Dumka [in Russian].
5. Marek, A., Junak, G., Okrajni, J. (2009) Fatigue life of creep resisting steels under conditions of cyclic mechanical and thermal interactions. *Archives of Materials Sci. and Engin.*, 40(1), 37–40.
6. Dombrovsky, F.S., Leshchinsky, L.K. (1995) *Serviceability of surfaced rolls of billet continuous casting machines*. Kiev, PWI [in Russian].
7. Oparin, L.I., Vasiliev, V.G., Bondarchuk, E.P. (1992) Improvement of fatigue strength of 15Kh13 type deposited metal. In: *Deposited metal. Composition, structure, properties: Transact.*, 51–54 [in Russian].
8. Makhnenko, V.I., Shekera, V.M., Kravtsov, T.G., Sevryukov, V.V. (2001) Effect of subsequent mechanical treatment on redistribution of residual stresses in surfaced shafts. *The Paton Welding J.*, 7, 2–5.
9. Bizik, N.K., Darchiashvili, G.I., Trapezon, A.G., Pismenny, N.N. (1986) Influence of surfacing of tin bronze on fatigue resistance of 40KhFMA and 10KhSND steels. In: *Surfacing in manufacture of machine and equipment parts: Transact.*, 100–103 [in Russian].
10. Ryabtsev, I.A., Senchenkov, I.K., Turyk, E.V. (2015) *Surfacing. Materials, technologies, mathematical modeling*. Gliwice, Wydawnictwo politechniki slaskiej [in Poland].
11. *Babinets A. A., Ryabtsev I. A. (2016) Fatigue life of multilayer hard-faced specimens. Welding International*, 30(4), 305–309. <https://doi.org/10.1080/01431161.2015.1058004>.

Received 15.11.2018



## FRONIUS UKRAINE LLC HOLDS THE SEMINARS

**May 15, 2019** — «Automation of Welding Processes»

**June 20, 2019** — «Robotization of Welding Processes»

### Fronius Ukraine GmbH

Browarskij r-n, s. Knjashitschi, ul. Slavy 24

07455 Kievskaya obl.

Tel.: +380 44 2772141

Fax: +380 44 2772144

sales.ukraine@fronius.com

<http://www.fronius.ua/>

# METHODS OF EVALUATION OF INCREASE OF FATIGUE RESISTANCE IN BUTT WELDED JOINTS OF LOW-CARBON STEELS AFTER HIGH-FREQUENCY MECHANICAL PEENING

V.A. DEGTYAREV

G.S. Pisarenko Institute for Problems of Strength of the NAS of Ukraine  
2 Timiryazevskaya Str., 01014, Kyiv, Ukraine. E-mail: [degtyarev@ipp.kiev.ua](mailto:degtyarev@ipp.kiev.ua)

There was investigated an effect of modes of high-frequency mechanical peening on increase of fatigue resistance of butt welded joints of steel St3sp (killed). Different technology of sample preparation for investigation allowed determining that a quantitative contribution in rise of fatigue limit of welded joints of residual compression stresses, deformation hardening of surface layer of a groove formed after peening of a narrow zone of weld fusion with base metal, and change of stress concentration after high-frequency mechanical peening makes 57, 37 and 6 %, respectively. It is shown that there is a correlation between the groove depth and depth of plastically deformed layer of material. The procedure was proposed for determination of the fatigue limits of butt welded joints after different modes of peening on groove depth and plastically deformed layer of material, using the experimental data of microhardness measurement as well as the change of amplitude of working tool oscillation in the investigated range. A depth of groove was determined depending on rate of high-frequency mechanical peening and amplitude of working tool oscillations as well as change of sample fatigue limit due to different technology of their manufacture. It is shown that increase of peening rate independent on the working tool oscillation amplitude promotes decrease of efficiency of improvement of welded joint fatigue resistance and at 0.4 m/min rate the fatigue limit from deformation hardening and total effect of all factors typical for high-frequency mechanical peening rises by 11 and 26 %, respectively. 14 Ref., 4 Tables, 7 Figures.

**Keywords:** *welded joint, fatigue limit, groove depth, rate of high-frequency mechanical peening, plastically deformed layer, microhardness*

Intensive development of technological methods for increase of fatigue resistance of welded metal structures and extension of their service life provokes significant attention to high-frequency mechanical peening (HMP) [1–3]. It is related with the fact that it can guarantee considerable rise of fatigue resistance of elements of metal structures and their life [4, 5] in manufacture as well as performance of repair-reconstruction works. It was proposed to use a groove depth [8] forming after peening of a narrow fusion zone of weld to base metal as a criterion of HMP efficiency control instead of rate of movement of working tool along the weld [6, 7]. A value of its optimum depth, equal to 0.14 mm, was determined and the parameters of HMP rate depending on amplitude of working tool oscillations were proposed. However, up to the moment the effect of various peening modes on the welded joint fatigue resistance remains unexplored. Since performance of a complex of full-scale experimental investigations is sufficiently expensive procedure as it takes long time and related with considerable consumption of the material then calculation evaluation of the butt welded joint fatigue resistance in comparison with separate experimental data is the most reasonable solution of the problem.

In this connection aim of the present work lies in calculation evaluation of the effect of HMP modes on increase of the fatigue limit of butt welded joints based on the results of measurement of groove or depth of plastically deformed layer of material under groove bottom using experimental data of microhardness measurement.

**Equipment, material and test procedures.** Butt welded joint of sheet steel St3sp (killed) made by semi-automatic welding in CO<sub>2</sub> was used as a material for investigation. Various order of preparation of test samples was used to evaluate the effect of HMP modes of welded joints and quantitative contribution into increase of their fatigue resistance of deformation hardening of the groove upper layer as well as residual stresses (RS).

In the first case the separate areas of welded plate of 1000×400 mm size with butt weld was subjected to HMP along weld to base metal fusion line by ultrasonic tool USP-300 [9] with oscillation frequency 22 kHz, deformation mechanism of which presented a 4-striker head with built in it 3 mm diameter rods. Peening was carried out at amplitude of working tool oscillation  $a$ , equal to 19 μm, and different given rate of its movement  $V$  (peening rate), equal to 0.232, 0.116 and 0.06 m/min, respectively, which was determined by relationship of length of treated weld to

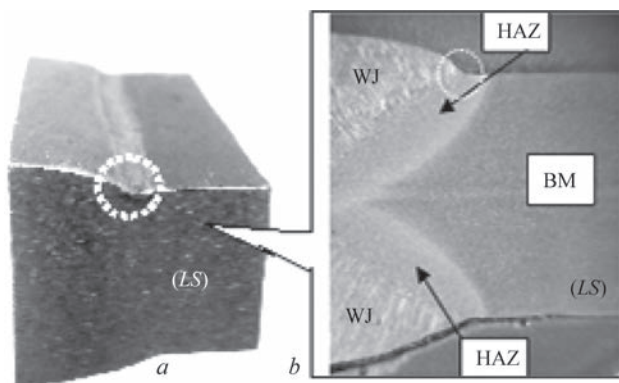


**Figure 1.** Appearance of template type (a), section surface after etching in LS plane of cross-section (b): L — rolling direction; S — direction normal to rolling plane; contour outlines groove profile; WJ — welded joint; HAZ — heat-affected zone; BM — base metal

time of treatment. After HMP the groove was formed depending on treatment rate and having 2.8–3.5 mm width and depth  $h$ , equal to 0.041; 0.062 and 0.143 mm, respectively. After that the plate was cut for samples (series 1) of 40×400×14 mm size with transverse weld, long side of which matched with rolling direction. It allowed considerable reduction of RS available after welding and next HMP of the plate.

In the second case the plate was firstly cut on the samples of the same size (series 2) and then each sample individually was subjected to peening with rate and amplitude of working tool oscillations similar to treatment of the first series samples. The groove of

the same size was formed after HMP. As a result, we managed to develop and keep compression residual stresses. Thus, in the samples of the first series the rise of welded joint fatigue limit was caused by presence of hardened layer and decrease of stress concentration coefficient, and in the second by additional effect of compression RS.

It should be noted that identical groove depth can be reached by combination of such parameters as treatment time allowing determining the rate at set width of sample and amplitude of tool oscillations. The paper does not cover the investigation of relationship of depth of the hardened layer and parameters of treatment at similar depth of the groove taking into account that a depth of plastically deformed layer is mainly reflected by microhardness and groove depth. It is proved by methodological investigations of hardening process optimizing carried at PWI [10].

After that one template of 40×40×14 mm size (Figure 1, a) was cut from each series of the samples treated at different HMP rate for metallographic examinations.

The metallographic examinations of the samples were performed on optical inverted microscope AXIOVERT 40 MAT. The sections were made on BUEHLER unit in (S–L) cross-section plane of welded joint normal to sheet rolling direction. Figure 1, b shows the surface of the section after etching in 4 % solution of nitric acid in ethyl alcohol. Measurement of microhardness was carried on microhardness meter PMT-3 according to GOST 9450–76 [11] at 1 N loading.

**Analysis of obtained results.** It is known that HMP results in deformation hardening of the material to some depth from groove surface. It is obvious that different groove depth as well as different depth of plastically deformed layer  $l_h$  (depth of hardened layer) will correspond to different modes of treatment.  $l_h$  with sufficient level of accuracy can be determined on change of microhardness  $H_\mu$ .

Measurement of microhardness was carried out in the welded joint cross-section normal to peening direction by parallel rows from the surface of the groove depth inside the material through equal intervals between the rows as well as each row on depth till reaching stable values of microhardness that corresponds to depth of material hardening layer  $l_h$ . Figure 2, a shows a scheme of microhardness measurement under the groove. Microstructure of heat-affected zone in the area of indentation corresponds to normalizing area (HAZ-2) with uniform fine-grain ferrite-pearlite structure (Figure 2, b). Besides, it was determined that different treatment rates were characterized with different maximum depth of hardening layer. It should also be noted that in the samples of the first and second series independent on technology of their manu-

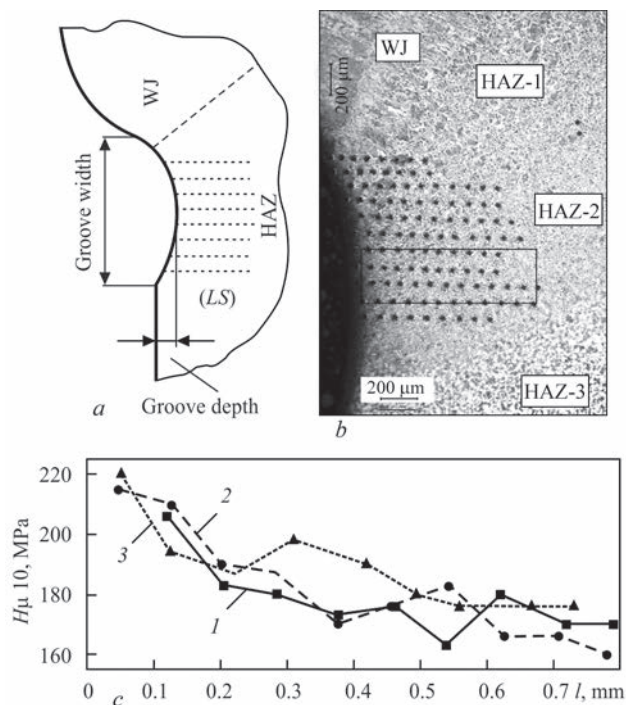


**Figure 2.** Welded joint zone with hardening layer in section plane (LS) after HMP effect with 0.116 m/min rate; a, b — scheme of measurement of microhardness under groove and microstructure with dents, respectively; c — change of microhardness  $H_\mu$  depending on depth  $l$  of material (HAZ-1, HAZ-2, HAZ-3 — areas of coarse grain, normalizing, incomplete resolidification, respectively)

facture the depth of the groove and hardened layer at comparable rates of peening are virtually the same. The similar values of hardened layer can also be explained by the fact that measurements were carried out on side surface of the sample, where effect of RS is virtually absent. Figure 2, *c* as an example shows the results of measurements of microhardness at material depth  $l$  after HMP of the sample with 0.116 m/min rate. Analysis of  $(H_\mu - l)$  dependence showed that in each of selected directions there is decrease of microhardness with removal from the surface into material depth. According to the expectations, the maximum depth of hardened layer is reached on the line matching to the maximum groove depth (curve 1) with gradual decrease at removal from its center. Later on the maximum  $l_h$  value will be used in calculations. It should also be noted that the values of microhardness are somewhat decreased with rise of HMP rate. The results of measurements of  $h$  and  $l_h$  in the samples of both series obtained after different rates of HMP are given in Table 1.

It is determined that decrease of peening rate provokes increase of depth of hardening layer and groove with a coefficient of proportionality after processing of the results using least square method being equal to  $K = h/l_h = 0.106$ . This allows calculating with small error a groove depth being set by any random values of depth of the hardened layer (see Table 1).

Analysis of effect of the hardened layer depth on hardening effect, appearing in rise of welded joint fatigue limit was carried out based on Figure 3. It represents experimentally determined fatigue limits of butt welded joints in the initial state ( $\sigma_R^\mu = 200$  MPa) [8] and 0.06 m/min HMP rate in the samples of the first ( $\sigma_R = 275$  MPa) and second ( $\sigma_R = 375$  MPa) series at working tool oscillation amplitude  $a = 19$   $\mu\text{m}$  as well as corresponding to them values of depth of the hardened layer. The calculation dependence of welded joint fatigue limit on current depth of hardened layer  $l_i$  in this case is the following:

$$\sigma_R^j = \sigma_R^\mu + Cl_i = \sigma_R^\mu + \frac{\sigma_R - \sigma_R^\mu}{l_h} l_i, \quad (1)$$

where  $C = \frac{\sigma_R - \sigma_R^\mu}{l_h}$  is the coefficient of proportionality having its value for each series of samples.

Using the known values of fatigue limits of the welded joint and experimentally determined  $l_h = 1.32$  mm (see Table 1) it was determined that  $C = 56.82$  MPa/mm for the samples of the first series and 132.6 MPa for the second. Assumption of proportional increase of the welded joint fatigue limit with rise of depth of the hardening layer, is proved by available references [12]. It should be noted that

**Table 1.** Value of maximum depth of hardened layer and groove in the samples of first and second series, obtained after HMP with different rate

HMP rate, m/min	Depth of hardened layer $l_h$ , mm	Groove depth $h$ , mm		Error, %
		Experiment	Calculation	
0.232	0.4	0.041	0.043	4.8
0.116	0.65	0.062	0.069	11
0.06	1.32	0.143	0.14	2.1

obtained in the work maximum depth of the hardened layer for the samples of second series is considered as limiting one, since its further rise, first of all, can have no hardening and there is rise of probability of underlayer fracture [12], and secondly, at large stresses it would be impossible to eliminate accumulation of significant cyclic inelastic deformations at the level of fatigue limit that eliminates application of elasticity theory formula [13]. In this case, the fatigue limit, determined at zero-to-compression harmonic stress cycle is considered as a limiting stress.

Thus, the proposed expression allows in a calculation way evaluating the fatigue limit of butt welded joint (dark points) from deformation hardening and change of stress concentration (line 1) as well as additional effect of residual compression stresses (line 2) at any depth of the hardened layer without laboriousness and long-term tests. Besides, the analysis of the obtained results indicates that increases of fatigue limit of the welded samples of the first series made 38 % (line 1) and maximum increase of fatigue limit of the samples of the second series was 87 % (line 2). It is easy to determine that portion of effect of compression RS on increment of fatigue limit at 0.06 m/min HMP rate made 57 % and at set in work [14] 14 % reduction of coefficient of stress concentration after HMP the rise of fatigue limit due to deformation hardening of material surface layer made 37 %, decrease of stress concentration was 6 %. However, portion of

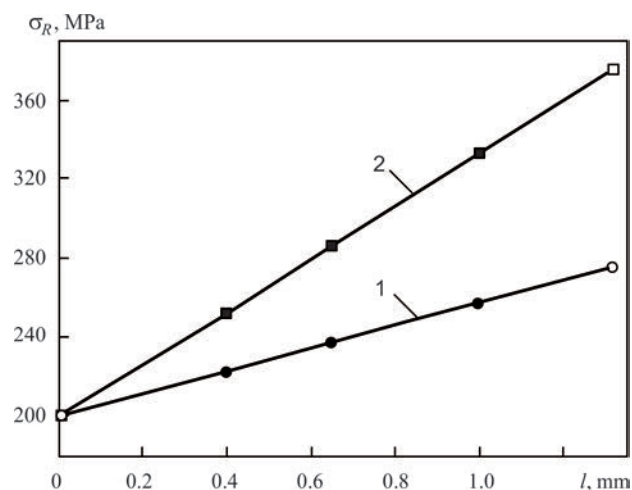


**Figure 3.** Calculation (dark points) and experimental (white points) depending on fatigue limits of hardened welded joints of the first (1) and second (2) series on depth of plastically deformed layer

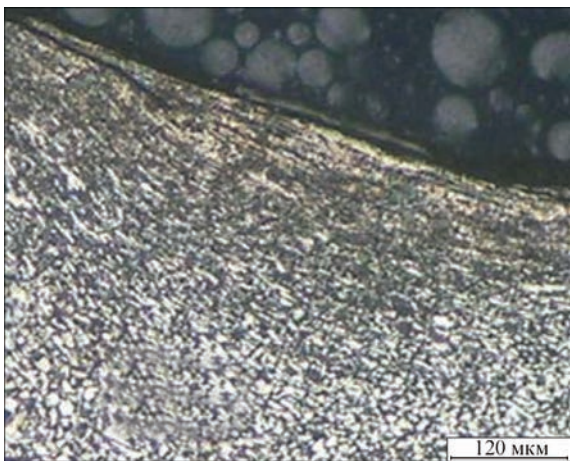


**Figure 4.** Microstructure of hardened layer under groove bottom in the zone of weld to base metal fusion

each factor requires additional experimental proof. It should be noted that deformation hardening of surface layer of the groove results not only in rise of physico-mechanical properties of the material, but also, as it is shown by metallographic examinations, forming of grains in the hardened layer under its bottom (Figure 4), depth of which depends on peening rate and visually varies in 200–250µm range. This factor can also influence the fatigue resistance of investigated material. However, in order to outline the portion of influence in rise of fatigue resistance of formed after HMP «fiber» structure of the hardened layer it is necessary to set up a special experiment. Thus, increase of the butt welded samples fatigue resistance in the absolute value due to compression RS, deformation hardening and change of stress concentration made 100, 65 and 10 MPa, respectively. Considering small contribution of stress concentration, it can be noted that after HMP the increase of fatigue resistance of the welded joints takes place as a result of influence of compression RS and deformation hardening of the surface layer of groove material.

Since measurement of  $l_h$  is related with specific technical difficulties, including presence of necessary equipment, and considering available linear dependence between  $h$  and  $l_h$ , rise of the fatigue limit after HMP of different rate can be easily calculated on the depth of groove as the simpler controlled parameter. In this case, a coefficient of proportionality, taking

into account earlier set dependence ( $K = h/l_h$ ) is determined as  $K_1 = (\sigma_R - \sigma_R^u)K/h$ . The expression for calculated determination of welded joint fatigue limit will be written as:

$$\sigma_R^j = \sigma_R^u + \frac{(\sigma_R - \sigma_R^u)K}{h} \frac{h_i}{K} = \sigma_R^u + \frac{(\sigma_R - \sigma_R^u)}{h} h_i, \quad (2)$$

where  $h_i$  is the current value of groove depth obtained after HMP of different rate.

Calculation values  $\sigma_R^j$  for each series of samples are given in Table 2. A good matching with the experimentally obtained fatigue limits should not go without mention. It should be noted that the groove depth ( $h = 0.14\text{mm}$ ) for this thickness of rolled stock is the optimum one [8] and its further rise can have no hardening.

It is known that the groove depth to significant degree depends on amplitude ( $a$ ) of working tool oscillations. The practice showed that in the most cases the welded elements of metal structures are treated at  $a$  varying in 19–26 µm limits. In this connection, using earlier obtained dependencies of the groove depth on HMP rate at 19 and 26 µm amplitudes [8], Figure 5 represents the diagrams, which allow setting the relationship between the depth of groove and peening rate at different amplitude of the working tool oscillations from the one side (Figure 5, *a*) as well as the fatigue limits of welded joints of both series (see Table 2) from other one (Figure 5, *b*), respectively. Analysis of the results presented in such form allows making several conclusions. At set rate of peening it is possible to determine the change of groove depth depending on amplitude of the working tool oscillations (Figure 5, *a*) as well as change of fatigue limit of the welded joints of the first and second series (Figure 5, *b*). It follows from the diagrams (Figure 5, *a*) that rise of treatment rate not only reduces the groove depth, but also effect of working tool oscillation amplitude on its change becomes less obvious since curves 1 and 2 match. This, on the one hand, results in decrease of fatigue resistance of the first (curve 1) and second (curve 2) series samples (Figure 5, *b*), and, on the other, influence of working tool oscillation amplitude on its change becomes less effective. At  $V = 0.4 \text{ m/min}$   $h$  has virtually no dependence on  $a$  that determines in turn the similar values of welded joint fatigue lim-

**Table 2.** Dependence of welded joint fatigue limits on depth of groove and corresponding to them HMP rate at different amplitude of working tool oscillations

Depth of hardened layer $l_h$ , mm	Depth of groove $h$ , mm	Fatigue limit, MPa		HMP rate, m/min	
		Calculation	Experiment	$a = 19 \mu\text{m}$	$a = 26 \mu\text{m}$
0.39	0.041	220*/250	–	0.4	0.4
0.58	0.062	233*/278	–	0.112	0.24
0.94	0.1	254*/325	–	0.075	0.125
1.35	0.143	277*/378	275*/375	0.06	0.09

\* — data deal with the samples of first series.

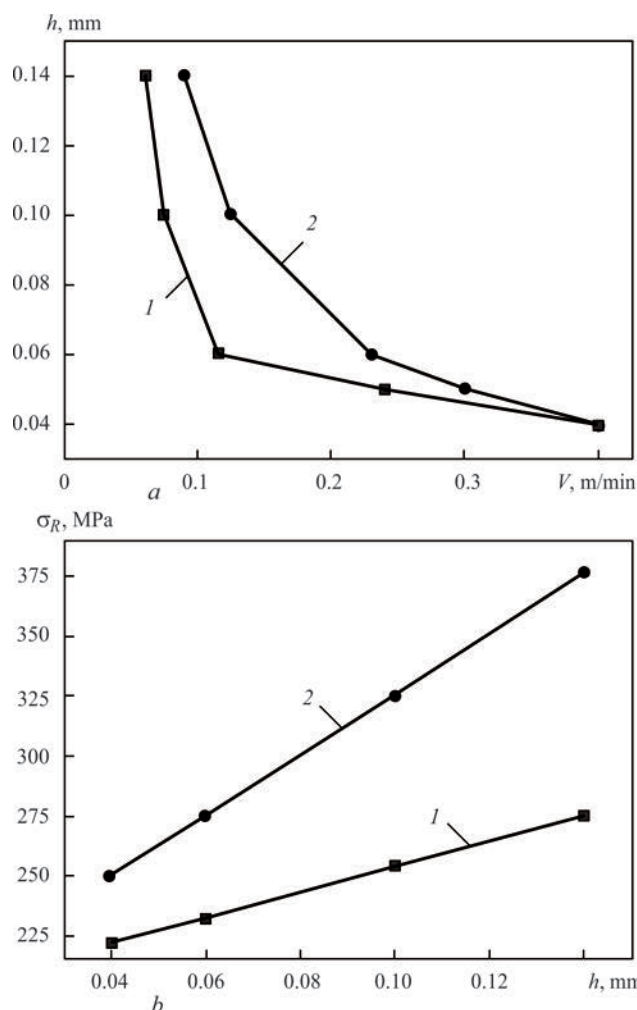


**Figure 5.** Dependence between groove depth and HMP rate at working tool oscillation amplitude 19 (1) and 26  $\mu\text{m}$  (2) —  $a$ , as well as fatigue limits of hardened welded joints of the first (1) and second (2) series —  $b$

it, which for the sample of the first and second series equal to 220 and 250 MPa, respectively. The analysis of the results also showed that rise of  $h$  provokes deviation of curves 1 and 2 (Figure 5,  $b$ ). This indicates that the place and order of application of hardening technology in the technological cycle of product manufacture has significant value.

Sometimes at repair-reconstruction works in difficult of access places of the element structures it is not always possible to get reliable determination of groove depth and it is easy to register peening rate. In this connection Figure 6 provides the dependencies of welded joint fatigue limits of both series on peening rate determined at working tool oscillation amplitude 19 and 26  $\mu\text{m}$ , respectively. Analysis of the obtained data shows that in each series the rise of  $V$  provokes not only reduction of the fatigue limits, but also decrease of difference between them. It follows from Figure that at  $V = 0.4$  m/min the efficiency of increase of welded joint fatigue resistance only due to deformation hardening (curves 1, 2) or mutual effect of mentioned factors (curves 3, 4) virtually does not

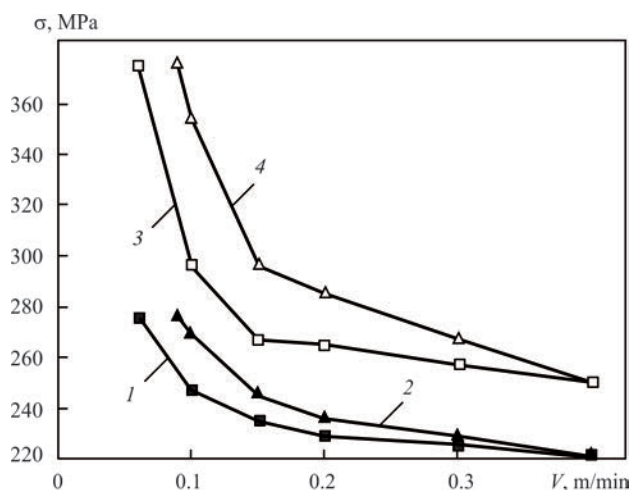


**Figure 6.** Dependence of fatigue limits of butt welded joints of first (1, 2) and second (3, 4) series on HMP rate in amplitude of working tool oscillations 19 (1, 3) and 26  $\mu\text{m}$  (2, 4)

depend on working tool oscillation amplitude. The fatigue limits have similar values, which by 11 % for the first series of the samples and 26 % for the second one exceed the welded joint fatigue limit in the initial state. Besides, it can be seen that independent on  $a$  the rise of peening rate results in insignificant decrease of difference of fatigue limits between both series.

Relative rise of the fatigue limits of the both series of welded joints, determined after HMP of different rate in the range of change of working tool oscillation amplitude from 19 to 26  $\mu\text{m}$ , following from the assumption on proportional increase of fatigue limit, illustrates well the dependencies given in Figure 7. Their calculation values at current oscillation amplitude of working tool  $a_i$  can be determined by equation in form of:

$$\frac{\sigma_R^i}{\sigma_R^u} = \frac{\sigma_{R1}}{\sigma_R^u} + \frac{\sigma_{R2} - \sigma_{R1}}{\sigma_R^u (a_2 - a_1)} (a_i - a_1), \quad (3)$$

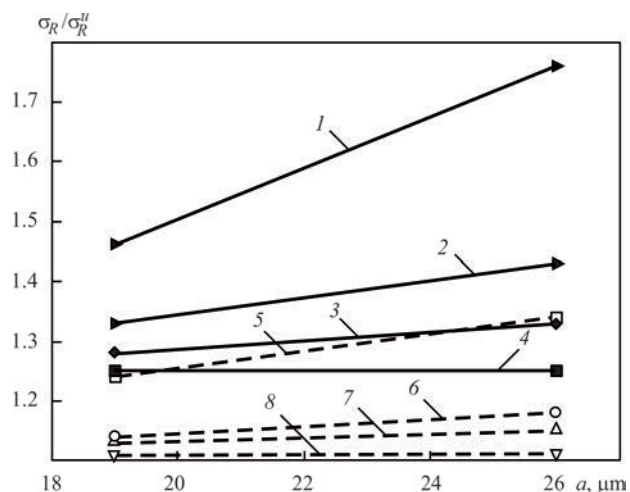


**Figure 7.** Relative increase of fatigue limits of butt welded joints of first (5–8) and second (1–4) series, determined after HMP with the different rate in range of change of working tool oscillation amplitude 19–26  $\mu\text{m}$ : 1 —  $V = 0.1$ ; 2 — 0.2; 3 — 0.3; 4 — 0.4; 5 — 0.1; 6 — 0.2; 7 — 0.3; 8 — 0.4

**Table 3.** Calculation values of fatigue limits of butt welded joints determined at different rates of HMP and amplitudes of working tool oscillations

V, m/min	Fatigue limit $\sigma_R$ , MPa		$\beta \cdot 10^{-2}$ , $\mu\text{m}^{-1}$
	$a_1 = 19 \mu\text{m}$	$a_2 = 26 \mu\text{m}$	
0.1	247*/295	269*/355	1.43*/4.29
0.2	229*/268	235*/290	0.57*/1.79
0.3	225*/255	230*/265	0.286*/0.714
0.4	222*/250	222*/250	0

\* — data deal with the samples of first series.

where  $\sigma_{R1}$  and  $\sigma_{R2}$  are the fatigue limits of each series of welded joints determined after different rate HMP at working tool oscillation amplitude  $a_1 = 19$  and  $a_2 = 26 \mu\text{m}$ , respectively (Table 3);  $\beta = \frac{\sigma_{R2} - \sigma_{R1}}{\sigma_R^u (a_2 - a_1)}$  is the coefficient having its value for each rate of peening;  $\sigma_R^u = 200$  MPa is the welded joint fatigue limit in the initial state.

It follows from the Figure analysis that increase of peening rate independent on amplitude of the working tool oscillations provokes decrease of efficiency of rise of the fatigue resistance of welded joint only due to deformation hardening (curves 5–8) or combination of all factors (curves 1–4). It should be noted that compression RS are more sensitive to  $V$  change since difference between 1–4 curves is more significant at different working tool oscillation amplitude. However, at  $V = 0.4$  m/min the difference between the fatigue limits of samples of the first and second series becomes the same independent on  $a$ . It indicates that contribution of compression RS in increase of fatigue resistance of welded joints independent on working tool oscillation amplitude is virtually the same.

It can be seen that at such rate of treatment the effect of only deformation hardening is also the same independent on  $a$ . Since reduction of peening rate and increase of the working tool oscillation amplitude provokes more intensive rise of the fatigue limits in the samples of second series, it is possible to make a conclusion that the most effective increase of fatigue resistance can be achieved by application of HMP technology via selection of the corresponding modes of hardening at the last stage of production of metal structure welded elements.

Thus, presented data gave the possibility, first of all, to determine the fatigue limits of butt welded joints after different modes HMP on groove depth or plastically deformed material layer, and secondly, to make more conscious choice of the optimum modes of HMP at various combination of its rate and amplitude of the

working tool oscillations considering the technology of manufacture of metal structure elements.

## Conclusions

1. The procedure was proposed for determination of fatigue limits of welded joints of low-carbon steel on groove depth and depth of plastically deformed layer of the material under its bottom in the weld to base metal fusion zone.

2. It is shown that there is satisfactory correlation dependence for butt welded joints between the groove depth and depth of plastically deformed layer obtained after different modes of high-frequency mechanical peening.

3. Efficiency of increase of welded joint fatigue limit of different manufacture technology depending on rate of high-frequency mechanical peening and working tool oscillation amplitude was determined.

- Roy, S., Fisher, J.W., Yen, B.T. (2003) Fatigue resistance of welded details enhanced by ultrasonic impact treatment (UIT). *Int. J. Fatigue*, **25**, 1239–1247.
- Wang, T., Wang, D., Huo, L., Zang, Y. (2008) Discussion on fatigue design of welded joints enhanced by ultrasonic peening treatment (UPT). *Ibid.*, **4**, 1–7.
- Zhao, X., Wang, D., Huo, L. (2011) Analysis of the S–N curves of welded joints enhanced by ultrasonic peening treatment. *Materials and Design*, **32**(1), 88–96.
- Marguis, G. (2010) Failure modes and fatigue strength of improved HSS welds. *Engineering Fracture Mechanics*, **77**, 2051–2062.
- Trufiyakov, V.I., Statnikov, E.Sh., Mikheev, P.P., Kuzmenko, A.Z. (1998) The efficiency of ultrasonic impact treatment for improving the fatigue strength of welded joints. *Intern. Inst. of Welding. IIW Doc. XIII-1745–98*, 12.
- Lobanov, L.M., Kirian, V.I., Knysh, V.V., Prokopenko, G.I. (2006) Improvement of fatigue resistance of welded joints in metal structures by high-frequency mechanical peening (Review). *The Paton Welding J.*, **9**, 2–8.
- Mikheev, P.P., Nedoseka, A.Ya., Parkhomenko, I.V. (1984) Efficiency of application of ultrasonic impact treatment for improvement of fatigue resistance of welded joints. *Avtomatich. Svarka*, **3**, 4–7 [in Russian].
- Degtyarev, V.A. (2011) Evaluation of effect of high-frequency mechanical peening modes of welded joints on their fatigue resistance. *Problemy Prochnosti*, **2**, 61–70 [in Russian].
- Prokopenko, G.I., Kleiman, Ya.I., Kozlov, O.V. et al. (2002) *Device for ultrasonic peening treatment of metals*. Pat. 47536, Ukraine [in Ukrainian].
- Knysh, V.V., Solovej, S.A., Bogajchuk, I.L. (2011) Optimisation of the process of strengthening of welded joints of 09G2S steel by high-frequency mechanical peening. *The Paton Welding J.*, **5**, 20–24.
- GOST 9450–76: Measurement of microhardness by indentation of diamond cone. Introd. 01.01.1977 [in Russian].
- Serensen, S.V., Kogaev, V.P., Shnejderovich, R.M. (1975) *Load-carrying capacity and strength design of machine parts*. Moscow, Mashinostroenie [in Russian].
- Manson, S.S., Muralidharam, U. (1987) Fatigue life prediction in bending from axial fatigue information. *Fatigue Fract. Eng. Mater. Struct.*, **9**(5), 357–372.
- Kirian, V.I., Knysh, V.V. (2008) High-frequency mechanical peening of welded joints of metal structures. *Svarochn. Proizvodstvo*, **11**, 36–41 [in Russian].

Received 24.10.2018

## HEAT TREATMENT OF WELDED JOINTS OF HIGH-STRENGTH RAILWAY RAILS (REVIEW)

R.S. GUBATYUK

E.O. Paton Electric Welding Institute of the NAS of Ukraine  
11 Kazimir Malevich Str., 03150, Kyiv, Ukraine. E-mail: [office@paton.kiev.ua](mailto:office@paton.kiev.ua)

In construction of high-speed continuous welded railway lines the high-strength rails, welded by different methods, have a mass application. With the appearance of high-strength rails with a high carbon content, the necessity of implementation of heat treatment operation of butt welded joints in a cycle of rail section manufacture became urgent. The aim of the presented review is the analysis of problems and forecasting the prospects of nowadays technologies of heat treatment of high-strength rail butt welded joints. Different methods of heat treatment used in industry were considered. Different schemes of heating and cooling of rail weld and their effect on formation of microstructure and mechanical properties of joint metal were analyzed. A review of references showed that the technology of high-frequency current heating with further hardening of a head is the most requested during heat treatment of butt welded joints of high-strength rails. 31 Ref., 6 Figures.

**Keywords:** *continuous rail track, high-strength rails, butt welded joints, heat treatment, hardness, microstructure, high-frequency currents, defects*

The world experience shows, that the promising development of railways requires the creation of high-speed railway lines. The solution of this task puts forward new requirements to the railway track and its main element: rails and their continuous joining along the entire length of the track.

In the last decade, a tendency to increase the intensity, speed and traffic density on railways is observed in the world, which makes it necessary to increase the reliability and service life of rails and causes a high level of requirements to them as to the hardness, contact-fatigue strength, resistance to formation of contact-fatigue defects and brittle fracture [1].

With an increase in the traffic speed and an increase in the mass of the transported cargoes, the dynamic effect both on the wheel pair, as well as on the railway track is increased. One of the main disadvantages of the link track is the presence of a butt joint. The rail butt joint is the place, where the «break» of the rail line occurs, which, despite the butt cover plates, reduces stiffness and increases deflection. This leads to the fact that when the rolling stock moves through the butt joint, the wheel hits the head of the receiving end of the rail. Shocks and impacts at the joints lead to intense wear on both the running gears of the rolling stock and the rails themselves. As a result of wheel strikes on the oncoming rail, crumpling and spalling of the rail head in the joint zone at a distance of 60–80 mm from the butt gap, fractures of rails across the bolt holes, fractures of cover plates and butt bolts occur [2].

In this regard, there is a tendency in the world to replace the butt bolted joints of railway rails by welded

joints. The continuous welded track is free from disadvantages of butt joints and has several advantages [3]:

- saving of metal due to reducing the number of butt joining;
- up to 30 % reduction in the costs for repair of track and rolling stock;
- increase in the service life of the upper structure of the track, as well as the rolling stock due to a decrease in the number of wheel strikes of cars and locomotives at the joint point of rail sections;
- reduction of the main specific resistance to the traffic of trains to 12 % and, in this regard, saving of diesel fuel and electricity for traction;
- reducing the volume of works on the straightening the track associated with deflections in the butt joints;
- absence of rail breaks across the bolt holes, one of the main types of breaks in the link track;
- improving the comfort conditions of passenger travel, reducing noise levels;
- reducing the pollution of the track with bulk cargoes and the environment with dusty cargoes;
- improving the reliability of electric rail circuits of automatic blocking, etc.

Nowadays, high-strength rails of such leading manufacturers as Voestalpine (R350NT, Austria), Nippon Steel (VS-350Ya, VS-350LDT, Japan), Corus British Steel (BS113A, Great Britain), PIETC (U75V, China), Azovstal Iron and Steel Works (K76F, Ukraine), OJSC Nizhny Tagil Metallurgical Plant (E76F, Russia), Novokuznetsk Metallurgical Plant (K76T, Russia) are widely applied. High-strength rails have characteristics of metal strength being 1.3–1.5 times higher than that in ordinary rails (Fig-

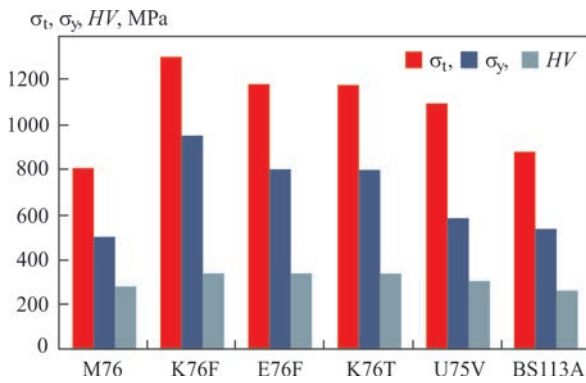


Figure 1. Strength characteristics of rails

ures 1, 2), while the requirements to ductile properties in accordance with standard indices remained at the same level [4]. In the production of high-strength rails, the production technology is used with continuous casting of steel and continuous rolling. Figure 3 shows the distribution of hardness in the base metal of high-strength rails in the vertical plane [5].

High-strength rails have a significant carbon content (0.9–1.1 %) for improvement of wear resistance. In the production of such rails, coarse carbides remain inside the austenite grains, thus reducing the ductility and impact toughness of pearlite structure after accelerated cooling. From the point of view of the structure of rail steel, the increase in its carbon content drastically changed the weldability of such steel. At the present stage of development of equipment for welding production technology, in terms of the main factor of steel weldability, high-carbon steel is close to high-strength medium-alloyed steels with a carbon content of 0.3–0.45 %. The value of indicates of carbon equivalent, calculated by the formula [6] for these steels, is approximately the same —  $S_{eqv} =$

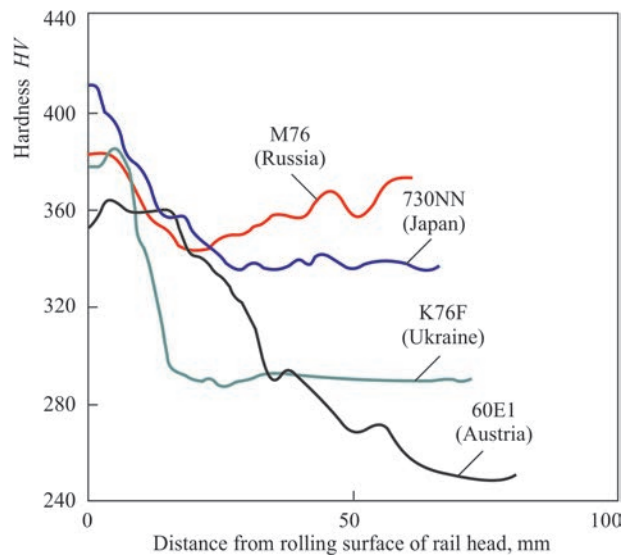


Figure 3. Distribution of hardness in base metal of high-strength rails in the vertical plane [5]

$= 0.80\text{--}1.0 \%$ . Thus, high-carbon rail steels are fair by the quality criterion of weldability, i.e. when it is impossible to provide metallic integrity of the joint without special technological measures and rational modes of welding [7].

Nowadays, in the world practice, the rails are welded by the following methods during the construction of continuous welded track [8]:

- pressure methods: flash-butt welding, gas pressure welding, induction welding, laser welding, friction welding;
- aluminothermic methods;
- electric arc methods: welding with stick electrodes, submerged-arc welding, shielded-gas welding, electro-slag welding, welding with flux-cored wires, etc.

The method of pressure welding is based on heating the rail ends to the temperature of plastic state and their pressing at a certain force. The ends of rails can be heated by electric current, gas torches, high-frequency currents, laser, plasma and heat evolved by friction. During pressure welding a filler material is not used, the ends of rails are welded together. When using pressure welding, the strength and reliability of welded rail joints is primarily determined by the correct choice of welding technology and modes.

Aluminothermic and electric arc methods differ significantly from pressure welding methods by the fact that a weld is 15–25 mm wide, and consists mostly of a filler material, having a cast structure [9]. The quality of welded rail joints and their life also depend on the properties of filler materials.

Among the abovementioned methods of rails welding, the electric flash-butt welding method became the most widely used [10]. This method provides a high quality of welded joint, high process efficiency, high automation and mechanization of the process and

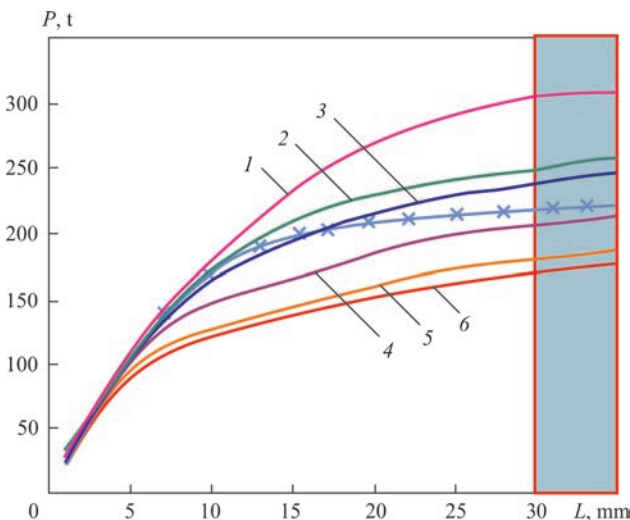


Figure 2. Dependence of loading during testing on static bending from deflection of rail [4]: 1 — NKMK E78KhS (Russia); 2 — NKMK, NTMK E76F, K76F (Russia, 2012); 3 — NKMK, NTMK E76F, K76F (Russia, 2003); 4 — Azovstal KF (Ukraine); 5 — U75V (PRC); 6 — Azovstal M76 (Ukraine)

availability of a system to monitor welding mode parameters.

For all welding methods the presence of heat-affected zone (HAZ) is typical. The resulting residual stresses in the HAZ metal lead to decrease in strength characteristics of welded joint. The width of the HAZ effect depends on the time of exposure of high temperatures to the base metal, mass of the filler material, method and welding parameters [11].

Every year the number of defect-proof welded rail joints increases, the number of rail breaks in welded joints also increases. These welding defects are observed in recent years when the rails of electric steel are used for construction of a continuous track [3, 12].

The zone of welded butt joints is a weak area of rail track. As practice shows, the number of defects in removed defective rails reaches 30 % in welds at a total weld length of not more than 2 % of rail section length. This is caused by varying homogeneity of microstructure in the regions of the weld and HAZ, as well as by creating an unfavorable residual stress diagram. During welding, the conditions are created for the formation of inner defects, which are stress concentrators and weaken the rail section with a weld, as well as for distortion of the rail in the weld zone with subsequent formation of deflections during service of saddles. Most of the rail defects occur in the head region. In the head, defects in the form of transverse cracks make up 33 %. They occur due to insufficient contact-fatigue strength of the metal, violations of technology of welding rails and inner defects. At the same time, the defects, caused by horizontal delamination of the rail head due to the presence of clusters of nonmetallic inclusions, amount to 17 %. Defects, resulting from vertical delamination of the head because of remnants of shrinkage cavity, are 19 %. The remaining volume of defects is caused by chipping of the layer deposited on the head rolling surface, side wear and crumpling of the rail head in the welded butt joint. Figure 4 shows the location of rail defects in the cross-section [6].

The main disadvantages which reduce the service life of rails are [11]:

- presence of residual stresses in the rail head, which occur as a result of cold straightening operation during manufacture;
- creation of weak areas with a lowered resistance to wear and crumpling in the HAZ after welding and local heat treatment of welds;
- noticeable decrease in impact toughness, crack resistance and critical size of fatigue cracks during hardening from rolling heating as compared to hardening after separate recrystallization heating.

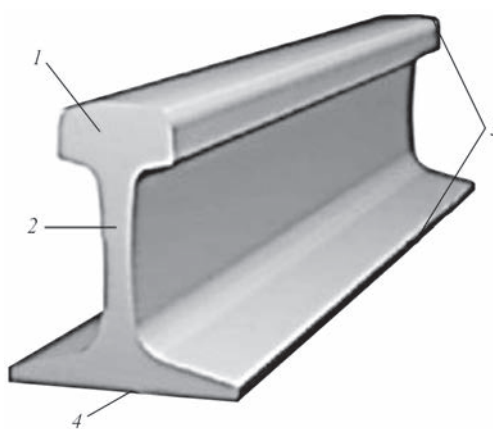


**Figure 4.** Location of rail defects across the cross-section [6]: 1 — in the rail head (74 %); 2 — in the web (7 %); 3 — other defects outside the joint (16 %); 4 — in the rail flange (3 %)

It is known [13], that a welded joint of rails has a coarse-grained structure and lower values of mechanical properties than the base metal. The metal of a welded joint zone, as compared to the metal of rolled rails differs by lower ductility, toughness and higher tendency to brittle fractures. In welded butt joints of high-strength rails, dips of hardness are observed, including the hardened metal layer of a rail head. In the rails of usual strength, the scattering of hardness in the welding zone varies within a small range of *HV* 10–30, and during welding of rails of increased and high strength, in the joints a significant decrease in hardness (on *HV* 100–150), and accordingly, wear resistance and fatigue limit of metal in the rail head are observed.

In the world practice, additional heat treatment (HT) of rail joints is increasingly used, which minimizes the results of high-temperature heating of high-strength rail steels during the process of welding [14, 15]. Additional HT of a rail joint increases its strength properties and refines the microstructure of a welded joint. The use of HT has a positive effect on service life of a welded joint of rails, since the fatigue strength limit is higher than the strength of a welded joint which was not subjected to HT. Brittle strength and impact toughness of the metal of welded rails is increased after local HT of joints, the increase in resistance to brittle fractures of welded rails of regular, enhanced and high strength increases the reliability of their operation in the track. This is especially important in the mass application of rails from the steels of new grades of continuous welded sections and rails in the regions with a severe climate, in express and high-speed lines [16].

In this regard, the problem of determining the optimal modes of HT of welded joints of high-strength rails is relevant. The solution of this problem will increase the service life and reliability of railway lines.

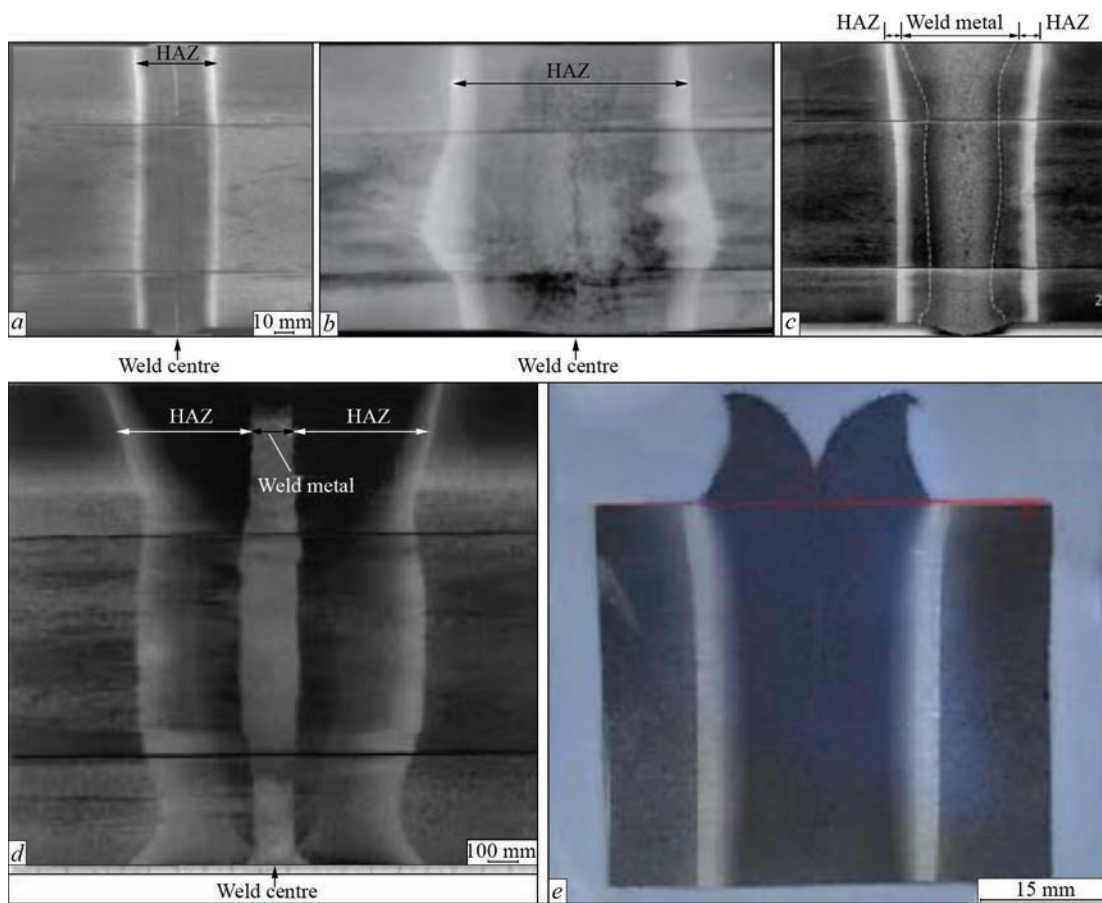


**Figure 5.** Macrostructures of welded rail joint made by different methods [17]: *a* — flash-butt welding; *b* — gas-pressure welding; *c* — aluminothermic welding; *d* — hidden arc welding; *e* — linear friction welding

The highest designed strength is in the rails with a homogeneous sorbite hardened structure of maximum dispersion with a hardness of  $HV\ 331\text{--}388$ , or rails with a homogeneous structure of tempered martensite or bainite. The service life of the rails is directly related to their hardness. Such parameters of rails microstructure as the value of distance between plates in pearlite, size of pearlitic colonies, presence of excessive ferrite also have a great influence on the properties of rails. It is known that pearlite structure is formed during diffusion transformation of austenite in a wide range of temperatures: from about  $720$  to  $450\text{ }^{\circ}\text{C}$  and, as a result, it has a different dispersion, estimated by the value of distance between plates, which can vary by more than an order: from about  $1.0$  to  $0.05\ \mu\text{m}$ . Accordingly, the steel hardness and other characteristics of mechanical properties are changed [17].

It is known (Figure 5) that flash-butt welding and arc welding have minimal zones of cast metal and HAZ. The aluminothermic joint has the largest zone of cast metal and HAZ, gas-pressure method has the largest HAZ of rail steel. In linear friction welding, the cast metal zone is minimal, and HAZ consists of several zones.

Figure 6 presents comparative results on distribution of hardness in a welded joint during welding using

different methods without and with heat treatment of the joint. It is seen that aluminothermic and gas-pressure welding have a dip of hardness in a larger area of a rail joint as compared to other methods [18].

Nowadays, a lot of works has been carried out to determine the rational technology of HT of rail joints of high-strength rails. In different countries of the world, the technologies of HT of welded joints have a radical difference. In Germany, to conduct the HT after welding a joint, the heating is performed by an exothermic powder, which is poured into the steel clinker, surrounding a welded joint, and ignited, burning of powder occurs at a temperature of  $370\text{--}430\text{ }^{\circ}\text{C}$ . A controllable cooling of a joint takes about 30 min, providing a complete pearlite transformation. In the recommendations of the Ministry of Rail Roads (India), in flash-butt welding of high-strength rails a controllable HT after welding should be performed. The HT process takes place in an asbestos pipe of 300 mm diameter, a length of 1 m, which is installed on the rail section with a weld and the joint is heated up to the temperature of  $850\text{ }^{\circ}\text{C}$  by four kerosene torches with a holding of about 10 min, after which the welded joint is moved to hardening device with a compressed dry air. The specialists of the Austrian Company Voestalpine Schienen GmbH recommend apply

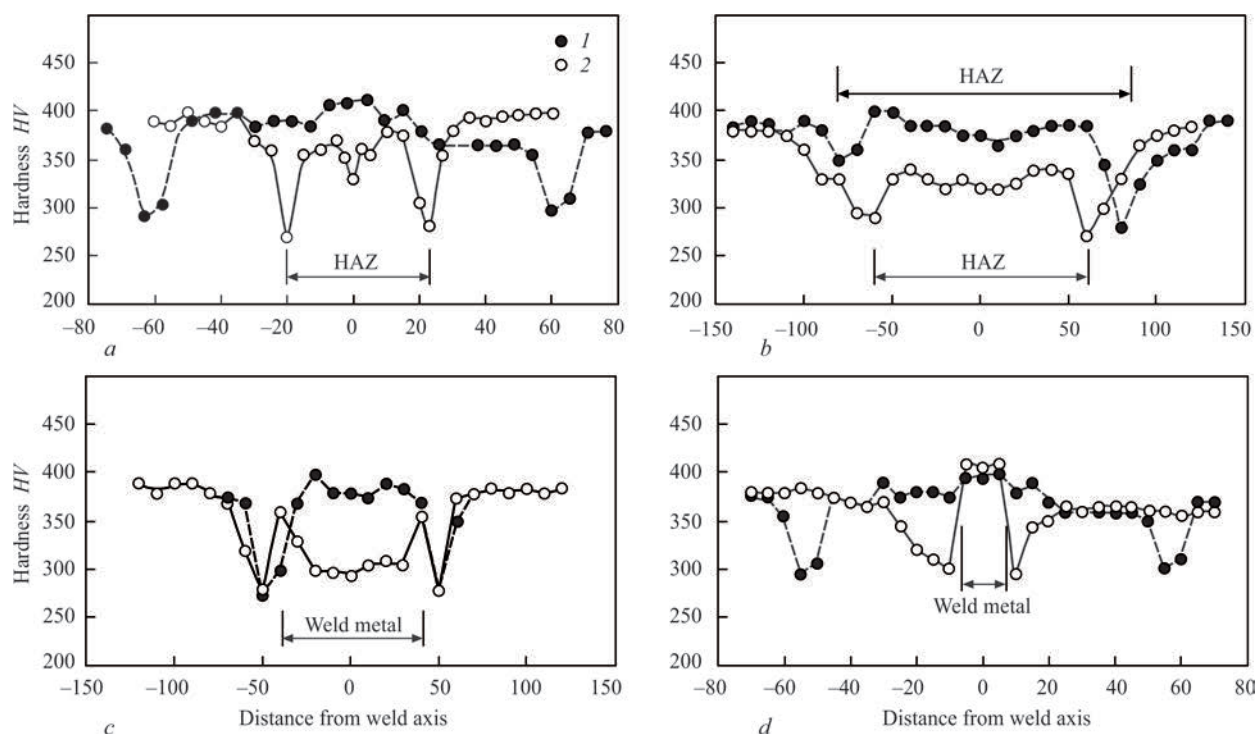


**Figure 6.** Distribution of hardness in the area of rail welded joint made by different methods [13]: *a* — flash-butt welding; *b* — gas-pressure welding; *c* — aluminothermic welding; *d* — hidden arc welding; 1 — after HT, 2 — welded joint

different HT after welding of high-strength rails of the own production of the type R350HT, R370CrHT, R400HT in the form of subsequent heating of a joint, accelerated cooling holding, etc. In the UK, the works were carried out to determine the optimal heating rate, influence of hardening conditions on distribution of residual stresses in a welded joint of high-strength rails and search for an acceptable cycle time. A welded joint was heated with a different heat flux from 75 to 120 kW/m<sup>2</sup> to the temperature of 650 °C and cooled at different rates from 2–5 °C/s. In the course of investigations it was found that the level of residual tensile stresses can be reduced by rapid heating of a welded joint immediately after welding. The results of accelerated cooling showed an improved hardness distribution as compared to the natural air cooling. The Rail Road Research Institute of Japan developed the technology of gas-pressure welding and HT of high-strength rails. After welding, when the temperature of a joint reaches 600 °C, it is reheated by special torches about 90 s up to the temperature of 1000 °C. Then the cooling by a special hardening device to a temperature of 300 °C occurs. In the USA, there is an experience in the construction of railways, using high-strength rails of Japanese production of hyper-eutectoid steel HE-X with a carbon content of 1.1 % and a length of 146 m, which are welded into 440-meter sections. Then, the entire welded section is passed through passing-by induction device for HT, which provides a uniform hardness and homogeneity of the structure over the entire length of a welded section. At

Qinghua University (China), research was carried out on the effect of HT on welded joints of U75Mn rails. HT was carried out by induction heating of the joint to a normalization temperature of 880 °C and tempering temperature of 600 °C. The research results showed that during normalization, the grain size in the welded joint is changed and the mechanical properties of the metal are improved, and the hardness is increased. At a temperature of 600 °C, the hardness parameters were even lower than those of a welded joint without HT [19–25].

In a number of works, it was proved that it is necessary to use a differentiated HT of welded joints, which consists in hardening of a rail head from repeated recrystallization induction heating of its entire cross-section with subsequent normalization of rail flange and web. As a result, the hardness in a rail head increases as well as the fatigue and brittle strength due to the welded joint metal structure refinement. According to the authors' opinion, the differentiated HT of welded rail joints eliminates the zonal heterogeneity of a weld metal [26].

In the opinion of specialists of Tomsk University (Russia), the technology with hardening using air-water mixture is unreliable, because an unfavorable hardened structure of martensite is formed in the metal of the head of a rail welded joint, exceeding the standard hardness of rail steel, which sharply decreases the resistance of rails to fatigue and brittle fracture. Such structural heterogeneity over the rolling surface of a joint leads to crumbling of these areas of metal [27].

The result of the carried out works on HT of welded joints in induction installations of the type ITSM-250/2.4 of the Russian production with a current frequency of 2.4 kHz is a restored hardness to the level of the base metal strength, moreover, a structure of hardened sorbite is formed in the rail head. The yield and fatigue strength of the metal of welded rails is not lower than that of the rolled ones. According to the authors of these works, to provide the strength and reliable operation of the tracks, HT of welded joints of rails of modern production with a high content of carbon and other alloying elements is obligatory [13, 27].

The Tomsk Company MagnitM developed a method of HT of welded rail joints, based on heating of the welded joint by the optimal scheme of temperature field distribution. This method of HT allows eliminating the self-tempering of the rail head after its cooling. Rail hardening is performed by a forced cooling with a compressed air, which is characterized by a more uniform and stable distribution of hardness at the rolling surface in the welded joint zone than during hardening with an air-water mixture. To carry out HT, an effective design of inductor was developed for heating the installation of UIN-100/RT-P type and different frequency of current of the induction heating source of 8.0–16.0 kHz was used [28].

The authors of the work [29] carried out investigations of the effectiveness of different HT methods. It was determined that the use of one-sided hardening cooling scheme, when the air hardening medium acts only on the rail head, leads to the fact that the joint zone, heated to a temperature above the critical one, sharply reduces the volume during cooling, which leads to its compression. The remaining high temperature in the flange leads to a plastic deformation, which causes the rail deformation and deflection on the flange. To eliminate the negative effect of stress in the rail flange, the authors propose a technology with the applying of a differentiated double-sided scheme of the hardening cooling. The scheme provides the hardening cooling of the rail head and subcooling of its flange to preserve the rail geometry and allows obtaining a favorable diagram of compressive stresses in the head and the flange and compensating tensile stresses in the web. After conducting HT, the microstructure of the weld metal in the rail head and flange is represented by sorbite, and in the web it is represented by lamellar and granular sorbite of a mixed morphology.

According to the author of the work [30], installations of the type UIN-001 have a design with an excessively wide inductor, which in the process of HT leads to an excessive increase in the HAZ, heating time and the effect of high temperatures on the rail

metal. Since the rail profile has a complex cross-sectional shape with different volumes of metal, then to have a uniform distribution of the temperature field over the cross-section the specialists of the E.O. Paton Electric Welding Institute proposed to reduce the current frequency to 2.4 kHz and apply a special design of inductors with magnetic conductors. Due to that, a magnetic coupling between the inductor and welded joint is improved, and a uniform distribution of the power input into the heated rail joint occurs. A part of the power, transmitted to the head and to the flange is increased as compared to that to the web, and it is decreased in the rail tongues, thus preventing their overheating. As a result, a uniform heating of the entire cross-section of the welded joint of the rail is provided with the allowable gradient of the temperature field drop. As a result, HT of welded joints positively changed the microstructure of the welded joint metal; the hardness was uniformly distributed across the HAZ width.

Different modern equipment, developed for the process of HT of welded joints of rails, allows carrying out HT process in the form of a single technological operation in one and the same induction equipment for various steel grades and different types and sizes of rails. This is provided by a rational choice of heat treatment mode.

Some recommendations exist as to conducting HT of welded joints of high-strength rails. At induction heating of a joint treated below the critical point  $A_1$  (690–730 °C) and a significant holding at this temperature, recrystallization and partial growth of grain sizes can occur. At such a holding, the carbides formed during welding can again dissolve in the ferrite matrix. At the same time, a slow cooling again promotes the formation of such carbides, which can lead to a decrease in the service life of rails. Therefore, during induction heating of rail steel it is recommended to perform a quick heating to a maximum temperature above the point  $A_1$ , with a minimum holding or without it, and to cool rapidly to the temperature of 600–650 °C. In this case, sorbite-shaped pearlite is formed with a degraded ferrite network, at the same time fine cementite dissolves in the ferrite matrix, which increases the weld hardness. In case of rapid cooling of steel, containing 0.71 % of carbon, in the temperature range  $A_1 < T < A_3$ , the austenitic grains transform into martensite and a hardened rail joint is formed. As is known, martensite has a high hardness and at the same time high brittleness. A slow cooling of <10 °C/s from the annealing temperature to  $A_1$  and a forced cooling with compressed air to a temperature of 510–420 °C can form a bainite structure, which has a high strength and impact toughness, but the hard-

ness of such a structure turns out to be higher than the standard hardness of rail steel [31].

It can also be said that the development of railways follows the path of construction of high-speed and cargo-intensive main lines, which make the operating conditions of a railway more severe and require the improvement of quality of both the rails themselves, as well as their welded joints. Manufacturers maintain trends to increase the carbon content in rail steel, develop new rail alloying systems and HT technologies, which improve their operational properties. To reduce damages of the rails, it is necessary to provide high hardness, wear resistance, contact-fatigue strength of the head metal and at the same time the plasticity and resistance to alternating loads in the web and flange. This review shows that despite great successes in the field of HT in improving the reliability of rail welded joints, the existing HT technologies do not provide a sufficient stability of service properties and do not fully allow obtaining the required operational characteristics of rail welds. Therefore, it becomes necessary to carry out further investigations and study the kinetics of phase transformations in a rail welded joint in the process of heating and cooling during HT, which will help to solve the specified problem. For today in the world there is no single established opinion on the performance of HT technological process by a number of parameters: heating source, power, type of hardening medium, temperature and time factors for welded joints of high-strength rails, with similar weight and geometry parameters. At HT there is no clear definition of the effect zone at HT, which, in turn, depends on the method of making welded joint of railway rails. Preferred are the methods for making welded joints with a minimum width of the HAZ, such as flash-butt welding of rails and subsequent HT of welded joint.

A widespread application in conducting HT of welded joints of high-strength rails was obtained by the method of high-frequency current heating, which has several advantages as compared to other methods. This method allows controlling the heating process, being controlled in terms of the required amount of energy input, including also at a certain metal depth, provides a more uniform heating of welded joint across the entire cross-section, reduces the heating time, and consequently, the effect of high temperatures on the welded joint metal. It should be noted that in the literature, the influence of the modes of induction heating and cooling on the structure of rail steel as well as the effect of the formed structure on the service life are almost not analyzed. Indeed, the cooling forms to a greater extent the structure of the metal and its properties.

One of the limiting factors for spreading of the technological process of HT with the high-frequency current heating of welded joints of railway rails is the complex process of determining the shape and design of the working member, i.e. inductor, which should meet all the requirements of the technological process of HT. The shape and design of the inductor depend on many characteristics: geometric (complex cross-sectional shape of rails, mass and dimensional indices of the components of a rail parts: heads, webs, flanges), electrical (operating frequency, electromagnetic parameters of the system), thermal (heating rate, holding time, cooling rate, distribution of heat fluxes in the complex geometry of metal volumes in the zone of welded joint and base metal), as well as the places of conducting HT of welded joints of railway rails (rail welding enterprise, field conditions, repair).

In this regard, an urgent task is to create a new complex of equipment for HT, which will meet the modern requirements to the determination of the optimal modes of HT of welded joints of high-strength rails to improve the life and reliability of railway lines.

In conclusion, let us note that the existing technologies of HT of welded joints of high-strength rails need further investigation of the process, as far as at the present stage the existing HT technologies do not fully provide a sufficient homogeneity of properties of welded joint and base metal.

Moreover, it is necessary to carry out further investigations on the effect of heating rates, holding and cooling time on the features of structure formation by controlling the thermal cycle modes in the temperature range of phase transformations and the effect on structural fraction of phase components in a welded joint, which determine its reliability and life.

The width of the zone of influence at the HT of welded joint is also not accurately determined. When studying the HT process, it is necessary to determine such a zone, which would maximize the homogeneity of welded joint with base metal of a rail and reduce its sensitivity to stress concentrators.

To solve the general problem, it is necessary to take into account the complex cross-sectional shape of welded rail and distribution of heat fluxes in the welded joint metal and along the rail axis. The application of methods of physical and mathematical modeling is important to determine the required heat fields, electromagnetic parameters of the system and phase transformations at HT of rail welded joint.

1. Gromov, V.E., Yuriev, A.B., Morozov, K.V. et al. (2014) Comparative analysis of structural-phase states in rails after volume and differential hardening. *Stal*, 7, 91–95 [in Russian].

2. Voronin, N.N., Prokhorov, N.N., Trynkova, O.N. (2012) Reserves of aluminothermic welding of rails. *Mir Transporta*, **2**, 76–83 [in Russian].
3. Zhadan, G.I. (2012) Assessment of measures on improvement of continuous welded rail track from viewpoint of resource-saving. *Zbirnyk Naukovykh Prats DonIIZT*, **32**, 263–268 [in Russian].
4. Kuchuk-Yatsenko, S.I., Krivenko, V.G., Didkovsky, A.V. et al. (2012) Technology and new generation of equipment for flash-butt welding of advanced high-strength rails for construction and reconstruction of high-speed railway lines. *The Paton Welding J.*, **6**, 22–26.
5. Kuchuk-Yatsenko, S.I., Didkovsky, A.V., Shvets, V.I. et al. (2016) Flash-butt welding of high-strength rails of nowadays production. *Ibid.*, **5-6**, 4–12. DOI: <https://doi.org/10.15407/as2016.06.01>.
6. Kostin, V.A. (2012) Mathematical formulation of carbon equivalent as a criterion for evaluation of steel weldability. *Ibid.*, **8**, 11–16.
7. Shtajger, M.G., Balanovsky, A.E. (2018) Analysis of technologies for welding of high-strength rails from position of structure formation in construction and reconstruction of high-speed railway lines. Pt 1. *Vestnik Irkutskogo Gos. Tekhn. Un-ta*, **22(6)**, 48–74. DOI: 10.21285/1814-3520-6-48-74 [in Russian].
8. Shevchenko, R.A., Kozyrev, N.A., Usoltsev, A.A. et al. (2017) Methods of producing of quality welded joint of railroad rails. In: *Proc. of 20th Int. Sci.-Pract. Conf. on Metallurgies, Innovations, Quality*. Novokuznetsk, SibGIU, 254–257.
9. Tikhomirova, L.B., Iliinykh, A.S., Galaj, M.S., Sidorov, E.S. (2016) Examination of structure and mechanical properties of aluminothermic welded joints of rails. *Vestnik YuUrGU. Seriya Metallurgiya*, **16(3)**, 90–95 [in Russian].
10. Kalashnikov, E.A., Korolyov, Yu.A. (2015) Technology of welding of rails in Russia and abroad. *Put i Putevoe Khozyajstvo*, **8**, 2–6 [in Russian].
11. Kozyrev, N.A., Usoltsev, A.A., Shevchenko, R.A. et al. (2017) Modern methods of welding of new generation rails. *Izv. Vuzov, Chyorn. Metallurgiya*, **60(10)**, 785–791 [in Russian].
12. Ermakov, V.M., Shtajger, M.G., Yanovich, O.A. (2016) Electronic certificate of rail. *Put i Putevoe Khozyajstvo*, **4**, 13–17 [in Russian].
13. Genkin, I.Z. (2003) Heat treatment of rail welded joints in induction units. *The Paton Welding J.*, **9**, 41–44.
14. Saita, K., Karimine, K., Ueda, M. et al. (2013) Trends in rail welding technologies and our future approach. In: *Nippon Steel & Sumitomo Metal Technical Report*. December, 105, 84–92.
15. Andreeva, L.A., Fedin, V.M., Bashlykov, A.V. et al. (2013) Thermal hardening of rail welded joints in industrial transport. *Promyshlennyy Transport XXI Vek*, **1**, 19–20 [in Russian].
16. Mashekov, S.A., Absadykov, B.N., Alimkulov, M.M., Smailova G.A. (2016) Problems of rail welding and their solution by mean of development of perspective methods of induction welding. *Information 1. Dokl. Nats. Akademii Nauk Respubliki Kazakhstan*, **305**, 19–21, ISSN 2224–5227 [in Russian].
17. Shur, E.A. (2006) Influence of structure on service stability of rails. Influence of properties of metallic matrix on service stability of rails. In: *Proc. of 2nd All-Russian Sci.-Techn. Seminar (Ekaterinburg, 16–17 May, 2006)*. Ekaterinburg, UIM, 37–64 [in Russian].
18. Shtajger, M.G., Balanovsky, A.E. (2018) Analysis of technologies for welding of high-strength rails from a position of structure formation in construction and reconstruction of high-speed railway lines (Review). Pt 2. *Vestnik IGTU*, **22(7)**, 41–68 [in Russian].
19. Zaayman, L. (2007) Continuous welded rail using mobile flash butt welding. *Civil Engineering*, **5**, 62–65.
20. (2012) Manual for flash butt welding of rails. Ministry of Railways of India, January.
21. Girsch, G., Keichel, J., Gehrman, R. et al. Advanced rail steels for heavy haul application – track performance and weld ability Intergrated Project (IP). *Thematic Priority 6. Project No. 5: Sustainable Development, Global Change and Ecosystems*.
22. Pointner, P., Joerg, A., Jaiswal, J. (2015) Definitive guidelines on the use of different rail grades. *Innovative track system*, **6**, 41–42.
23. Jilabi, Abdul (2015) Welding of rail steels. In: Thesis for PhD Degree, University of Manchester, Faculty of Engineering and Physical Sci.
24. (2015) Continuous path in the United States on the Union Pacific network. *Railway Gazette International*, **8**, 42–43.
25. Gong, L., Zhu, L., Zhou, H.X. (2017) Effect on hardness and microstructures of rail joint with ultra-narrow gap arc welding by post weld heat treatment. *Engineering Materials*, **737**, 90–94.
26. Khlyst, S., Kuzmichenko, V., Khlyst I., Gontar, A. (2013) Experience of conducting of differentiated heat treatment of rails by air method according to the technology «TEK-DT» on industrial unit TEK-DTO-20-13.6. *Inzhenerye Resheniya*, **1**, 1–4 [in Russian].
27. Babenko, P.G., Zeman, S.K. (2002) *Software-hardware of automation of technological processes*. Tomsk, Tomsk Un-t [in Russian].
28. Feshchukov, A.N., Ruban, V.V., Zeman, S.K. (2013) Complex of high-frequency induction heater for heat treatment of rail welded joints in track conditions. In: *15th Int. Sci.-Pract. Conf. on Modern Engineering and Technologies*, 256–258.
29. Rezanov, V.A., Fedin, V.M., Bashlykov, A.V. et al. (2013) Differentiated hardening of rail welded joints. *Vestnik VNIIZhT*, **2**, 28–34 [in Russian].
30. Panteleymonov, E.A. (2018) On the problem of heat treatment of welded joints of railway rails. *The Paton Welding J.*, **3**, 36–39. DOI: <https://dx.doi.org/10.15407/as2018.03.08>.
31. Mashekov, S.A., Absadykov, B.N., Alimkulov, M.M., Smailova, G.A. (2016) Problems of rail welding and their solution by mean of development of perspective methods of induction welding. *Information 2. Dokl. Nats. Akademii Nauk Respubliki Kazakhstan*, **305**, 22–28, ISSN 2224–5227 [in Russian].

Received 21.09.2018

**FEBRUARY 1, 1941** Production of Sherman tank began in the USA. Compared to riveted tank M-3, it had a larger caliber gun (75 mm), cast or welded turret. Pullman-Standard Company participated in fulfillment of the program on all-welded tank production. It developed the technology of welding the hull and turret. A conveyor line for hull assembly and welding was organized. Multilayer manual arc welding was performed in the downhand position, and after that the structure was installed into positioners. Automatic submerged-arc welding in equipment developed already in 1940, was used only for producing the heaviest part — tank wheels from low-carbon steel.



**FEBRUARY 2, 1933** All-Ukrainian Academy of Sciences (AUAS) adopted a resolution on setting up the Electric Welding Institute on the base of the Electric Welding Committee and Electric Welding Laboratory of AUAS. Evgeny Oscarovich Paton (1870–1953) was appointed Director of the Institute.



**FEBRUARY 3, 1938** Birthday of V.G. Fartushny (1938–2018), President of the Welding Society of Ukraine, specialist in the field of welding high-alloyed corrosion-resistant steels, mechanization and automation of welding production, equipment for thermal coating and robotic complexes. He took an active part in development and testing of Vulkan unit, in which welding in space was performed in 1969. During 1980–2004 he was Director of All-Union Design Institute of Welding Production. V.G. Fartushny is author of about 100 scientific publications and inventions.



**FEBRUARY 4, 1952** At the start of 1952 B.E. Paton and B.I. Medovar developed the process of electroslag remelting (ESR) at the Electric Welding Institute for the first time, in order to produce high-quality metals. At ESR metal refining is achieved by changing the slag composition and process temperature mode.



**FEBRUARY 5, 2005** Sea fighter (FSF-1), experimental ship of the US navy, was tested. Its hull has a smaller water-plane area, ensuring high stability even on rough seas. The ship was one of the first, in manufacture of which friction stir welding began to be applied at assembly of metal panels.



**FEBRUARY 6, 1989** An experiment was performed in Yantar unit on deposition of thin-film coatings by the method of thermal electron beam evaporation and condensation, in order to study the features and dynamics of the process in space environment.

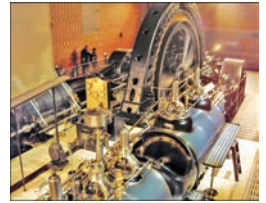


**FEBRUARY 7, 1950** R. Sarazin, French inventor, proposed a method and machine for continuous coating of electrodes. In keeping with his invention, the wire was unwound from the bundle at wheel rotation. It was then straightened in rollers and entered in extrusion press, which was followed by its cutting into separate electrodes, and feeding by a conveyor for drying.



\*The material was prepared by the company Steel Work (Krivoy Rog, Ukraine) with the participation of the editorial board of the Journal. The Calendar is published every month, starting from the issue of «The Paton Welding Journal» No.1, 2019.

**FEBRUARY 8, 1988** ABB Concern (Asea Brown Boveri Ltd.) was founded. It is a Swedish-Swiss Company, specialized in the field of electrical and power engineering and information technologies. ABB Company is actively pursuing manufacture of industrial robots, including those for welding operations. The Concern has its representative offices in more than 100 countries of the world. Production facilities are located in the territory of Germany, Switzerland, Sweden, Italy, France, Czechia, India, China, USA, Portugal, Brazil, Finland, Estonia and other countries.



**FEBRUARY 9, 1915** Birthday of G.P. Sakhatsky (1915–1992), known scientist and specialist in the field of cold welding of nonferrous metals and alloys. In his works he set forth the main principles of resistance butt welding and features of joint formation on such materials as high-carbon and high-alloyed steels, copper, and aluminium alloys of different alloying systems.



**FEBRUARY 10, 1938** Birthday of V.P. Larionov (1938–2004), known Russian scientist in the field of strength and reliability of structures, operating under extreme climatic conditions of the North, academician of RAS. He obtained fundamental results in the field of materials physics, metallurgy and kinetics of welding processes.

**FEBRUARY 11, 1965** Scientists of E.O. Paton Electric Welding Institute — A.E. Asnis and I.M. Savich — for the first time developed the equipment, flux-cored wire and technology of mechanized wet underwater welding. The technology has found wide application in repair of underwater pipelines and structures as well as afloat ships.



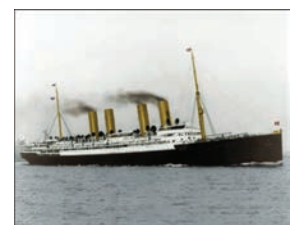
**FEBRUARY 12, 1981** President of the AS of USSR acad. B.E. Paton was awarded with the Lomonosov Gold Medal — the highest award of AS of USSR — for outstanding achievements in the field of metallurgy and metal technologies.

**FEBRUARY 13, 1951** In the beginning of 1951 E.O. Paton Electric Welding Institute together with Novokramatorsk Machine-Building Plant developed a process and technology of vertical electroslag welding of metal of up to 2000 mm thickness. For the first time in the world the new method was used in welding of stator of hydraulic turbine for Mingachevir Hydro Power Station.

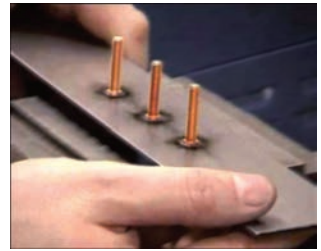


**FEBRUARY 14, 1917** Birthday of S.M. Gurevich, a well-known scientist in the field of metallurgy and welding of titanium and refractory metals. For the first time in the world S.M. Gurevich developed a technology of submerged-arc welding of titanium. He participated in the development of the methods of electroslag welding and electroslag remelting of titanium, argon-arc welding over flux layer with flux-cored wire. S.M. Gurevich is the author of almost 600 scientific papers, including more than 100 patents for invention.

**FEBRUARY 15, 1938** The second transatlantic liner Leviathan, initially constructed as German liner Vaterland, was recycled. On April 6, 1917 the USA entered the World War I and Vaterland was impressed by American authorities. Three months after it was renamed in «Leviathan». After repair using welding it was subjected to sea trials. They were successful, the vessel built up impressive speed of 27.48 knots. Leviathan carried military cargos in North Atlantic, transported troops in Europe. The vessel has transported in total more than 100 thousand soldiers for 19 voyages.



**FEBRUARY 16, 1912** Capacitor-discharge welding and device for its realization was patented. Staff member of Westinghouse Electric Corp. L.V. Chubb experimenting with electric capacitors found that the wire is welded to aluminum plate in passing through them of accumulated electric discharge. This observation allowed making some conclusions, namely discharge ruined strong oxide film complicating soldering and, that provided the possibility to get sound joint of aluminum wires. The capacitor-discharge welding at once started to be used in electric engineering (welding of silver, tungsten and other contacts).



**FEBRUARY 17, 1982** R.I. Lashkevich died. He was a talented designer and researcher in the field of development of welding equipment. He developed a series of original welding apparatuses, units, machines and devices such as roll-welding mills for mine cars, first models of apparatuses for electroslag welding, first in the USSR through-pass mill for automatic welding of large-diameter pipes, heads for resistance welding of main pipelines and another unique welding equipment.



**FEBRUARY 18, 1914** Birthday of V.V. Podgaetsky (1914–1991), a well-known scientist, Honored Master of Science and Engineering of Ukraine. He made a fundamental contribution in welding metallurgy, in particular, investigation of interaction of metal, slag and gases, causes of formation of pores, cracks and other defects in weld metal. Published 215 scientific papers, including 23 monographs.

**FEBRUARY 19, 1948** V.P. Nikitin, a well-known scientist in the field of electrical engineering, welding and electromechanics was awarded with an honorary title «Honored Master of Science of RSFSR» for outstanding achievements in the field of science. The main works of V.P. Nikitin are dedicated to investigation of physical processes in electric arc and development of electric machines and apparatuses for arc welding. He designed a structure of one-body transformer-regulator for arc welding, which found application in industry. In 1926–1929, V.P. Nikitin being a professor of Ekaterinoslavsk Mining Institute was simultaneously a consultant at many Ukrainian and Russian enterprises.



**FEBRUARY 20, 1986** On February 20, 1986 the Soviet Union launched the scientific orbital station «Mir», replacing the orbital stations «Salyut» and became for about 15 years a single in the world manned space laboratory for long-term scientific-technical experiments and investigation of human body in space. Further on the solar-cell batteries designed at the E.O. Paton Electric Welding Institute were deployed at the station.



**FEBRUARY 21, 1920** On February 21, 1920, the State Commission on Electrification of Russia (GOELRO plan) was established. Later, in the GOELRO plan, the name of the future construction: the Dnieper Hydroelectric Station appeared. On March 15, 1927 on the rock «Love» a red flag with the inscription «Dneprostroy began» was set. During its construction, autogenous cutting and welding, electric welding, devices for butt joining of reinforcement bars and other mechanisms became widespread.



**FEBRUARY 22, 1937** Date of birth of V.M. Sagalevich (1937–1995), Professor of the Bauman Moscow State Technical University, a scientist in the field of welding, welding strains and stresses. The works of Professor V.M. Sagalevich are devoted to the problems of strength, theory of welding strains and stresses, including deformations of thin-sheet and thin-walled structures during welding.



**FEBRUARY 23, 1934** The French inventors R. Sarrazin and O. Moneiron received a patent for the electrode coating of their development, which included the compounds of alkali and alkaline earth metals (feldspar, marble, chalk and soda). Due to the low ionization potential of such elements as sodium, potassium, calcium, the arc was easily excited and maintained in burning.



**FEBRUARY 24, 1988** Date of death of James Rosati (1911–1988), an American sculptor who created his sculptures by welding of stainless steel. His most famous works were created since the 1960s, where a special role was occupied by a stainless steel sculpture «Ideogram» of 23 feet height. About forty monumental sculptures of James Rosati are located in the United States of America and other countries.



**FEBRUARY 25, 1936** Date of birth of O.K. Nazarenko (1936–2014), a famous scientist in the field of electron beam welding, a corresponding member of the NAS of Ukraine. He provided physical and technical grounds for the ability of avoiding defects in welded joints during breakdowns in electron gun by short-time removing of accelerating voltage. On this basis, he created perfect power sources, developed principles of automatic electron beam guiding along a welded joint, and created corresponding systems which use secondary electron emission from the welding zone as a source of information. With his participation the technology and equipment for electron beam welding of rocket and gas turbine engines was introduced into the industry of Ukraine.



**FEBRUARY 26, 1934** The first plant for the production of the «people's» car Volkswagen was opened. The first produced car was the famous VW Beetle. This is the most popular car in history, produced without additional consideration of the basic design. In total, 21,529,464 cars were manufactured. In its development Ferdinand Porsche (later founder of the second variant of the Tiger tank) was involved, who was keeping contact with Ford and other pioneers and actively introduced new technologies at the plant. Welding provided reliability and quick assembly of the car in the conveyor.



**FEBRUARY 27, 1917** J.H. Lincoln published one of his patents in the field of welding. He is the founder of Lincoln Electric Company, which became an American multinational company, producing equipment for arc welding, robotic welding, plasma and gas cutting. In 1909, for the first time in history, the company manufactured a welding apparatus. In 1911, Lincoln Electric produced the world's first portable welding apparatus with a controlled voltage.



**FEBRUARY 28, 1962** At the end of February, at the general meeting of the Academy of Sciences of the Ukr.SSR, a new membership of the Presidium was selected. Boris Evgenievich Paton, Academician of the Academy of Sciences of the Ukr.SSR, became the President. Today, the NAS of Ukraine includes 174 institutes. The number of its associates is over 30,000 members.

